



Durham E-Theses

An Assessment of Basement Inheritance in SE Brazil

ALVES-DE-MATOS, MARIA,ANTONIA

How to cite:

ALVES-DE-MATOS, MARIA,ANTONIA (2017) *An Assessment of Basement Inheritance in SE Brazil*, Durham theses, Durham University. Available at Durham E-Theses Online:
<http://etheses.dur.ac.uk/12198/>

Use policy

The full-text may be used and/or reproduced, and given to third parties in any format or medium, without prior permission or charge, for personal research or study, educational, or not-for-profit purposes provided that:

- a full bibliographic reference is made to the original source
- a [link](#) is made to the metadata record in Durham E-Theses
- the full-text is not changed in any way

The full-text must not be sold in any format or medium without the formal permission of the copyright holders.

Please consult the [full Durham E-Theses policy](#) for further details.



An Assessment of Basement Inheritance in SE Brazil

Master of Science by Research
Department of Earth Sciences
Durham University
2017

Maria Antonia Alves de Matos
Ustinov College

Table of Contents

Contents

| | |
|-------------------------------------------------------------------|------|
| Table of Contents..... | ii |
| Table of Figures..... | iv |
| Abstract..... | viii |
| Declaration..... | ix |
| Copyright..... | ix |
| Acknowledgments..... | x |
| 1 Introduction | 1 |
| 1.1 Study Area..... | 8 |
| 2 Regional Geology and Tectonic Framework | 9 |
| 3 Methodology..... | 14 |
| 3.1 Remote Sensing | 14 |
| 3.2 Geophysical data..... | 17 |
| 3.4 Fieldwork..... | 18 |
| 3.5 Methodology Approach in the Field | 21 |
| 3.5.1 Reactivation vs Reworking vs Inheritance | 21 |
| 3.5.2 Structures in a strike slip/wrench regime | 23 |
| 3.5.3 Rheology | 24 |
| 3.5. 4 Faults, Joints and veins..... | 25 |
| 4 Structural Geology | 26 |
| 4.1 The Rio Santana Graben..... | 26 |
| 4.1.1 Location 1 (UTM: 23K 649344 7507989)..... | 27 |
| 4.1.2 Location 2 (UTM: 23K 651592 7510592) | 29 |
| 4.2 Volta Redonda Basin | 31 |
| 4.2.1 Location 6/7 (UTM: 23K 599896.9 7514777.4)..... | 33 |
| 4.2.2 Location 28 (UTM: 23K 577396 7513051) | 35 |
| 4.3 Resende Basin | 37 |
| 4.3.1 Location 9 (UTM: 23K 559770.2 7520585.9) | 39 |
| 4.3.2 Location 10 (UTM: 23K 559924.5 7533609.9) | 42 |
| 4.3.4 Location 13 (UTM: 23K 562514.9 7538179.2) | 44 |
| 4.4 Taubate Basin..... | 46 |
| 4.4.1 Location 27 (Taubate basin) (UTM: 23K 474139 7470288) | 47 |

| | |
|---------------------------------------------------------------------------------|-----|
| 4.5 Tamoios Highway: Embu Domain and Coastal Complex | 50 |
| 4.5.1 Location 22 (UTM: 23K 0422175 7421654) | 51 |
| 4.5.2 Location 23 (UTM: 23K 427548 7417600) | 53 |
| 4.5.3 Location 24 (UTM: 23K 443030 7400035) | 57 |
| 4.6 Sao Paulo Basin | 61 |
| 4.6.1 Location 0 (UTM: 23K 362778 7403387) | 63 |
| 4.7 Lineaments Analysis (Comparison of Remote Sensing and Fieldwork data) | 74 |
| 5 Control of the local structures – Discussion | 79 |
| 6 Conclusion | 94 |
| Appendix 1 | 96 |
| Appendix 2 | 97 |
| Appendix 3 | 98 |
| References | 100 |

Table of Figures

| | |
|--------------------------------------------------------------------------------------------------------------------------------------------------------------------------------------------------------------------------------------------------------------------------------------------------------------------------------------------------------------------------------------------------------------------------------------------------------------------------------------------------------------------------------------------------------------------------------------------------------------------------------------|-----------|
| <i>Figure 1: Area of study showing the main basins part of the Continental Rift of Southeast Brazil (CRSB). Volta Redonda Basin, Resende Basin, Taubaté and São Paulo Basin.</i> | <i>8</i> |
| <i>Figure 2: Mylonitic fabric showing dextral sense of movement at the Santana Graben in the state of Rio de Janeiro</i> | <i>10</i> |
| <i>Figure 3: Fig 3a: Lithology by CPRM (Companhia de Pesquisa de Recursos Minerais) Brazilian Geological Service, 2007 http://geobank.cprm.gov.br/. In the next page figure 3b is diagram summarising the tectono-stratigraphy evolution of each studied basins based upon literature. Figure 3c in the following page is the diagram in figure b with added the findings of this project.</i> | <i>11</i> |
| <i>Figure 4: From clockwise, hillshade illumination from angles 45 °, 125 °, 315 ° and 225 °. Using ArcGIS 10.2</i> | <i>15</i> |
| <i>Figure 5: In Fig.a above the lines were then separated into colours to help visualize the different orientation of each group. This method helped to give the area regional, large scale structural features. Figure 5b (anti-clockwise): Close up of lineaments of locations 1,2,3, and 4. Changing the scale during the lineaments pick-ups helped to judge the faults tips. Here fault tips were determined by the intersection of the lines or following the shadows of the structures, assuming that the structure would terminate where its shadow terminates</i> | <i>16</i> |
| <i>Figure 6 : The DEM image above (90m) is displaying the seismic events recorded in the SE Brazil until 2013 (data from IAG-USP/Instituto de Astronomia e Geofisica-Universidade de Sao Paulo. The red triangles are the events recorded. In blue the drainage system by CPRM (Companhia de Pesquisa de Recursos Minerais) Brazilian Geological Service, 2007. http://geobank.cprm.gov.br/</i> | <i>17</i> |
| <i>Figure 7: lineation taken from locality 6 at Volta Redonda basin</i> | <i>18</i> |
| <i>Figure 8: The locations are concentrated on the four basins before mentioned, Volta Redonda, Resende, Taubaté and São Paulo; therefore the locations above represent the outcrops visited within these main areas, which has been described in Chapter 2. Some of these locations have been not considered to the aim of this project and therefore not added to the analyses.</i> | <i>20</i> |
| <i>Figure 9: Diagram taken from Holdsworth, Hand et al. (2001) demonstrating zones of reactivation and reworking and its controlling parameters.</i> | <i>21</i> |
| <i>Figure 10: Diagram taken from Holdsworth, Butler et al. (1997)</i> | <i>22</i> |
| <i>Figure 11: Structures expected in strike slip settings: a) Restraining and releasing bends form where the fault changes direction. b) “Flower structures” formed as a result of oblique extension (top), or compression (bottom), where smaller structures link to larger faults (Woodcock and Fischer, 1986). c) Riedel shears form complex geometries in response to strike-slip deformation and occur at different scale (Tchavchenko 1970 ref.). Modified from McClay (1991). (Ashby 2013)</i> | <i>23</i> |
| <i>Figure 12: A and B in this figure demonstrate the different types of abutting joints as per Rives, Rawnsley and Petit (1994) and the shapes found in the field. The smaller fractures abutting against the NW-SE structures suggest the former are younger.</i> | <i>25</i> |
| <i>Figure 13: Example of cross-cutting relationship in the field, with E-W fault cross-cutting the pegmatite veins infill in the basement rock.</i> | <i>25</i> |
| <i>Figure 14: Example of a reverse fault in the Tamoios Highway location. The S fabric indicating the sense of movement of the fault.</i> | <i>25</i> |
| <i>Figure 15 : The Rio Santana graben is at the west of the city of Rio de Janeiro ~25km. The first 2 locations of the project were recorded there.</i> | <i>26</i> |
| <i>Figure 16: Figure 16a is the stereographic representation of the data from this outcrop. Fig. 16b Diagram of the relay ramp feature in the area (Gontijo-Pascutti, Bezerra et al. 2010). Fig.16c is a sample of the foliation in the rock, showing dextral sense of movement and micro boundinage within the matrix.</i> | <i>27</i> |
| <i>Figure 17: Figure 17a is the Stereonet projection of the structures in the dyke. The surface of the dyke has been constantly eroded by the river water current and it makes it difficult to identify the relationship between them. Because the uncertainty to classify the fractures and joints the structures were kept in one colour – black at the stereographic projection. In fig 17b the structures that could possibly be joints are shown in blue. Possible riedel fractures also showing a sinistral sense of movement in the figure 17b (fainting orange just behind Dr Julio Almeida who was used for scale.</i> | <i>29</i> |

| | |
|--------------------------------------------------------------------------------------------------------------------------------------------------------------------------------------------------------------------------------------------------------------------------------------------------------------------------------------------------------------------------------------------------------------------------------------------------------------------------------------------------------------------------------------------------------------------|-----------|
| <i>Figure 18: A geological map from (Gontijo-Pascutti, Bezerra et al. 2010) where the dykes mapped in the area (in green) show direction NE-SW.</i> | <i>30</i> |
| <i>Figure 19 : Location map with red dot marking the basin</i> | <i>31</i> |
| <i>Figure 20: Stratigraphic column of Volta Redonda (Negrão, Mello et al. 2015)</i> | <i>32</i> |
| <i>Figure 21: Fig. 21a is the stereographic projection of its structures recorded. Fig. 21b shows an example of boudanige in the outcrop suggesting the extensional regime in the area.. Fig. 21c shows a normal fault that at first sight can be classified as a reverse fault, but it is a normal fault with an oblique component. Fig. 21d shows the lineation imprinted in the fault which are slickenlines in the fault.</i> | <i>33</i> |
| <i>Figure 22: 22a stereographic projection showing parallel lines to the foliation and possible reactivation fractures E-W orientated (black.) The vectors represent the transport direction. Fig. 22b the dyke intrusion is offset by the NNW-SSE fracture.</i> | <i>35</i> |
| <i>Figure 23: Map showing the points visited within the Resende Basin. Locations 9, 10, 11, 13. Location 12 was too close to location 13 and no relevant information was observed to justify its inclusion in the final report. Location 9 is seen at the hangwall of one of the main faults in the west side of the basin, whereas the other three outcrops are located on the footwall of the fault.</i> | <i>37</i> |
| <i>Figure 24: Chronostratigraphy for the Resende Basin (Ramos, Mello et al. 2006)</i> | <i>38</i> |
| <i>Figure 25 : Outcrop in location 9 is a brecciate fault rock, showing very fine grains, heavily weathered and located at the border of the Resende basin. Fig 25a is the stereographic representation of the structures recorded in the outcrop, the dominant orientation is NE-SW and the slickenline suggest an oblique fault. Fig. 25b displays the fault core layers aligned. At Fig. 25c the yellow dashed lines display a network of fractures/minor faults that possibly pre-date the fractures in solid red lines.</i> | <i>39</i> |
| <i>Figure 26: Thin section of sample showing field of view 1000µm , the red lines represent possible micro-structures for this outcrop. Quartz veins, shear zone and brittle micro-fractures. The quartz vein seems to have been offset by a microfracture, and the shear zone stops at an intersect point. The yellow dashed lines here are indicating a possible sinistral shear movement.</i> | <i>40</i> |
| <i>Figure 27: Second location at the Resende basin, Fig. 27a is the stereographic projection of the planes measured at the location there was no indication of reactivation neither kinematics were possible to be collected. Fig 27b shows the outcrop follows the trend of the area, with high angle fractures NE-SW and NW-SE</i> | <i>42</i> |
| <i>Figure 28: An outcrop in the Resende basin, the fractures displayed in this outcrop are similar to the outcrop back in Volta Redonda (location 28) with NW-SE being crosscut by NNE-SSW and by a more consistent set of ENE-WSW strike.</i> | <i>44</i> |
| <i>Figure 29: Another outcrop at high elevation, granitoid showing fabric showing preferential orientation and displaying joints. Fig. 29a is the stereographic projection of the fractures measured, Fig. 29b is showing two different sets of joints typical of uplifted areas and Fig. 29c is a panoramic view of the location looking towards N-NE, the scarp swarm orientation is marked by the red lines.</i> | <i>44</i> |
| <i>Figure 30: Map location of the outcrop visited at Taubate Basin, it is an active quarry at the border of the east side of the basin.</i> | <i>46</i> |
| <i>Figure 31: Chronostratigraphy column of Taubaté basin (Torres-Ribeiro 2004)</i> | <i>46</i> |
| <i>Figure 32: The stereonet displays its fractures in Fig 32a. The high angle dips faults cut through the moderately dipping foliation (green line), the gouges trace an almost parallel with the deeply steep ENE-WSW fault sets. The slickensides imprinted in zeolite in the fracture wall (Fig. 32b).</i> | <i>47</i> |
| <i>Figure 33: Geological sketch of the northern coast of the São Paulo state. The Camburu Shear Zone (CSZ) limiting at north</i> | <i>50</i> |
| <i>Figure 34: Location of the outcrop in Fig. 34a. Stereographic projection is shown in Fig. 34b. Figure 34c shows an inset of the sinistral sense of movement (red arrows) imprinted in the fabric with quartzo feldspathic veins (pink), cohesive corridor marked in red plain lines, and in dashed line a small possible microfault offsetting the red lines and veins. Still in Fig 34c crenulations displaying the Figure 34d displays the different sets of fractures/faults within the outcrop in Fig 34e.</i> | <i>51</i> |
| <i>Figure 35: Fig. 35a is the location of the outcrop, 35b is the stereographic projection of the data recorded. Fig. 35c is the Google image of the anticline structure at the location of the outcrop, the measurement were taken from the opposite hand side of the highway. In 35d if a close insight of pegmatite veins, showing W microfold and possibly microfaults striking E-W cutting through these veins. Fig 35e the slickensides imprinted in one of the the NE-SW fault plane outcrop. In Fig 36 a close up of the outcrop striking NW- SE.</i> | <i>53</i> |

| | |
|----------------------------------------------------------------------------------------------------------------------------------------------------------------------------------------------------------------------------------------------------------------------------------------------------------------------------------------------------------------------------------------------------------------------------------------------------------------------------------------------------------------------------------------------------------------------------------------------------------------------------------------------------------------------------------------------------------------------------------------------------------------------------------------------------------------------------------------------------------------|-----------|
| <i>Figure 36: Fig 36 shows part of the anticline pictured in Fig 35c, the vein striking SSE-NNW has perfect left-lateral strike lip fault and cut through cleavage of the structure. The dashed red lines are striking E-W, layers displaying a fabric showing preferential orientation but with hollow space in between the beddings probably resulting of dissolution of minerals. On the left corner the riedel diagram for dextral strike slip fault.</i> | <i>54</i> |
| <i>Figure 37 (anticlockwise): Fig. 37a is the map location of the outcrop, while Fig 37b stereographic projection; Fig. 37c displays the listric fault in the outcrop being cut-off by the E-W predominant fault set in the outcrop. Fig 37d pictures the fault gouge, and the fig 37e is an inset of the fault gouge in the reactivated foliation dipping south.</i> | <i>57</i> |
| <i>Figure 38: Thin section of the fault gouge sample taken from the location. Fig 38a is in PPL (plain polarized light). In Recrystallized quartz veins and frictional grain boundary corridor can be observed . Possible microfaults in dashed red lines.</i> | <i>59</i> |
| <i>Figure 39: The quarry visited at São Paulo basin is marked with the red dot.</i> | <i>61</i> |
| <i>Figure 40: Chronostratigraphy column of São Paulo basin.. Modified from Riccomini et al. (2004). .</i> | <i>62</i> |
| <i>Figure 41: Fig 41a is the stereographic projection of its linear/plane structures, the lineation recorded here shows oblique to dip slip fault, the foliation rotated anti-clockwise in apparently two stages, 25° each, adding up to a 50° change in its strike. Fig. 41b is the basement gouge displaying secondary fractures. Fig 41c is an example of fossil plants which are very common within the Itaquaquecetuba formation of the Sao Paulo basin. These fossils have been dated back to Pleistocene, the fine upwards is characteristic of fluvial deposits. Fig. 41d is a picture of a flower structure displayed on the outcrop, the red lines are represent the original shape of the structure while the black lines represent the secondary that developed as faulting progressed under different stresses regimes locally.</i> | <i>63</i> |
| <i>Figure 42(clockwise): Fig. 42a display the fault bending in the outcrop that occurred when the NW-SE fault joined the NNE basement fault. Fig. 42b is the inset of the structure marked with the red square in Fig. 42a. The riedel fractures are marked in blue (R and R'), the yellow dashed lines are possibly reactivated foliation which offset the fault line of the fault wedge. The solid red lines represent the fault line NW-SE. The basement rocks are augen gneiss (the dark one get its colour due to the contact with the running water from the quarry and Sandstone consistent of fluvial sediments. Red arrows indicating sense of movement. The solid yellow lines suggest a possible secondary fractures relationship that seems to repeat across the basement plan.Dashed white lines displaying the curvature of the faults.</i> | <i>64</i> |
| <i>Figure 43: Fig. 43a and b shows a panoramic view of the outcrop with its different beddings within the Pleistocene sandstone. The black lines separate the beddings showing distinctive structures and textures, these beddings are following a NE-SW orientation, similar to the deflected foliation of the basement. A small angular unconformity is also marked with a purple dashed line. At the base of the outcrop gravel and some parts of the basement are still exposed. The red dashed lines are indicating fractures and red lines are faults where displacement is observed.</i> | <i>65</i> |
| <i>Figure 44: In this figure a better exposure of the outcrop beddings, sedimentary structures indicate a fluvial environment. The solid black lines are contact between the beddings whether they are discontinued or fractured. The solid red lines are faults recorded in the sediment and the red dashed lines are possible fractures.</i> | <i>66</i> |
| <i>Figure 45: Inferred paleostress based on remote sensing lineaments inferred on the fault wall of the Pleistocene sandstone, according to Riedel diagram.</i> | <i>67</i> |
| <i>Figure 46: Another point of the same outcrop in Fig. 46a, a negative flower structure indicates that the structures enjoyed a transtensional regime. Here is possible to observe water responsible for heavily weathered and reduced basement directly. The water also causes the erosion within the beddings leaving karstic like cavities structures cut across the beddings, which are marked by the solid black lines. The solid red lines are fault lines, and the dashed lines are used suggest fractures. The throw between unit A and B, suggests a syn-sedimentary process that might have been influenced by pre-existing basement structures, and the stream (blue) (Fig. 46b) running down the outcrop seems to follow the direction to the heavily weathered basement slope towards S.</i> | <i>68</i> |
| <i>Figure 47: The flower structure from Fig. 41c seen from another angle emphasizing the main fault planes. It shows the contact between the basement and sandstone, in red dashed lines infer tensile faults showing sinistral vergence.</i> | <i>69</i> |
| <i>Figure 48: Figure 48a the diagram suggests that the youngest fractures propagate towards the stress perturbations. Figure 48b The pink dashed lines in the picture on the left represents the fault NNE-SSW and the green dashed lines represents the NNW-SSE.White dashed lines represent faults from the NNE-SSW set going through the same dynamic with the older E-W fault set.</i> | <i>73</i> |

| | |
|------------------------------------------------------------------------------------------------------------------------------------------------------------------------------------------------------------------------------------------------------------------------------------------------------------------------------------------------------------------------------------------------------------------------------------------------------------------------|----|
| <i>Figure 49: Figures A represent the azimuth of the structural lineaments and B has been separated by length. The colours are representing the different sets of the lineaments by orientation; the longer fractures are orientating NE-SW and are the ductiles lineaments reactivated at late cretaceous. The shorter yellow lines, representing the brittle fractures E-W and N-S, likely to have been created under different tectonic regime.</i> | 74 |
| <i>Figure 50: The lines in this map represent the brittle structures in the area, E-W and N-S orientations.</i> | 77 |
| <i>Figure 51: The yellow lines are ductile features, primarily formed during the amalgamation of Ribeira belt during the Neo-Proterozoic.</i> | 78 |
| <i>Figure 52: Stratigraphic column for the CRSB with tectonic regime according to Riccomini, Sant'Anna et al. (2004).....</i> | 82 |
| <i>Figure 53: Taxaquara fault cross cutting the Sao Paulo basin, the dashed line inferring that the fault disappear towards the Santos basin</i> | 93 |
| <i>Figure 54: Zalan 2005 inferred grabens within the shallow part of the Santos basin area. Implying them to be from Cenozoic age, reflecting the same geometry of the onshore rift system and the basement anisotropy influence in the formation of new structures. Dykes and faults are cross cutting these grabens, suggesting tectonic activities that reactivate transfer zones, possibly during the Paleogene. Modified from Zalán and Oliveira (2005)</i> | 93 |
| <i>Figure 55: Sketch taken from (Rodriguez 1998) modified from (Riccomini 1989)</i> | 94 |
| <i>Figure 56: sketch based on the faults crosscutting the Sao Paulo basin from Rodriguez (1998)</i> | 94 |
| <i>Figure 57: First attempt to create different angles through hillshade of the DEM map of 30m resolution. Because of the poor quality of the results as above it was decided to use the results for the 90m resolution.(picture on the top displaying hillshade process on 90m resolution)</i> | 96 |
| <i>Figure 58: Rose diagrams representing the different orientations of the area, separated the structures in group based on their azimuth.</i> | 98 |
| <i>Figure 59: Rose diagrams comparing regional to local structures orientations</i> | 99 |

Abstract

SE Brazil, especially the Central Segment of the Ribeira belt, in theory is an ideal place to investigate reactivation of pre-existing structures or basement-influenced faulting due to its position on the South Atlantic margin and large area of basement exposure, however it offers several obstacles due to its high rates of weathering and erosional processes, and amongst others, difficulty in correlating the brittle history with neotectonic processes.

This project focused on finding at outcrop scale evidence for basement inheritance or basement influence in the deformation processes of the area and present day tectonics. Fieldwork and remote sensing analysis were used as well as alternative solutions to acquire data and these results were integrated with previous publications.

The area displays predominantly steeply dipping fault structures that are consistent with its main basin architecture and in particular the Santos basin which sits parallel to the study area. The area has a geological history that differs from its surroundings due to its geological setting. The Central segment of the Ribeira belt is where the Continental Rift of SE Brazil Tertiary basins are localised. These basins are evidence of relatively recent deformation histories and are great assets to investigating local control to geological structures. Many outcrops were visited, and at the end only the ones offering a good display of information were used to provide evidence to support inheritance/influence of the basement and are described in this report. Few structures displayed reactivation evidence, whereas basement influence could be observed throughout the area considering the criteria necessary to infer it i.e. stereonet analysis data showing how the basement faults/fractures displays similar orientation through different rocks of different age creating the basins architecture. Reactivation evidence is more complex to achieve, given the necessity to access the

subsurface faults and its behaviour (Holdsworth, Butler et al. 1997). More time and resources would be necessary to uncover reactivation evidence for the onshore continental margin, this would be also vital to understand intraplate seismic activity in the area and beyond. The difference between inheritance (influence) and reactivation terms are discussed more in depth in Chapter 3.5 Section 3.5.1.

Declaration

I confirm that no part of the material presented in this thesis has previously been submitted by me or any other person for a degree in this or any other university. In all cases material from the work of others has been acknowledged.

Copyright

The copyright of this thesis rests with the author, Maria Antonia Alves de Matos. No quotation from it should be published without their prior written consent and information derived from it should be acknowledged.

Acknowledgments

Firstly I would like to thank my supervisor Prof. K.J.W. McCaffrey for his guidance and patience over the last months. Secondly Dr. Edward Dempsey for his support throughout the fieldwork and the time I have spent in the department, Dr. Julio Almeida from UERJ for his assistance in the fieldwork and all the conversations about the area, my driver and fellow geology student Aimee Guida, the best driver in the world. I also would like to say thank you for the Ustinov College Norman Richardson Postgraduate Research Fund and Santander Mobility Grant for their financial support to our fieldwork. To the Durham Earth Sciences department I would like to express how grateful I am for being part of. And lastly but the most important for me to my family that without their support I would have not be able to accomplish this work.

1 Introduction

Reactivation or the influence of basement faults on later tectonic events has been identified in the uplifted parts of passive margins from Upper Cretaceous to Paleogene in Norway, Greenland (Lundin and Dore 2002); Portugal, Morocco (Zitellini, Rovere et al. 2004) and Angola (Hudec and Jackson 2004), Scotland (Holdsworth, Stewart et al. 2001).

The SE Brazil passive margin displays a wide range of geological structures, fault-rock assemblages and exhumed high-grade metamorphic rocks. Within the Province of Mantiqueira, in the southern part of Brazil, a complex of mobile belts formed during the Brasiliano Orogeny (Almeida, Hasui et al. 1981). Many papers have been published describing the geological development of the Brazilian southeast passive margin (Almeida, Hasui et al. 1981, Riccomini 1989, Almeida and Carneiro 1998), nevertheless the onshore area lacks studies of how the pre-existing structures influence on the continental architecture of the region and its seismicity. One of the reasons might be that it is classified as a passive margin, hence there have not been many studies and few seismic stations have been deployed in the region. These stations data were useful to help in the delimitation of the area of study of these project, the identified seismicity led to areas where pre-existing structures in the basement could have been reactivated, adding to the region's geological framework and its architecture in the present day.

The limited data available show that small magnitude seismic events in the area have been recorded and these are typical of intra-plate regions and according to Sykes (1978) such events concentrate mainly in pre-existing zones of weakness, areas created by the latest orogeny that predating the opening of oceans.

Riccomini, Peloggia et al. (1989) concluded that active tectonism in the Serra do Mar rift system (where part of our area of study is located) is still present at least as residual tectonism (the author has not explained what type of residual tectonism in his paper) - this residual tectonism would come from tectonic movements that acted in the area through the Holocene to late Pleistocene. They based this conclusion upon the compatibility of the stress field determined from focal mechanisms of induced seismic activity in his area of study with the regional present day stress system of the passive margin. Assumpção, Barbosa et al. (1997) however attributed the majority of these seismic events to the presence of a hydroelectric plant and reservoir on the Paraíba do Sul River causing induced seismicity. After investigation, the results of which were presented in the ICOLD (International Commission of Large Dam), only one seismic event at 3.0 M (in 1977) was attributed to the Paraíba do Sul reservoir with its water depth at 88m (Assumpção, Ribotta et al. 2008). Considering the seismicity recorded in the surroundings of this area, a more thorough investigation of these events (induced and natural) should be considered in order to determine the influence of the mesoscale structures in these localities.

The thermal history of the margin has been extensively studied with results indicating uplift episodes occurred in SE Brazil. Apatite fission track (AFT) analyses conducted by several authors were used to investigate the uplift of the area (Gallagher, Hawkesworth et al. 1994, Saenz, Hackspacher et al. 2003, Tello Saenz, Hadler Neto et al. 2005, Cogné, Gallagher et al. 2011, Karl, Glasmacher et al. 2013). The thermal history suggests a first reactivation of basement structures at approximately 120 Ma, correlating with the opening of the South Atlantic. Saenz, Hackspacher et al. (2003) based on the cooling history of the Serra do Mar and Serra da Mantiqueira suggested, based on a rapid cooling record, that rapid uplift during the Early Cretaceous, was caused by tectonic movements during the opening of the Atlantic, and a more linear cooling through the Paleogene until the Neogene, which the authors

attributed to erosion causing uplift by isostasy. Saenz, Hackspacher et al. (2003), also suggests another rapid uplift during the Neogene and tectonic activation during the Plio-Pleistocene. These authors suggest that these events correlate with some of the main Santos basin unconformities: The Upper Cretaceous, Palaeocene, Oligocene, and Neogene unconformities.

Hiruma, Riccomini et al. (2010), studied the denudation history of the Bocaina Plateau on the Serra do Mar. The authors focused on the influence of the Gondwana breakup tectonics on the erosion during that period, using apatite fission track analysis. Clastic sedimentation in the area was attributed to uplift of the Serra do Mar during the Late Campanian-Maastrichtian period. The thermochronology data analysed by the authors support a denudation history associated with tectonothermal events formed during different time periods that included the Cenozoic. In their paper, the authors suggested that the most recent cooling phase was associated with the origin and evolution of the continental rift and reactivation of the basement terrains. Hiruma, Riccomini et al. (2010) also suggested that the changes in the intraplate compression to extension occurred during the period when the Nazca plate subduction process was dominant; however a shift from extension to compression reflected the onset of Atlantic ridge push based on geomorphology studies. They suggested that the persistence of tectonic landforms of the *Altos Campos* landscape system, despite the action of the humid tropical processes, could be an indication of recent tectonic activity.

Cogné, Gallagher et al. (2011), used (U-Th)/He isotopic ratios and fission track data to analyse post-rift reactivation in the area constraining the Mesozoic and Cenozoic exhumation. In their samples, two cooling stages in the Late Cretaceous and the Neogene were found in the area of the Serra do Mar near Ilha Bela. They recorded a total of 2-3 km regional denudation, concluding that the onshore region has not been inert since the continental break-up, attributing this erosional process not just to climate change but also to tectonic processes.

The rapid cooling episode in the Neogene coincides with the reactivation of the CRSB (Continental Rift Southeast Brazil), this reactivation has been attributed to a regional right-lateral transpression (Cobbold, Meisling et al. 2001).

Another aspect that might be considered when addressing the influence of the basement pre-existing structures is the effect of fluid passing through these structures. The SE Brazil area has acted as a conduit for the passage of fluids/magmas and displays complex thermal history (Gallagher, Hawkesworth et al. 1994, Saenz, Hackspacher et al. 2003, Ribeiro, Hackspacher et al. 2005, Tello Saenz, Hadler Neto et al. 2005, Cogné, Gallagher et al. 2011, Siga Jr, Cury et al. 2011, Curvo, Tello S et al. 2013, Karl, Glasmacher et al. 2013).

This complex history could cause rheological changes and long-term weakening associated with faulting and shear zone processes (Holdsworth, Butler et al. 1997, Holdsworth, Stewart et al. 2001). Assumpcao, Schimmel et al. (2004), based on a study of the distribution of earthquake epicentres, proposed that a thinner lithosphere with a weaker upper mantle cover may concentrate stresses in the brittle upper crust. They concluded that this stress concentration in the upper crust is due to weakness of the upper mantle caused by a high geothermal gradient.

Salomon, Koehn et al. (2015) analysed the stress fields of the South Atlantic conjugate margins of SE/S Brazil and NW Namibia. According to these authors, the data were processed following the “stress inversion via simulation” method developed by (Sippel, Scheck-Wenderoth et al. 2009). These data showed agreement with paleostress studies in the area of SE Brazil by other authors (Ferrari 2001, Riccomini, Sant’Anna et al. 2004, Ribeiro, Hackspacher et al. 2005, Cogné, Cobbold et al. 2013). The results showed two major strike-slip trends, one reflecting a compressional SW-NE direction during the Cretaceous up to Late Eocene and a second trend reflecting E-W compression from Oligocene to present. The authors also suggested a minor strike-slip regime with N-S compressional element, with a

minor extensional trend showing distinctive extensional directions within the Paraná-Etendeka basalts and the Botucatu / Twyfelfontein sandstone. According to Salomon, Koehn et al. (2015), in SE/S Brazil, reactivation is either absent or of minor magnitude, due to the shear zones not being oriented favorably for renewed slip to take place, but it contrasts with the area between Rio de Janeiro and Sao Paulo state, where considerable reactivation has been observed as postulated by previous authors (Riccomini 1989, Saenz, Hackspacher et al. 2003, Cogné, Gallagher et al. 2011, Franco-Magalhaes, Cuglieri et al. (2013)). Taking into consideration that this area is farther south than my study area, it is interesting that the complexity they noted in the northern part of their study area (Ponta Grossa dyke swarm) is similar to that found in data recorded during the field work for this project, which will be discussed further in this dissertation.

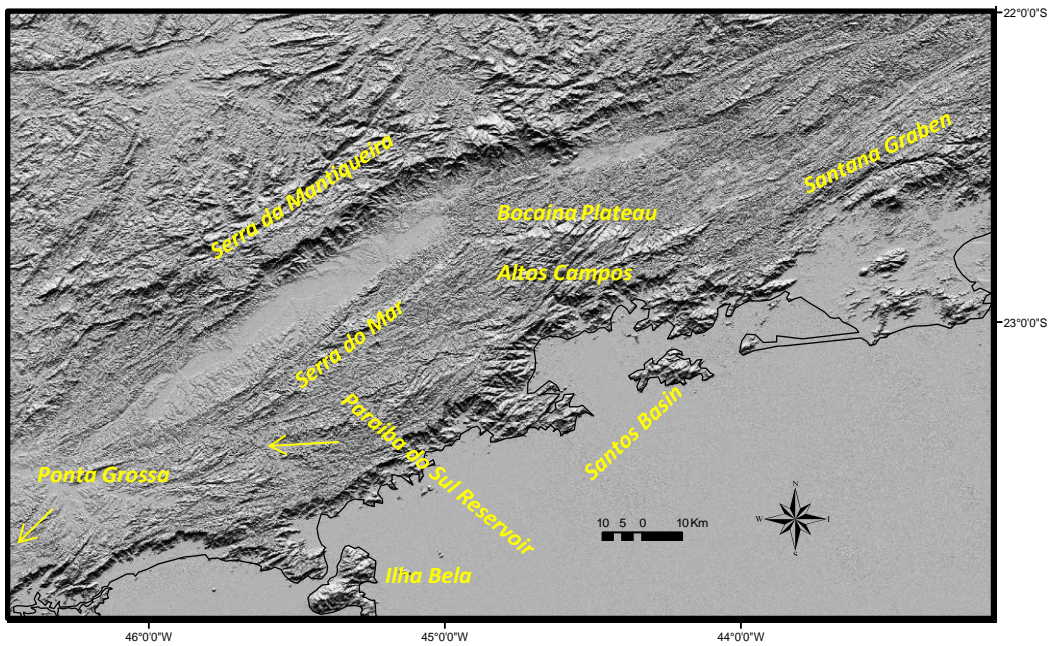
The Tertiary basins in the Continental Rift of Southeast Brazil are a reactivation response by the large structures in the Ribera Belt shear zones to the Cenozoic tectonic events, as postulated by some of the authors aforementioned. The influence of the basement pre-existing structures might still be influencing (by reactivation) the architecture that is forming at present day, but controls on the later structures are still not clear (either basement reactivation or formation of new smaller structures). Little relevant field work analysis has been executed to record small scale geological structures within the onshore passive margin of Brazil, possibly due to the difficulty of finding good outcrops in the heavily weathered region.

The aim of this study is to identify and characterize using remote sensing interpretation and fieldwork analysis evidence that might suggest that pre-existing structures have been reactivated by the observed brittle tectonics and how this influences the possible neotectonic/active tectonics of the continental margin of onshore SE Brazil. The project is an

exercise to explore methods to ascertain whether the characteristics of the passive margin of SE Brazil fit a model in which basement inheritance plays an important role.

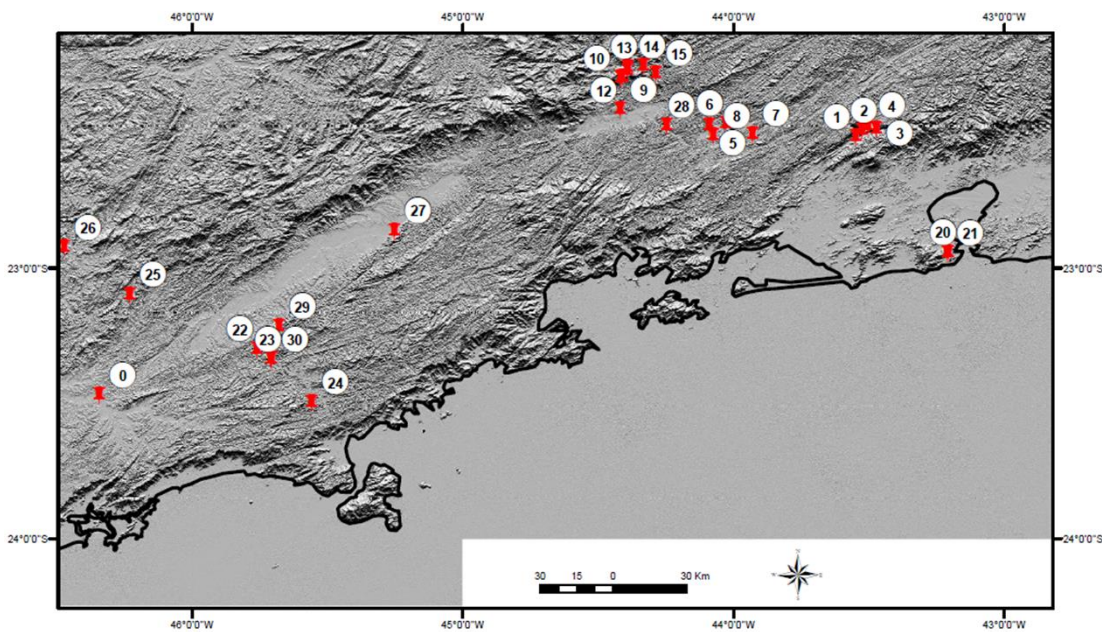
The first idea was to investigate and relocate earthquake focal mechanisms in the area, from literature and direct from sources, unfortunately, some obstacles made this a difficult task. The lack of seismic activity in the past has not compelled the authorities to invest in seismic stations of sufficient numbers to record with accuracy the seismic activities in the area, thus the use of seismic data was not possible in this project. The approach adopted was a combination of fieldwork and remote sensing to study the geological structures at different scales, mesoscales at outcrop scale and microscale through thin sections analysis. Field work took place over 15 days and samples of fault rocks were taken. The ArcGIS map created through remote sensing helped to understand the location and nature of structures that would be found in SE Brazil.

The structures mapped display characteristics of reactivated structures where basement inheritance/influence (these terms will be explained in the following chapter) could be suggested, however new structures have also been created. The microstructures within the samples may be able to provide information on the nature of the latest events, since they were taken from fault rocks created during reactivation processes in the area, reactivation in the area as according to (Cobbold, Meisling et al. 2001, Gontijo-Pascutti, Bezerra et al. (2010), Cogné, Gallagher et al. 2011, Franco-Magalhaes, Cuglieri et al. 2013). For examples, one of these reactivation events formed structures associated with the CRSB (Continental Rift of Southeast Brazil). Therefore reactivation of the basement for these basins is well known, whether reactivation continued during development of young structures is still an open question.



Map 1: The locations above are the ones mentioned specifically in the text above as the areas of study by previous works. The Santos Basin by Cobbold, Meisling et al. (2001) the area of Ilha Bela by Cogné, Gallagher et al. (2011), Alto Campos at the Bocaina Plateau has been studied by Hiruma, Riccomini et al. (2010), Santana Graben by Gontijo-Pascutti, Bezerra et al. (2010). The Ponta Grossa locality is not located within the area of study of this project, but has been explained in the text that Salomon, Koehn et al. (2015) points out the difference between the area in Ponta Grossa and the area between Rio de Janeiro and Sao Paulo where the occurrences of seismic activity is more pertinent in the later, which is at north of his area of study which happened to be confirmed by the geophysical data acquired through the IAG-USP/Instituto de Astronomia e Geofísica-Universidade de Sao Paulo (Fig. 6).

These localities related to the core of this present work given their dealing with tectonic events in the SE Brazil. Reactivation and tectonic uplifts have been suggested and postulated by the authors above mentioned.



Map 2 : Localities visited for this work

1.1 Study Area

The area also known as the Mantiqueira Province (Almeida, Hasui et al. 1981) includes the Serra do Mar and Serra da Mantiqueira, two of the most important geomorphotectonic features in the area (Fig. 1). These two mountain ranges formed the Paraíba do Sul River Valley, where the Tertiary Basins of Taubate, Resende, and Volta Redonda are located (Fig. 1). It lies between the two major cities in Brazil, Rio de Janeiro and Sao Paulo, and is also the location of the Paraíba do Sul reservoir in Sao Paulo state and Angra dos Reis nuclear plants I, II and III situated within Rio de Janeiro state and borders the offshore Santos Basin, that has recently become the largest hydrocarbon complex in the country (Fig. 1).

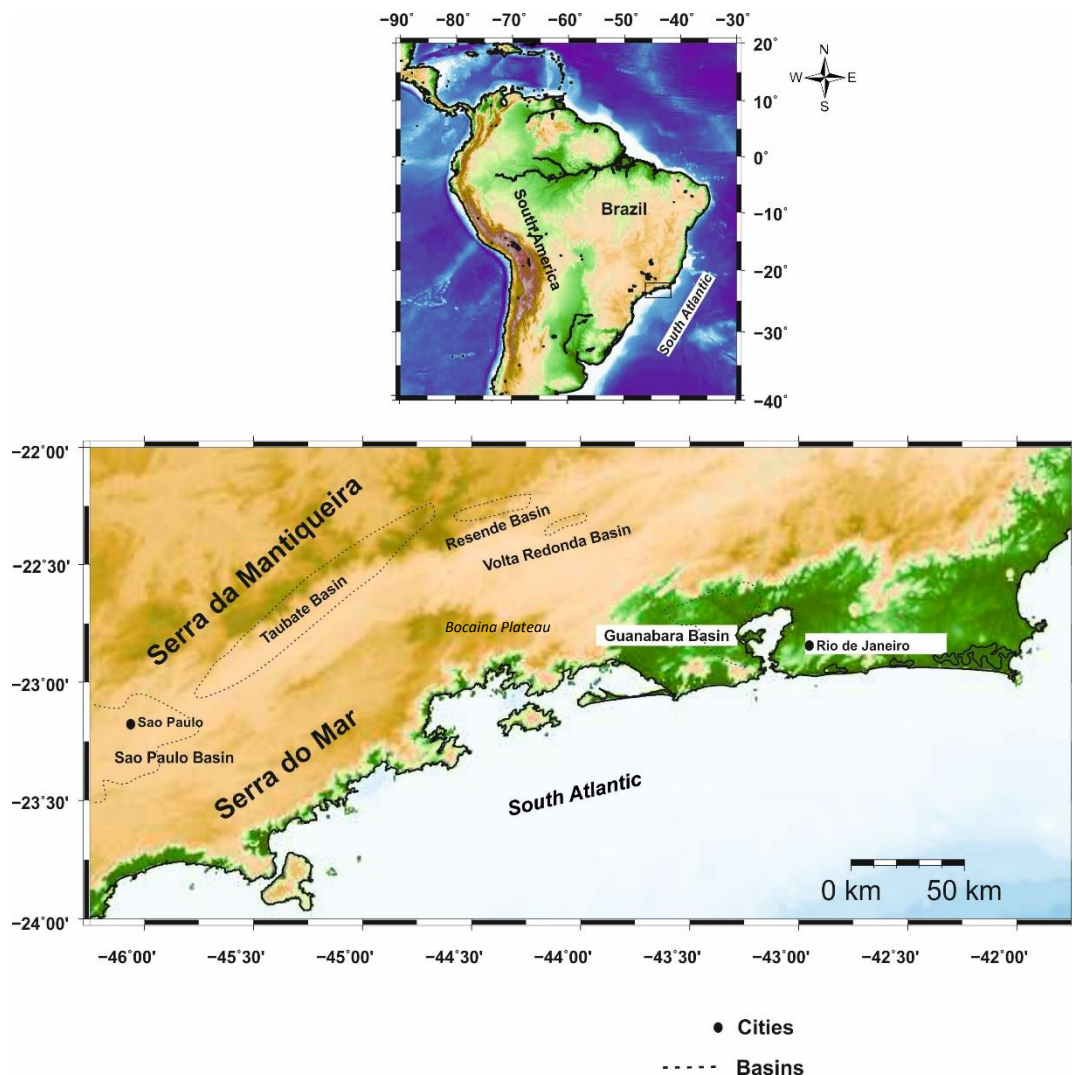


Figure 1: Area of study showing the main basins part of the Continental Rift of Southeast Brazil (CRSB). Volta Redonda Basin, Resende Basin, Taubaté and São Paulo Basin.

2 Regional Geology and Tectonic Framework

The Ribeira Belt is a Neoproterozoic orogenic complex formed during the collision of West Gondwana (Hackspacher, Juliani et al. 2001), its main lithologies comprise high grade gneisses displaying mylonitic fabrics with pegmatite veins (Fig. 2) formed by sinistral and dextral transcurrent tectonism (Riccomini 1989). According to Heilbron, Valeriano et al. (2008) the belt terranes and microplates were progressively accreted in a complex diachronous docking of Neoproterozoic magmatic arcs and older cratonic fragments through four main tectonic events between *c.* 640-510 Ma. The Occidental Terrane contains two distinct units; one made up of Palaeoproterozoic orthogneisses with amphibolites, migmatites and minor granulites and a second one made up of ortho-granulites also of Palaeoproterozoic age (Heilbron, Valeriano et al. 2008). The Embu and Paraiba do Sul Terranes are comprised of hornblende-bearing orthogneisses unit and a metasedimentary siliciclastic sequences with dolomitic marble and calc-silicate lenses (Heilbron, Valeriano et al. 2008).

Apatite fission track (AFT) analyses conducted by several authors investigated the uplift of the area (Gallagher, Hawkesworth et al. 1994, Saenz, Hackspacher et al. 2003, Tello Saenz, Hadler Neto et al. 2005, Cogné, Gallagher et al. 2011, Karl, Glasmacher et al. 2013). The thermal history suggests a first reactivation at approximately 120 Ma, correlating to the opening of the South Atlantic. Saenz, Hackspacher et al. (2003) based on the cooling history of the Serra do Mar and Serra da Mantiqueira suggested based on a rapid cooling record that rapid uplift during the Early Cretaceous, was caused by tectonic movements during the opening of the Atlantic, and a more linear cooling through the Paleogene until the Neogene, which the author attributes to erosion causing uplift by isostasy. Saenz, Hackspacher et al. (2003) also suggests another rapid uplift during the Neogene and tectonic activation during the Plio-Pleistocene. He suggests that these events correlate with some of the main Santos

basin unconformities: The Upper Cretaceous, Paleocene, Oligocene, and Neogene unconformities.

Karl, Glasmacher et al. (2013) divided the south of Brazil in 3 blocks, separated by old reactivated fractures zones and determined the thermal history of the blocks calling them Northern, Central and Southern blocks. The area of study in this project lies within the Northern block, for which Karl, Glasmacher et al. (2013) calculated an exhumation rate of 0.1mm/a initially then decreasing to 0.05mm/a for the last 20Ma. He suggests that the diversity in timing and rates of exhumation in that area were an indication of different sources of influence for the uplift.

During the formation of the CRSB (Continental Rift of Southeast Brazil) in the Late Cretaceous/Early Neogene, pre-existing shear zones were reactivated to form a series of Cenozoic basins (including the Taubate, Resende, and Volta Redonda basins) (Cogne, Cobbold et al. 2013).



Figure 2: Mylonitic fabric showing dextral sense of movement at the Santana Graben in the state of Rio de Janeiro

The Taubate, Resende and Volta Redonda basins are elongated features which display similar orientation to the Ribeira belt shear zones trends which can be observed in the DEM map in Figure 8 due to its strong ductile foliation. A dextral sense of kinematics can be seen from the

lithographic map of the area shown in Figure 3, as the major units form right stepping features. They are orientated NE-SW parallel with the Serra do Mar.

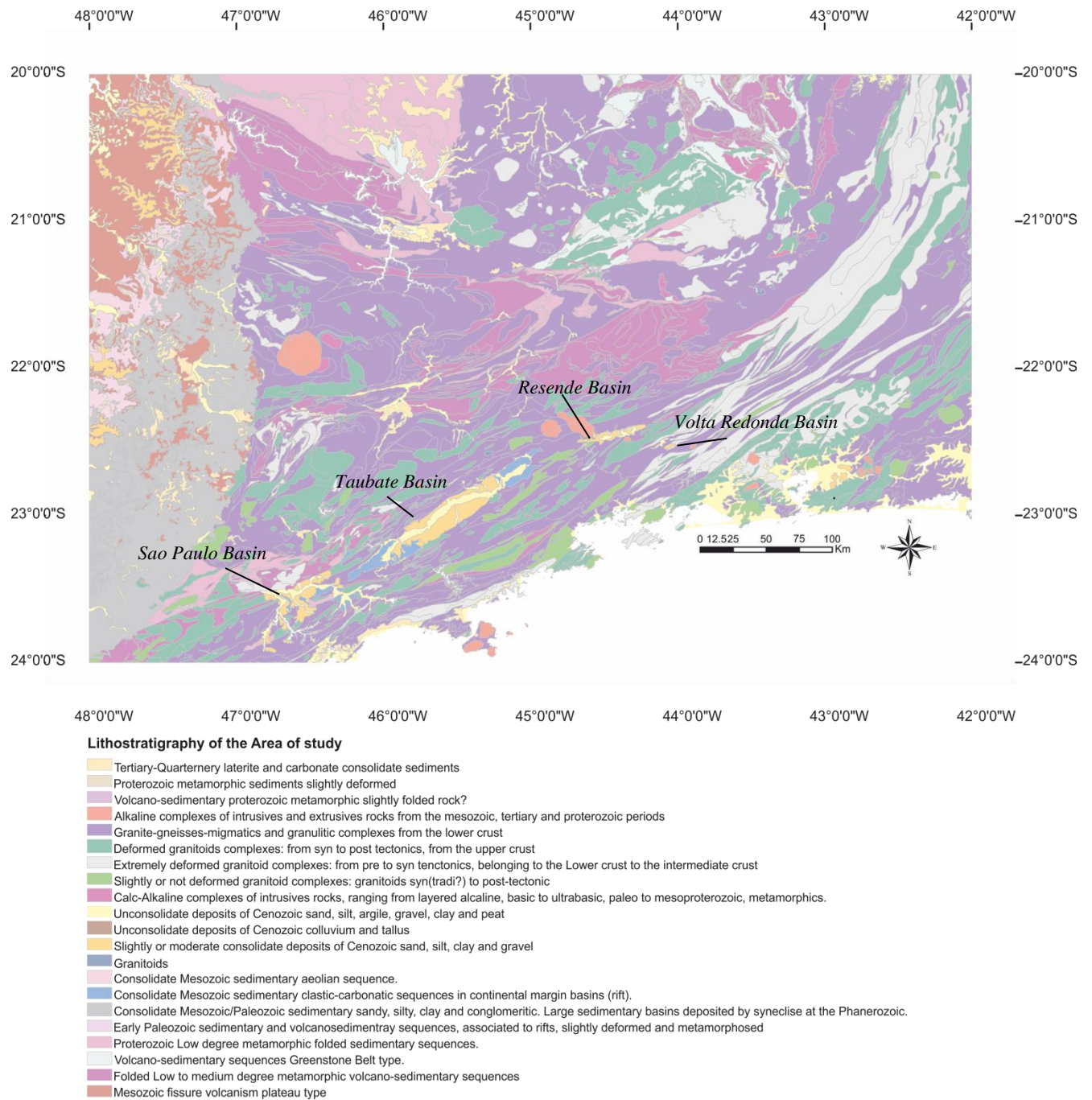


Figure 3: Fig 3a: Lithology by CPRM (Companhia de Pesquisa de Recursos Minerais) Brazilian Geological Service, 2007 <http://geobank.cprm.gov.br/>. In the next page figure 3b is diagram summarising the tectono-stratigraphy evolution of each studied basins based upon literature. Figure 3c in the following page is the diagram in figure b with added the findings of this project.

| TIME (ma) | Geochronology | | Volta Redonda Basin | TE according to Negrão, 2015 based upon Sanson (2006). | Resende Basin | TE according to Albuquerque (2004) | Taubaté Basin | TE according to Cogné, Cobbold et al. (2013) | São Paulo Basin | TE according to Riccomini (2004) | | |
|--------------------------|---------------|-------------|-------------------------|--------------------------------------------------------|----------------------------|------------------------------------|------------------|---------------------------------------------------|-----------------------|----------------------------------|------------------------|-------------------|
| | Period | Epoch | | | | | | | | | | |
| Lithostratigraphy | | | | | | | | | | | | |
| 10 | Quaternary | Holocenic | Alluvium | Extension NW-SE | Alluvium | Extension NW-SE | Alluvium | E-W Compression (based upon the world stress map) | Alluvium | E-W Compression | | |
| | | Pleistocene | | | Transcurrent Dextral E-W | | | | | Extension | | |
| | Tertiary | Neogene | Pliocene | | | | | | | | Transcurrent Dextral | |
| | | | Miocene | | Transcurrent Dextral E-W | Floriana Formation | | Pindamonhangaba Formation | Transpressional E-W | | Transcurrent sinistral | |
| | | | Oligocene | | Transcurrent sinistral E-W | | | São Paulo Formation | Quiescence Period | Itaquaquecetuba Formation | São Paulo Formation | Extension NNW-SSE |
| | | | | Pliocene | | | | | | | | |
| | | Paleogene | Eocene | | Basalt Casa de Pedra | Extension NW-SE | | Resende Formation | Trans-tensional NE-SW | Resende Formation | | |
| | | | | | Resende Formation | | | | | | | |
| | | | Paleocene | | Quatis Riverside | | Quatis Riverside | | | | | |
| | | | | | | | | | | | | |
| CRETACEOUS | | | Alkaline Volcanic rocks | | | | | | | | | |
| PROTEROZOIC | | | Basement | | | | | | | | | |

Figure 3b

TE - Tectonic Events

| TIME (ma) | Geochronology | | Volta Redonda Basin | TE according to Negrão, 2015 based upon Sanson (2006). | Resende Basin | TE according to Albuquerque (2004) | Taubaté Basin | TE according to Cogné, Cobbold et al. (2013) | São Paulo Basin | TE according to Riccomini (2004) | This work (Based upon literature and fieldwork) No tectonic event have been recorded |
|--------------------------|---------------|-------------|-------------------------|--------------------------------------------------------|--------------------|------------------------------------|---------------------------|---------------------------------------------------|------------------------|----------------------------------|--------------------------------------------------------------------------------------|
| | Period | Epoch | | | | | | | | | |
| Lithostratigraphy | | | | | | | | | | | |
| 10 | Quaternary | Holocenic | Alluvium | Extension NW-SE | Alluvium | Extension NW-SE | Alluvium | E-W Compression (based upon the world stress map) | Alluvium | E-W Compression | Alluvium |
| | | Pleistocene | | | | | | | | | |
| | Tertiary | Neogene | Pliocene | Transcurrent Dextral E-W | Floriana Formation | Transcurrent sinistral E-W | Pindamonhangaba Formation | Transpressional E-W | Transcurrent sinistral | Pindamonhangaba Formation | |
| | | | Miocene | | | | | | | | Transcurrent sinistral E-W |
| | | Oligocene | Pinheiral Formation | Tremembé Formation | Resende Formation | Resende Formation | | | | | |
| | | Paleogene | | | | | Eocene | Basalt Casa de Pedra | Extension NW-SE | Resende Formation | Trans-tensional NE-SW |
| | Paleocene | | Quatis Riverside | Quatis Riverside | Quatis Riverside | | | | | | |
| | 20 | | | | | | | | | | |
| | 30 | | | | | | | | | | |
| | 40 | | | | | | | | | | |
| 50 | | | | | | | | | | | |
| 60 | | | | | | | | | | | |
| CRETACEOUS | | | Alkaline Volcanic rocks | | | | | | | | |
| PROTEROZOIC | | | Basement | | | | | | | | |
| | | | Guanabara Graben | | | | | | | | |

Figure 3c: Summary of previous authors and the lithostratigraphy examined in this body of work

TE – Tectonic Events

3 Methodology

The methodology used in this project was divided into three different scales for the area: Regional scale, Local scale and micro-scales. At regional scale, structures were mapped using remote sensing. At local-scale exposures were visited throughout the basins in the study area (Fig. 1). Samples were collected for micro-scale analysis. The kinematics and geometry of brittle faults that were collected during the fieldwork are used to investigate what controls fractures at a local scale and the relationship with basement structures.

3.1 Remote Sensing

The first method used was to pick lineaments on SRTM 90m and later 30m resolution satellite images. The satellite images were downloaded respectively from the SRTM website (<http://srtm.csi.cgiar.org/SELECTION/inputCoord.asp>) and TOPODATA website (<http://www.webmapit.com.br/inpe/topodata/>). Hillshade images were created in ArcGIS software and were used to help visualize the structures under different angles of light (Fig. 4). Unfortunately the TOPODATA at 30m resolution did not produce a good hillshade illumination (Appendix 1; Fig. 57) Not sure if this was an specific technical issue with the department ArcGIS edition, but this situation led to the choice to work with the 90m resolution for hillshade plates. This of course did not produce as much clear lineaments as it could have with the 30m DEM. To compensate this, a decision to work with variable scale was taken between 1:250,000 to 1:100,000. This would facilitate to pick lineaments too small to be correctly traced under a fixed scale. To determine the “tips” of these segments, the trace

of each of these lineaments were stop whenever the ending of the lineaments was encountered an obstacle; this would assess the length of the segment, not the age relationship of the fault, the same approach was taken to determine the start of the segments. ArcGIS would not estimate the length of these lineaments because it would only give the length of each segment created to add up to a single lineament (several segments to create one long feature). To address this problem, an add-on Polar Plots for ArcGIS from Jenness Enterprises (http://www.jennessent.com/arcgis/polar_plots.htm) was installed to ArcGIS to make it possible to calculate the length of each complete lineament and azimuth. Each lineament was given different colours to help visualise and group their orientations into different sets using ArcGIS (Appendix 2 Table 4). These data were afterwards input into GEOrient™ software creating rose diagrams for their attributes. The result helped to establish a model for the trend of these linear structures and to compare with the data collected in the field, establishing the regional trends to the brittle and ductile structures.

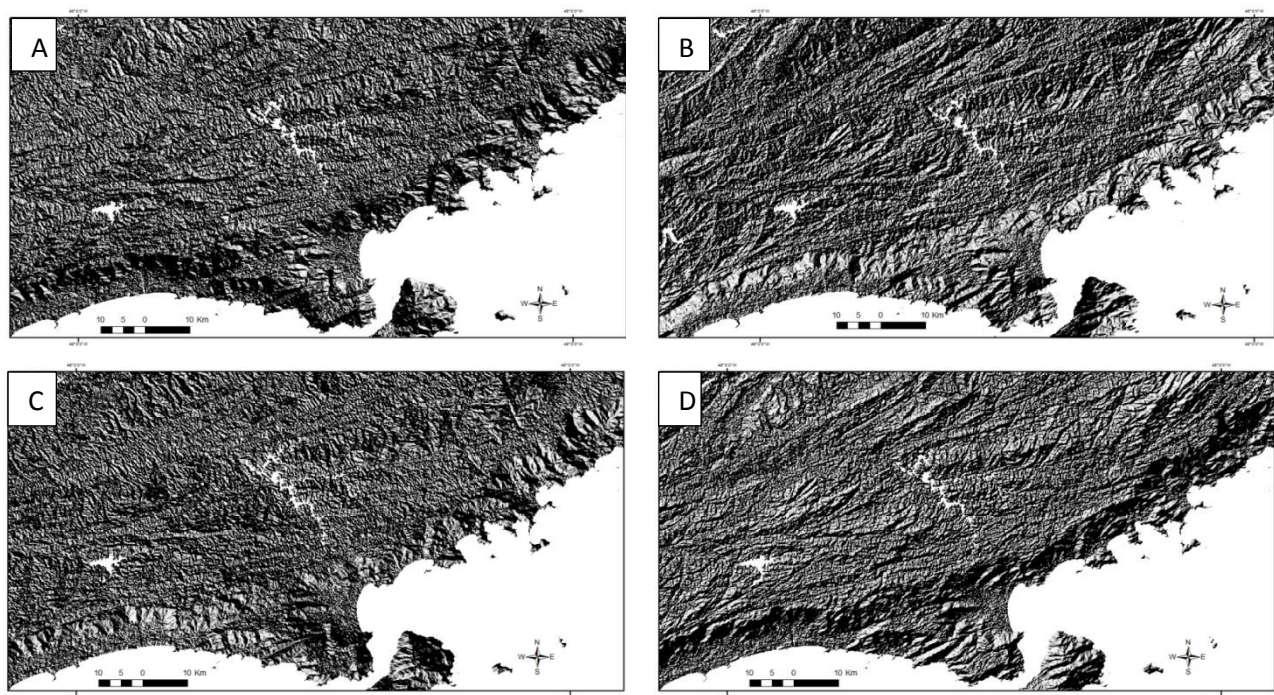
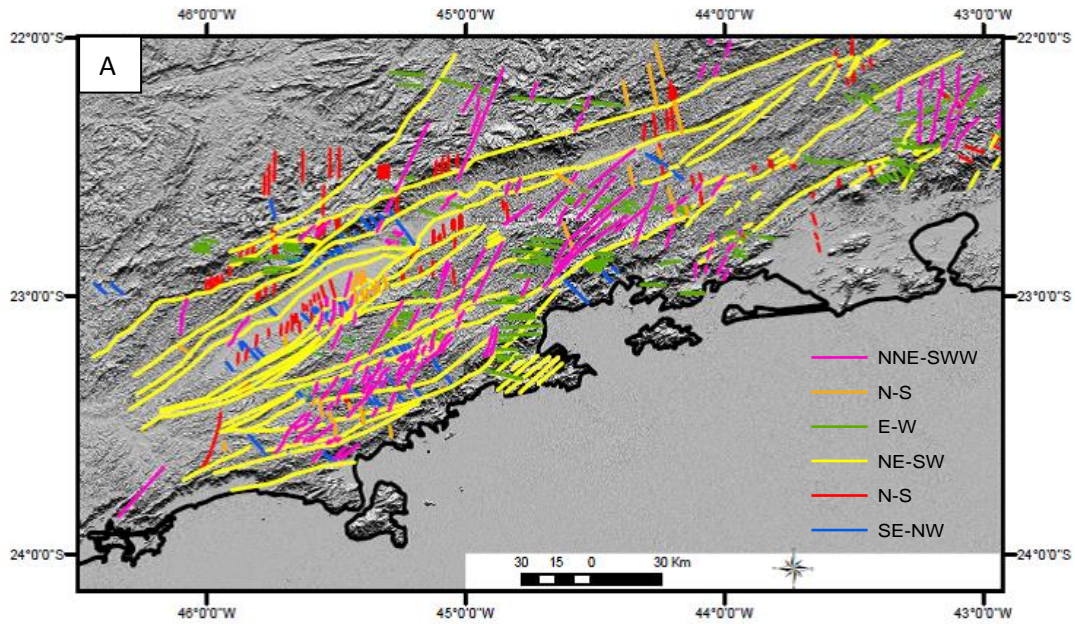
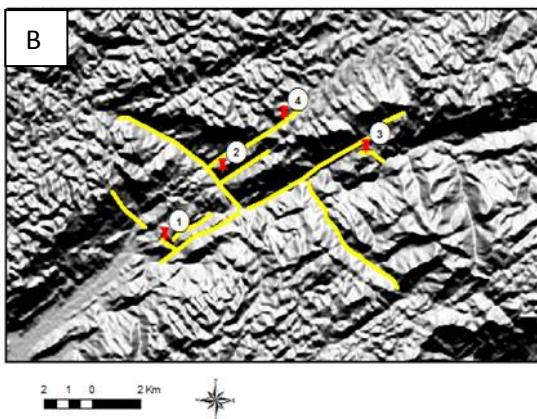


Figure 4: From clockwise, hillshade illumination from angles 45° , 125° , 315° and 225° . Using ArcGIS 10.2



*Figure 5: In Fig.a above the lines were then separated into colours to help visualize the different orientation of each group. This method helped to give the area regional, large scale structural features. **Figure 5b (anti-clockwise):** Close up of lineaments of locations 1,2,3, and 4. Changing the scale during the lineaments pick-ups helped to judge the faults tips. Here fault tips were determined by the intersection of the lines or following the shadows of the structures, assuming that the structure would terminate where its shadow terminates*



Though this method is a great resource to map linear structures it does not allow to distinct the type structures i.e. valleys and ridges and can lead to a number of uncertainties. For this particular case, the climate conditions also has to be accountable for; due to rapid weathering process

in tropical regions and its frequent rainfalls and flash floods and many of its features (i.e. kinematic evidence) are eroded. Another aspect adding to its uncertainties is that when assessing these features in the field the structures were not as available as in the topographic imagery suggests, much of these features are covered with the vegetation making it difficult access. The numbers in the figure 5b are locations visited in the area and concur with the locations in map 2.

3.2 Geophysical data

As previously stated, the lack of geophysical data available for the onshore SE Brazil made it difficult to correlate the seismic events with geological structures in the surface. Some data were obtained from the IAG (Institute of Geophysics and Astronomy of Sao Paulo). The Figure 6 shows the area with most seismicity recorded in the area of study.

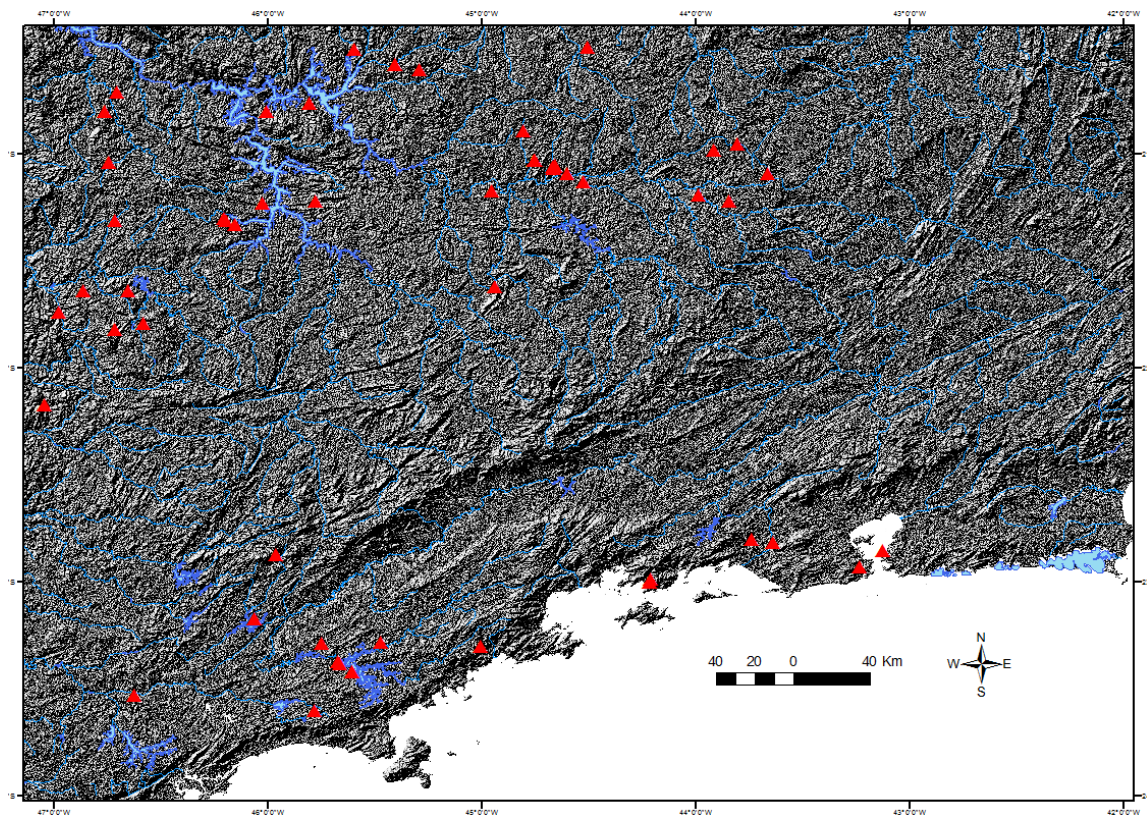


Figure 6 : The DEM image above (90m) is displaying the seismic events recorded in the SE Brazil until 2013 (data from IAG-USP/Instituto de Astronomia e Geofisica-Universidade de Sao Paulo). The red triangles are the events recorded. In blue the drainage system by CPRM (Companhia de Pesquisa de Recursos Minerais) Brazilian Geological Service, 2007. <http://geobank.cprm.gov.br/>

3.4 Fieldwork

Fieldwork data were collected during a 3 week period in the study area during which 22 locations were visited. The quality of the outcrops ranged between excellent and very poor. The best outcrops visited were found in the quarries, due to the constant and deep excavation. The tropical climate of the region changes very quickly the conditions of the outcrops through weathering, and for that reason the lineation in particular found within the rocks were extremely faint to non-existent. The fieldwork was mainly concentrated on the structural geology of the area, so detailed analysis of its stratigraphic column was not considered for the scope of this research.

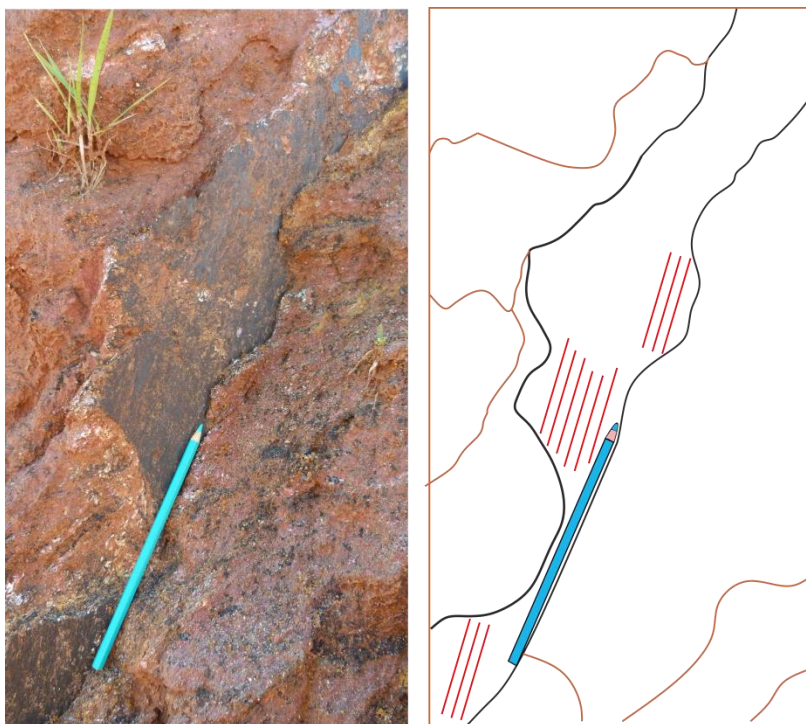


Figure 7: lineation taken from locality 6 at Volta Redonda basin

The area was accessed by car due to the large distances between quarries and road-cuts with fresh outcrops. The field work took place in two phases, in Rio de Janeiro, measurements of the faults and fractures were taken with a stratum compass that measured the dip and dip direction of the fractures and subsequently the values were converted into strike and dip using Geolcalc™. Later a Silva™ compass was used in the São Paulo area. The magnetic deviation for SE Brazil was calculated 22° W.

The measurements taken were strike azimuth, dip and pitch (rake) of each fracture in the outcrop. This information was inserted in a spreadsheet that can be found in Appendix 3. The process of stress inversion was applied where possible using MyFault™ software (version 1.05) and GEORient™ 9.5.1. was used to create stereographic projections of the data acquired. Oriented hand-specimens were also collected from the fault rocks in order to access the micro-scale features.

The figure below shows the map of the area visited with the outcrops locations marked, locations 16,17,18 and 19 were removed from the study due as they were not relevant to this specific research. The location at the Sao Paulo basin is called 0 for logistic purposes. All these locations will be described and analysed in the following section.

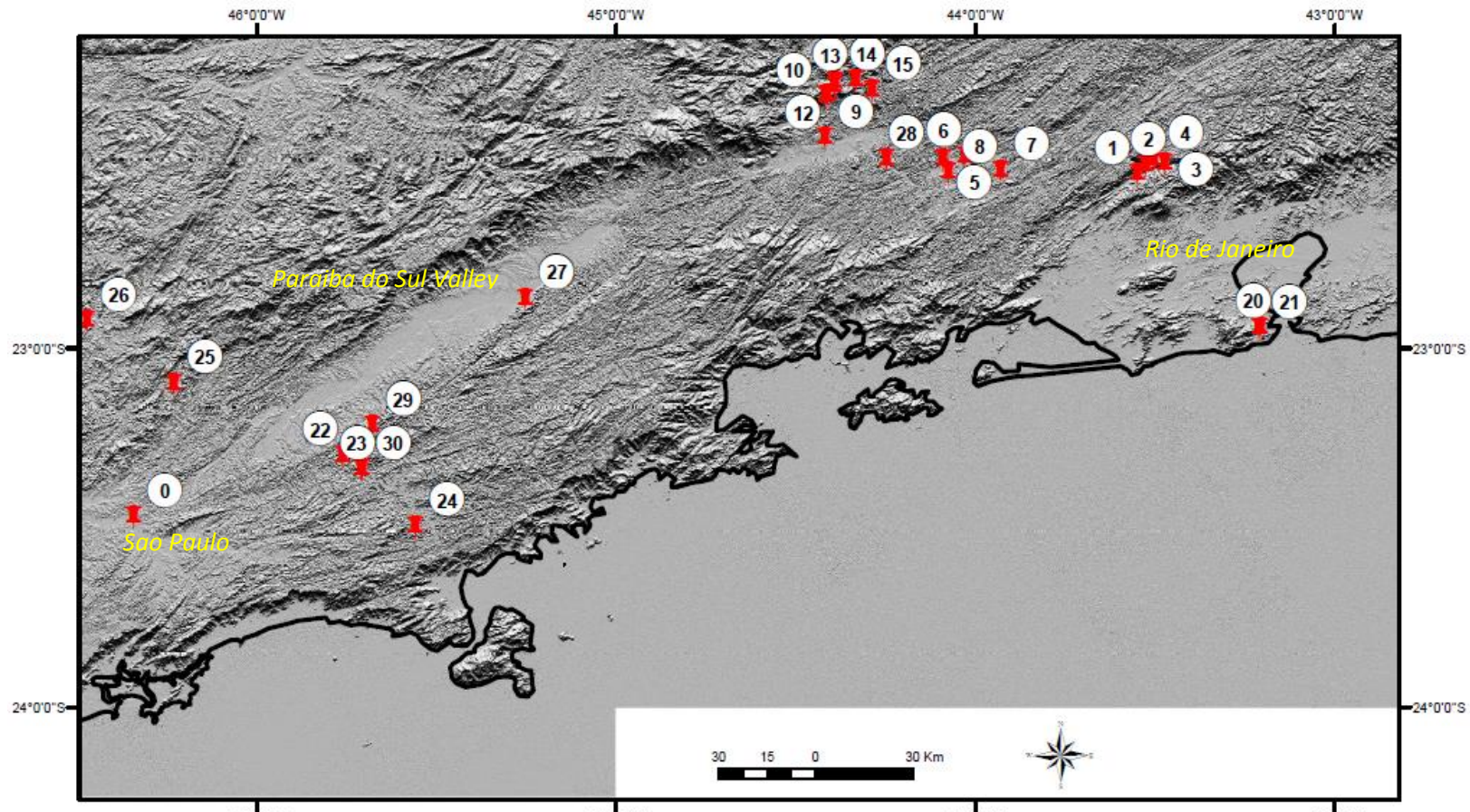


Figure 8: The locations are concentrated on the four basins before mentioned, Volta Redonda, Resende, Taubaté and São Paulo; therefore the locations above represent the outcrops visited within these main areas, which has been described in Chapter 2. Some of these locations have been not considered to the aim of this project and therefore not added to the analyses.

3.5 Methodology Approach in the Field

The model produced via DEM in ArcGIS suggests a strike-slip regime existed in the region, comprising of long faults with branches with an anastomosing pattern and smaller fractures at an orthogonal angle to the former. The next step was to find structures in the field that could demonstrate typical strike slip/wrench fault system and areas of possible reactivation.

3.5.1 Reactivation vs Reworking vs Inheritance

Reactivation and Reworking are two related process according to Holdsworth et al (1997, 2001) responsible for the rejuvenation of the lithosphere and pre-existing crust. Reactivation involves geologically distinct displacement events (intervals >1 Ma) and is normally responsible for the rejuvenation of discrete structures whereas reworking means that the same crustal/lithospheric-scale volume goes under repeated metamorphism, deformation and magmatism.

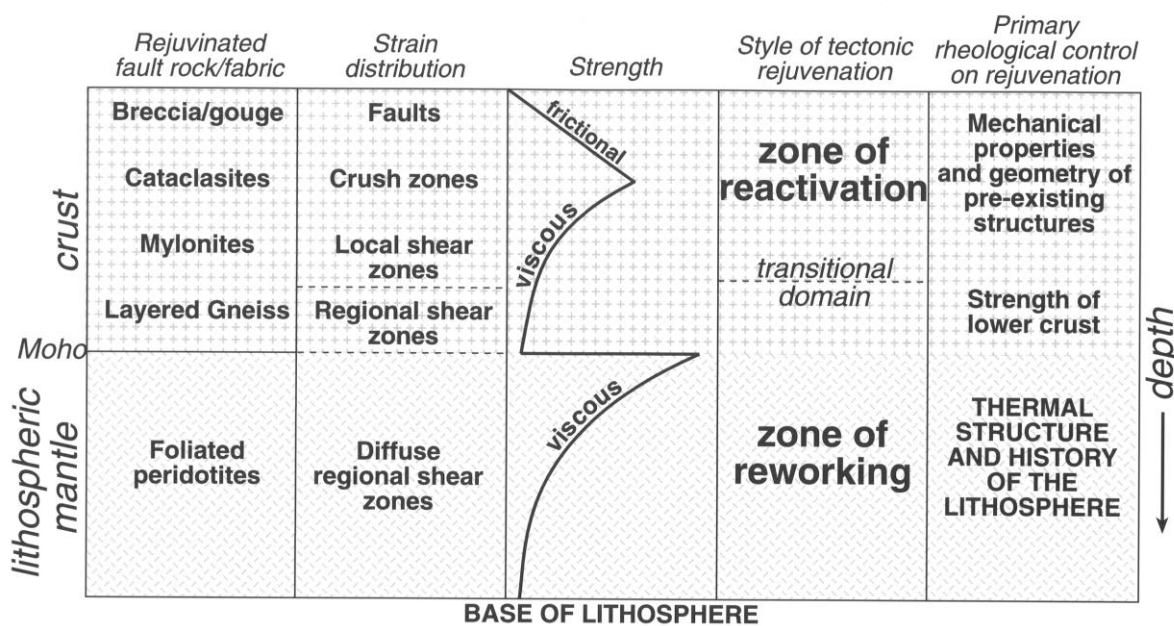


Figure 9: Diagram taken from Holdsworth, Hand et al. (2001) demonstrating zones of reactivation and reworking and its controlling parameters.

Inheritance is not a term commonly defined in the literature, according to Misra and Mukherjee (2015), Tectonic Inheritance deals with the influence of pre-existing or pre-rift elements on the

geometry, genesis and propagation of rift-related faults and strongly controls the architecture of continental rifts and passive margins. According to the authors, the parameters controlling the architecture of rifts and passive margins are strength, crustal and lithospheric thicknesses, thermal state and strain rate which correspond to the same parameters for reactivation according to Holdsworth, Hand et al. (2001) (Fig 9).

This dissertation deals primarily with inheritance; assessing the influence of the pre-existing faults geometries of the SE Brazil present day architecture. The criteria Figure 10 were used to help in the assessment of the influence of the pre-existing structures in the architecture of the Tertiary basins in this work.

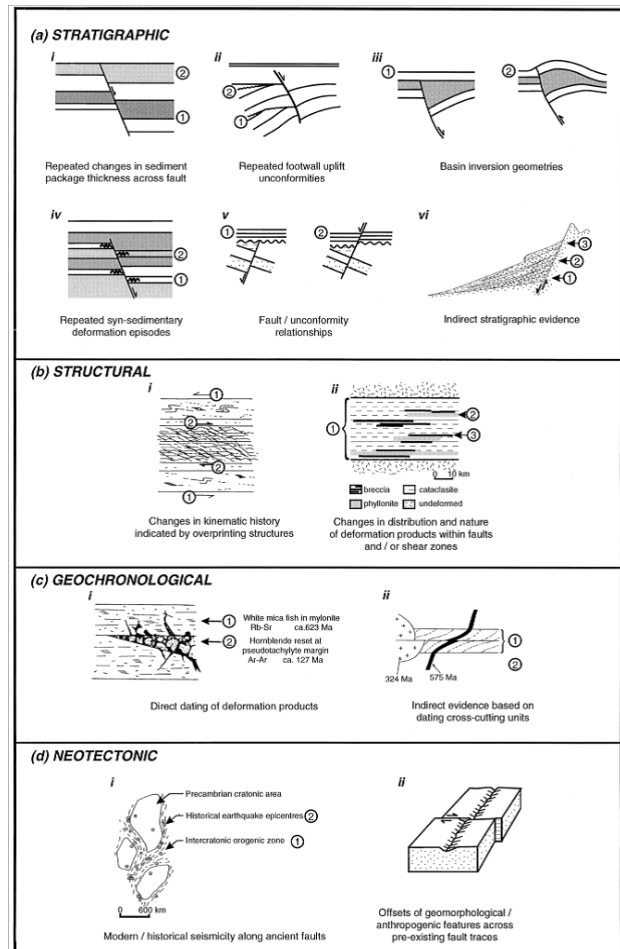


Figure 10: Diagram taken from Holdsworth, Butler et al. (1997)

3.5.2 Structures in a strike slip/wrench regime

When working with the DEM to build the remote sensing map for the area, it was noted a typical strike-slip geometry, displaying possible riedel-shears that are subsidiary to the long, ductile faults from the Ribeira Belt.

These geometric relationships display typical geometries for transtensional/transpressional fault zones, as suggested by the diagram in figure 11. When in the field this model were used to verify these faults relationships, key outcrops features were noted, such as flowers structures, angle of the branch fractures in relationship to the main faults, offset of faults indicators such crosscut veins and bed boundaries to determine sense of direction.

Strike-slip form a number of geometries at different scale as the diagrams below demonstrate (Fig. 11)

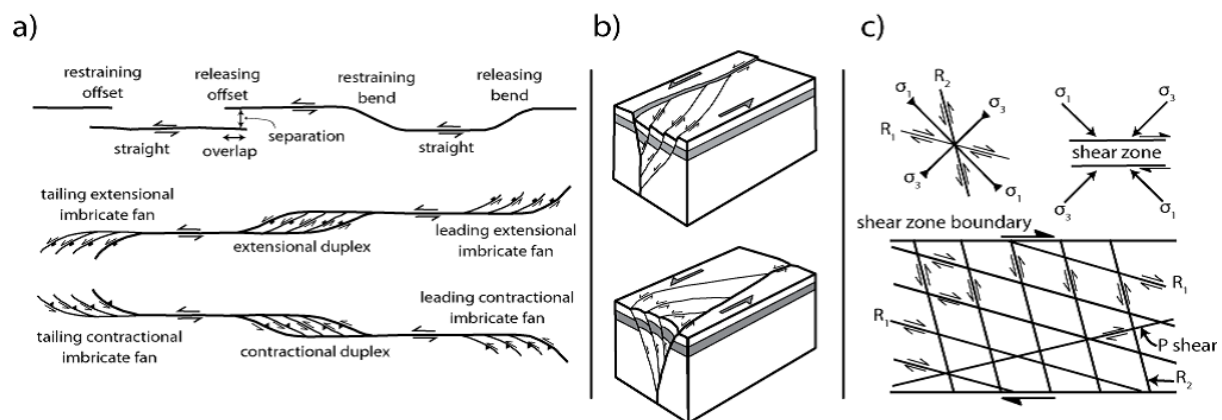


Figure 11: Structures expected in strike slip settings: a) Restraining and releasing bends form where the fault changes direction. b) “Flower structures” formed as a result of oblique extension (top), or compression (bottom), where smaller structures link to larger faults (Woodcock and Fischer, 1986). c) Riedel shears form complex geometries in response to strike-slip deformation and occur at different scale (Tchavchenko 1970 ref.). Modified from McClay (1991). (Ashby 2013)

The riedel shear diagram can be used to infer regional strain ellipse associated with a wrench/strike slip fault system and it was crucial to the work in the field helping to determine kinematics of the structures, i.e relative sense of movement of the structure. The Riedel shear R_1 is the synthetic and R_2 is the antithetic system and very often displacements are minor (McClay 1991).

R_1 is the first subsidiary fracture to occur; these fractures develop at an acute angle, typically 10-20° clockwise for a dextral main fault, anticlockwise for a sinistral strike-slip fault. Their acute angle with the main fault plane points in the direction of the relative sense of movement on the main fault. This angle is equal to $\phi/2$, where ϕ is the theoretical material internal friction angle. R_2 shears, the antithetic faults (i.e. with a sense of displacement opposite to the bulk movement) oriented at a high angle (approximately 75°) clockwise to a dextral, anticlockwise to a sinistral main fault plane).

3.5.3 Rheology

Rock strength is one of the primary factors to control the process above mentioned (Holdsworth, Stewart et al. 2001). The rock composition in SE Brazil indicates retrograde metamorphism where phyllosilicates are widely distributed replacing feldspar grains, the presence of hydrous minerals such as amphibolites indicates the weakening of the rock related to the retrograde mineral growth or alteration by hydrous fluids, this could be a case of weakening of the mid-crust suggesting the capability of the area to undergo reactivation (Imber, Holdsworth et al. 1997). According to Vauchez, Tommasi et al. (1998) mechanical anisotropy in the lithosphere underlies the classical concept of structural inheritance that was frequently invoked to explain the systematic reactivation of pre-existing tectonic structures, but possibly only when applied to local tectonic structures. Foliations are 'pervasive' fabrics while widely spaced isolated zones of weakness are defined as 'discrete' zones, the sediments in the area show strong foliation being favourable to faulting occur following the anisotropy of the rocks.

3.5.4 Faults, Joints and veins

Faults, joints and veins were used to determine the age relationship, sense of direction amongst other correlation between these structures and the tectonic events in the area. The fractures patterns most commonly in the area were conjugate joints and abutting structures (Fig.12b). Cross-cutting relationships were also observed (Fig.14); mainly using veins displacement, slickenlines were recorded where possible. The pictures below are examples found in the field, figure 12b is located at Location 13, figure 13 is nearby Location 24 and figure 14 is part of the structures measured in Location 0. They will be mentioned in their respective locations interpretation section as they are part of the data analysed giving important evidence to the structural geological history in the area.

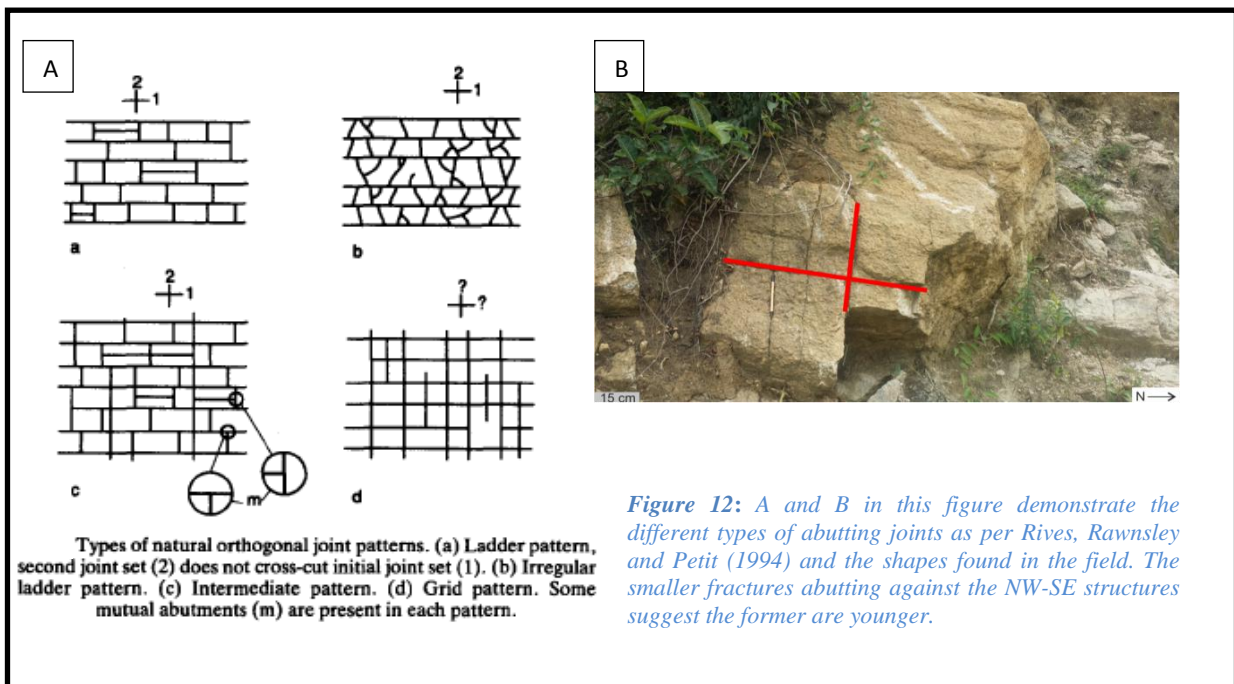


Figure 13: Example of a reverse fault in the Tamoios Highway location. The S fabric indicating the sense of movement of the fault.



Figure 14: Example of cross-cutting relationship in the field, with E-W fault cross-cutting the pegmatite veins infill in the basement rock.

4 Structural Geology

4.1 The Rio Santana Graben

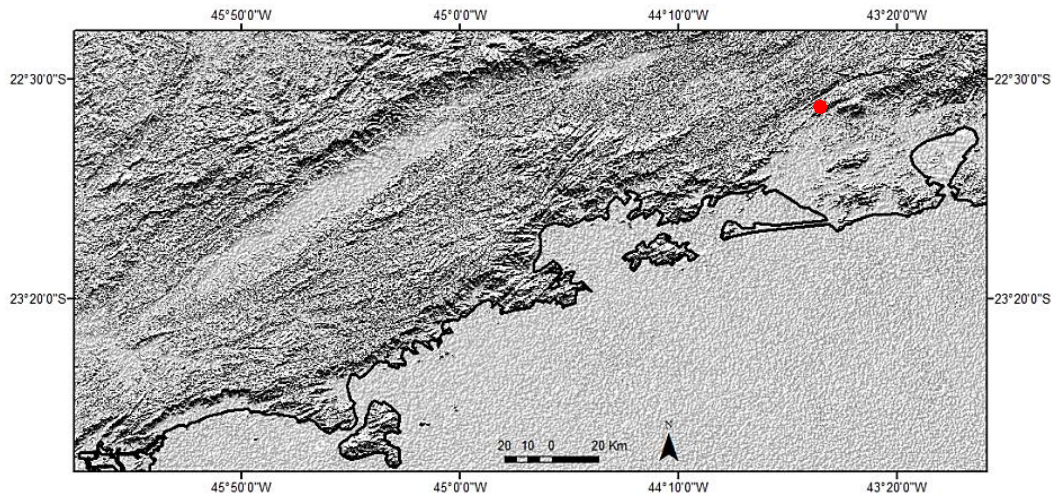


Figure 15 : The Rio Santana graben is at the west of the city of Rio de Janeiro ~25km. The first 2 locations of the project were recorded there.

The Rio Santana graben is an NE elongated 15 km long and 2 km wide Cretaceous sedimentary-filled trough whose basement displays a dextral sense of movement. It is located near the mylonitic shear zone of *Arcadia Areal* to the northwest of the city of Rio de Janeiro (Fig. 15) and its faults were reactivated during two major events 1) the Cretaceous and 2) the Cenozoic (Gontijo-Pascutti, Bezerra et al. 2010). According to Gontijo-Pascutti, Bezerra et al. (2010) it has two depocentres which are separated by a relay ramp (Fig. 16b).

4.1.1 Location 1 (UTM: 23K 649344 7507989)

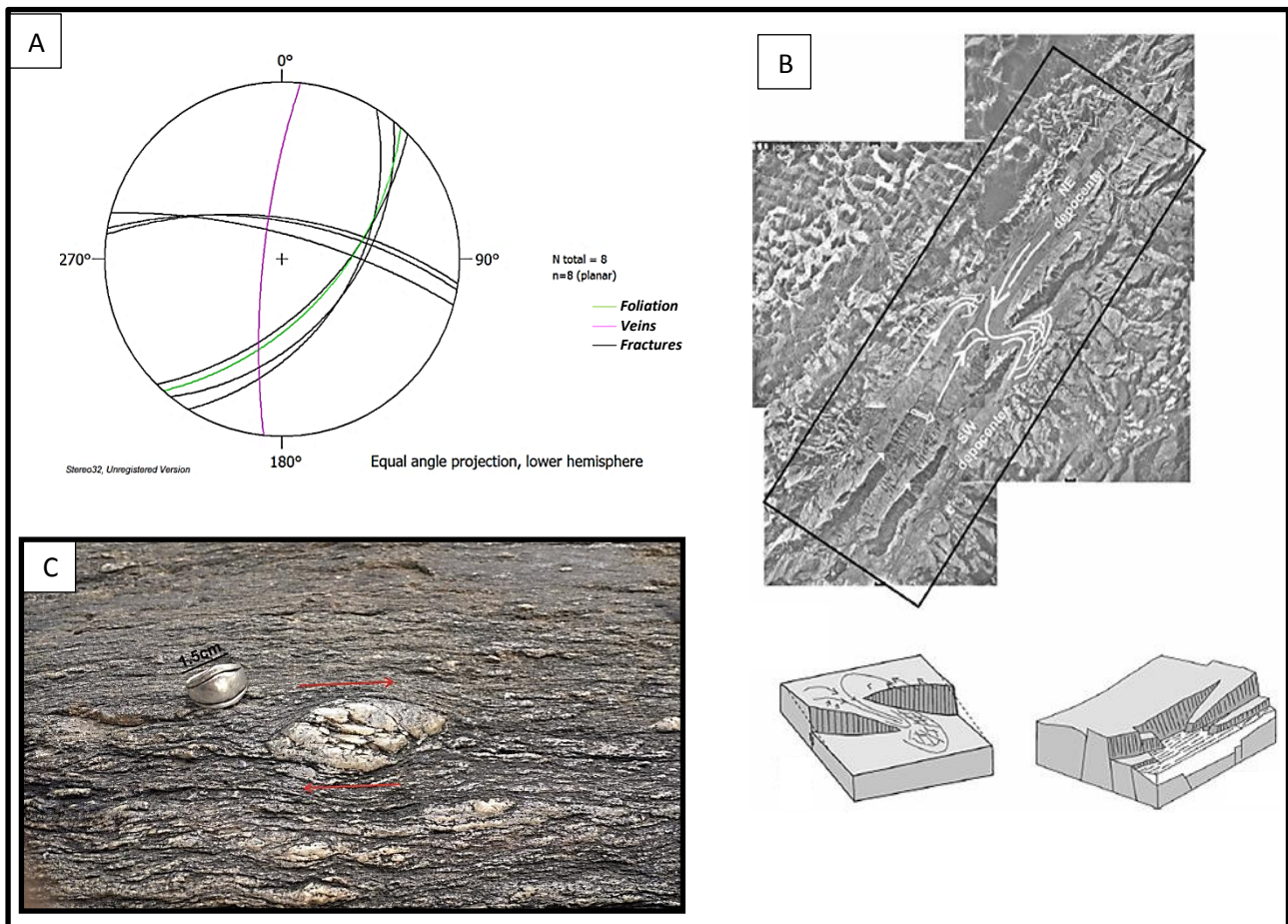


Figure 16: Figure 16a is the stereographic representation of the data from this outcrop. Fig. 16b Diagram of the relay ramp feature in the area (Gontijo-Pascutti, Bezerra et al. 2010). Fig.16c is a sample of the foliation in the rock, showing dextral sense of movement and micro boudinage within the matrix.

Outcrop description:

The outcrop at location 1 in the Santana graben is at a small waterfall in a stream running towards the Rio Santana. The main rock is a paragneiss showing mylonitic texture with porphyroclasts of feldspar measuring up to 6cm. The fractures trend E-W dipping north within the waterfall showed a sinistral sense of movement.

Outcrop-scale structures:

The basement foliation is a steeply-dipping fabric that has a dextral sense of movement (Fig. 16c). Folds of the fabric and stretching lineation were observed as having been cut through by fractures. The folds represent the ductile nature of the outcrop prior to the fractures. NE-SW trending fractures formed parallel to the foliation, and a variation in elevation that coincides with this trend could represent a throw of 7m. No crosscutting relationship has been observed between the E-W and NE-SW structures, but an age relationship could be established between the NE-SW and the quartz vein which has a N-S orientation and pre-date the NE-SW set.

Interpretation:

The fractures parallel to the basement fabric illustrate the influence of the orientation of the fabric on the brittle NE-SW fractures. The vertical displacement of 7m within the Neoproterozoic rock could represent the Cenozoic reactivation attributed for the CRSB (Continental Rift of Southeastern Brazil) by Riccomini (1989). The N-S structure pre-dating the NE-SW is indicative of a previous brittle deformation event in the area, possibly Upper-Cretaceous - which coincides with the opening of the Atlantic - since the Santana graben genesis has been dated back to the Paleogene (Gontijo-Pascutti, Bezerra et al. 2010)

4.1.2 Location 2 (UTM: 23K 651592 7510592)

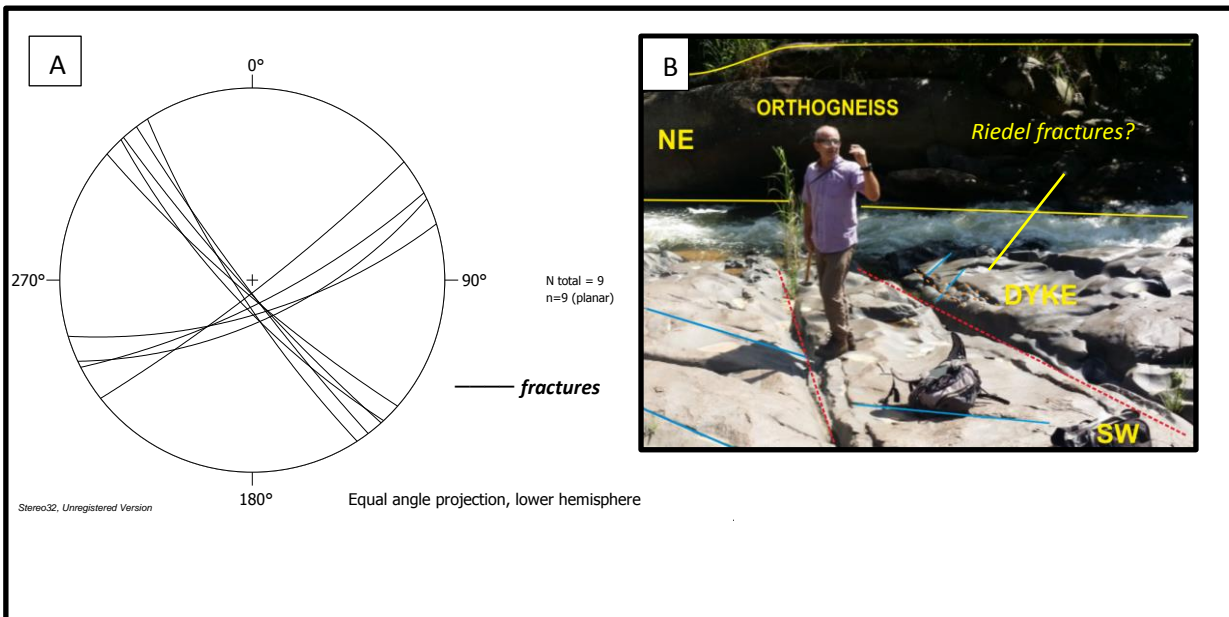


Figure 17: Figure 17a is the Stereonet projection of the structures in the dyke. The surface of the dyke has been constantly eroded by the river water current and it makes it difficult to identify the relationship between them. Because the uncertainty to classify the fractures and joints the structures were kept in one colour – black at the stereographic projection. In fig 17b the structures that could possibly be joints are shown in blue. Possible riedel fractures also showing a sinistral sense of movement in the figure 17b (faint orange just behind Dr Julio Almeida who was used for scale).

Outcrop description:

This exposure located at 380m elevation and situated 350m northwest of the RJ-125 highway, was the second outcrop visited within the Cenozoic Rio Santana graben. The River Santana here exposes a contact between the dyke and the orthogneiss rock (Fig. 17b). The dyke is possibly Cretaceous, formed during Late Jurassic and Early Cretaceous (Gontijo-Pascutti, Bezerra et al. 2010)

Outcrop-scale structures:

The fractures in the outcrop display different orientations, NW-SE and NE-SW (Fig 17a). The surface of the outcrop has been heavily polished/eroded by the contact with the water, which makes the relationship between these structures difficult to discern. The cooling joints of the dyke were not possible to identify due to the margins not being visible, thus the igneous intrusion orientation

also was not possible to be determined. The brittle minor faults (possible Riedel shears) present within the dyke showed orientations suggesting sinistral oblique movement.

Interpretation:

It was not possible to identify the orientation of the dyke due the non-recognition of its chilled margins, however according to Gontijo-Pascutti, Bezerra et al. (2010) in their geological map of the area it is orientated NE-SW (Fig. 18), and it could be part of the Serra do Mar or Santos-Rio de Janeiro dyke swarms of Mesozoic age. Considering the alleged orientation of the dyke and the sinistral sense of movement inferred by the riedel fractures, it is possible to suggest that the outcrop has contemporaneous tectonic activity as in location 1. If the Mesozoic age for the dyke is confirmed, it would indicate tectonic activity reactivating the faults that control the graben prior to its development and could be associated with the opening of the Atlantic. This would suggest reactivation of these features during the brittle event that formed the Santana Gabren.

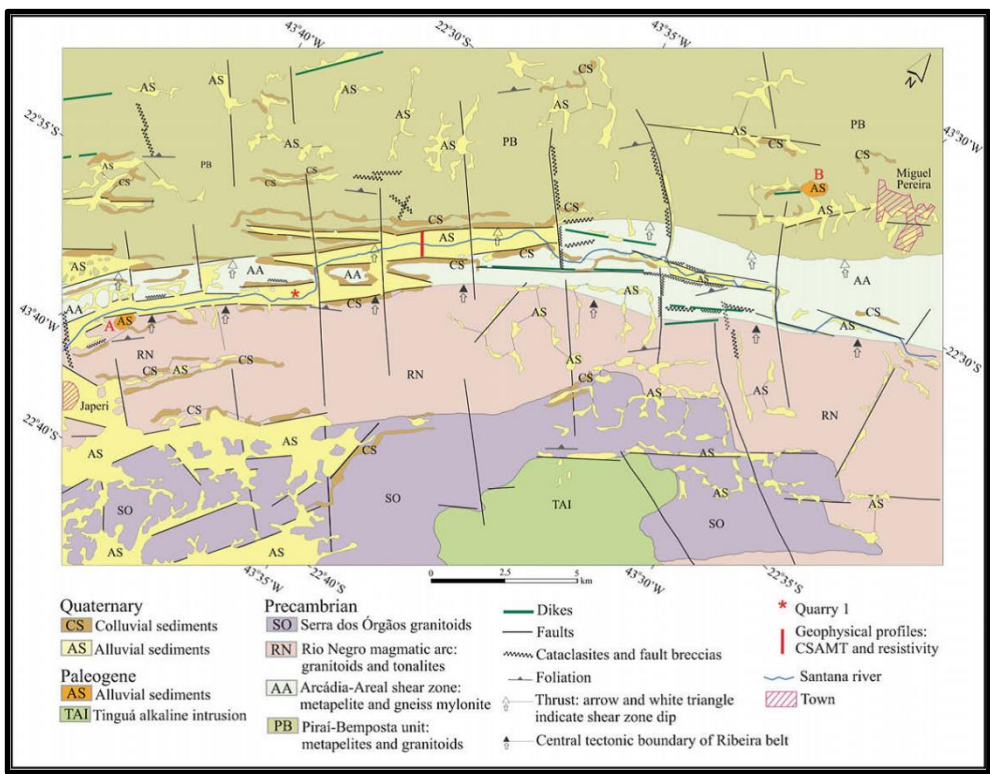


Figure 18: A geological map from (Gontijo-Pascutti, Bezerra et al. 2010) where the dykes mapped in the area (in green) show direction NE-SW.

4.2 Volta Redonda Basin

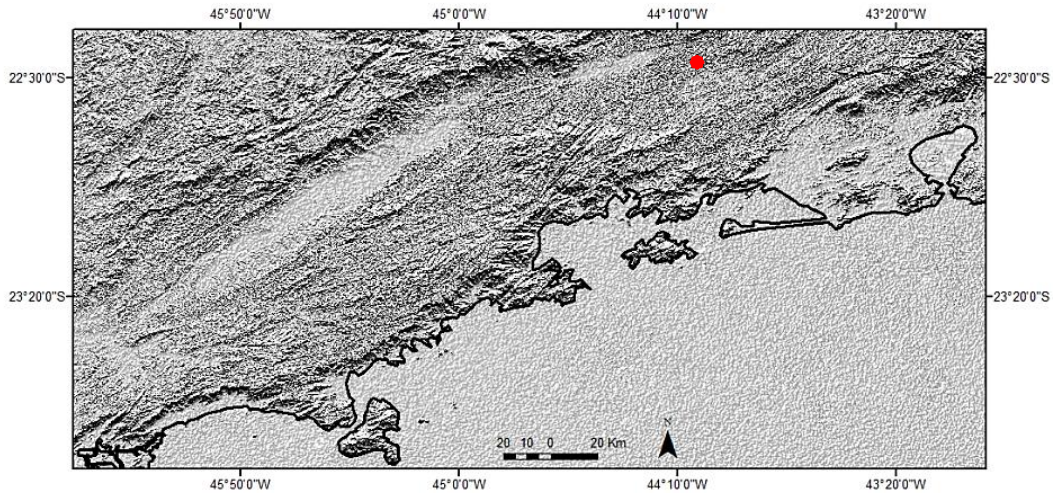


Figure 19 : Location map with red dot marking the basin

Volta Redonda was the smallest basin visited during this study. According to Sanson (2006) the stratigraphy of the basin shows Palaeogene sediments belonging to the following formations:

- Ribeirão dos Quatis Formation: Ribeirão dos quatis represents the pre-rift phase of the Volta Redonda basin evolution, which was deposited overlying the Pre-Cambrian basement. It is 10m thick, composed of quartzose conglomerate interbedded with arkosic arenite and thick layers of pelites due to a later cycle of fluvial progradation. (Negrão, Mello et al. 2015)
- Resende Formation: This also occurs in the Resende Basin (see section 4.2.3). The formation is associated with the main sedimentation phase of the basin occurring during the Eocene (Ramos, Mello et al. 2003). The sediments unconformably overly the basement highs; the facies of the formation are interbedded well-stratified feldspathic sandstones with fine conglomerates and mudstones with poorly sorted rudites (Negrão, Mello et al. 2015).
- Casa de Pedra Basanite Formation: Negrão, Mello et al. (2015) described this formation as made of basanitic volcanic rocks comprising ultramafic alkaline composition and showing aphanitic

texture with microphenocrysts and vesicles, they also suggested two pulses of magma. This formation can be observed in between the Resende Formation and the Pinheiral Formation and is of Eocene age according to Ar-Ar dating by Ramos, Mello et al. (2003)

Pinheiral Formation: These deposits are Palaeogene in age and were unconformably deposited on the basement, Resende Fm and locally the Casa de Pedra Fm. Lithologically, this formation shows frequent truncated architecture, of conglomeratic stratified arenite layers, and layers of pelite of decimetric thickness, the latter formed during periods of fluvial drowning (Negrão, Mello et al. 2015).

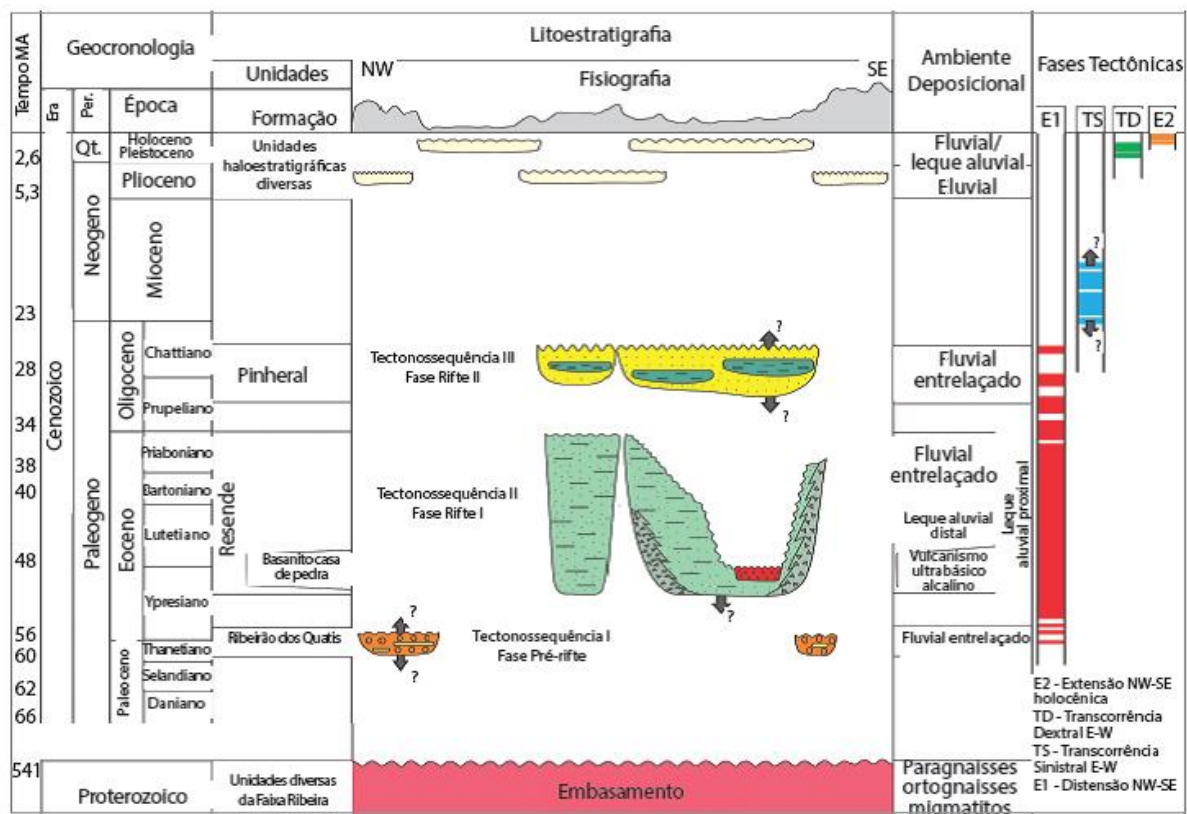


Figure 20: Stratigraphic column of Volta Redonda (Negrão, Mello et al. 2015)

4.2.1 Location 6/7 (UTM: 23K 599896.9 7514777.4)

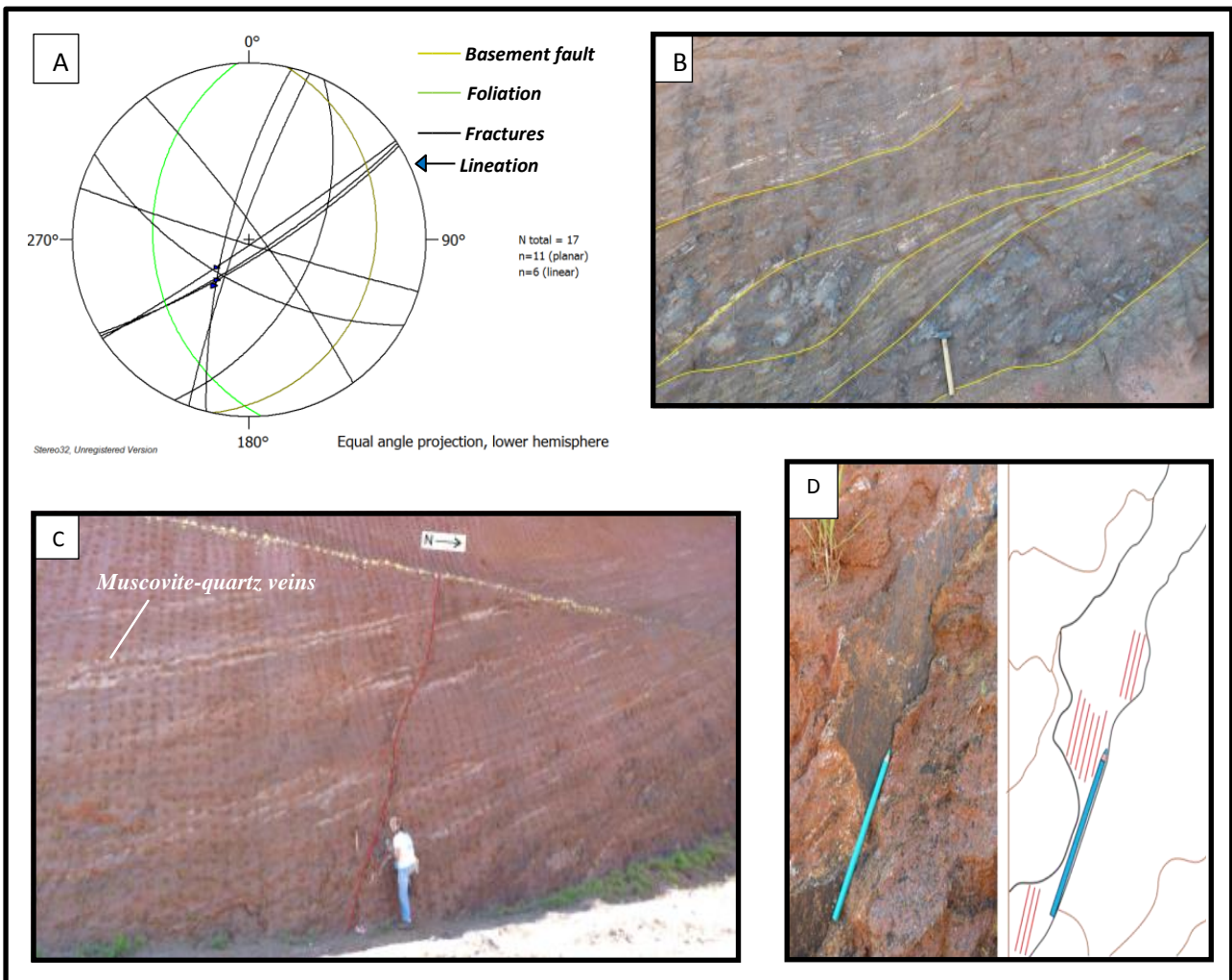


Figure 21: Fig. 21a is the stereographic projection of its structures recorded. Fig. 21b shows an example of boudanage in the outcrop suggesting the extensional regime in the area.. Fig. 21c shows a normal fault that at first sight can be classified as a reverse fault, but it is a normal fault with an oblique component. Fig. 21d shows the lineation imprinted in the fault which are slickenlines in the fault.

Outcrop description:

A large outcrop by the BR-393 just at the exit to Volta Redonda is located in a road cut measuring 280m in width and 20m high. The rock is a high-grade metamorphic rock from deep crustal level that is heavily weathered. The red colour is possibly attributed to a high level of manganese content in the parent rock. It possibly belongs to the Formation Pinheiral of Paleogene age.

Outcrop-scale structures:

The main foliation is orientated N-S and is moderately west dipping and the main fault in the outcrop trends NE-SW (Fig. 21c) steeply dipping to the SE. The slickenlines observed on the fault plane shows a movement in a dip slip direction but with $\sim 50^\circ$ of obliquity to the fault plane. The offsets are caused by a dextral normal movement as suggested by the lineation (Fig. 21d). Boudinage of the more mafic layers was also observed in the outcrop within the foliation (Fig. 21b). Distinct sets of fractures were recorded within the outcrop with a fracture in the basement rock observed orientating N-S. Muscovite-Quartz veins following the foliation were also observed (Fig. 21c)

Interpretation:

The angle between N-S west dipping foliation and the basement fault N-S east dipping is 51.5° , their dip are 33° and 19° respectively, striking the same orientation. These data suggest a reverse/thrust fault, even though aforementioned relationship has not been observed in the field. The NE-SW fault (Fig. 21c) is a high oblique fault (suggested by the dip-slip and strike slip components showed in the stereographic representation); and post-date the structures aforementioned therefore a second tectonic event is proposed. The slickenlines in the main NE-SW has a 55° pitch confirming a high angle of movement, adding to this context the obliquity of the fault, it could represent a reverse fault reactivated during the latter extensional period, possibly during the Cenozoic Transcurrent Dextral regional paleostresses suggested by Riccomini (1989).

4.2.2 Location 28 (UTM: 23K 577396 7513051)

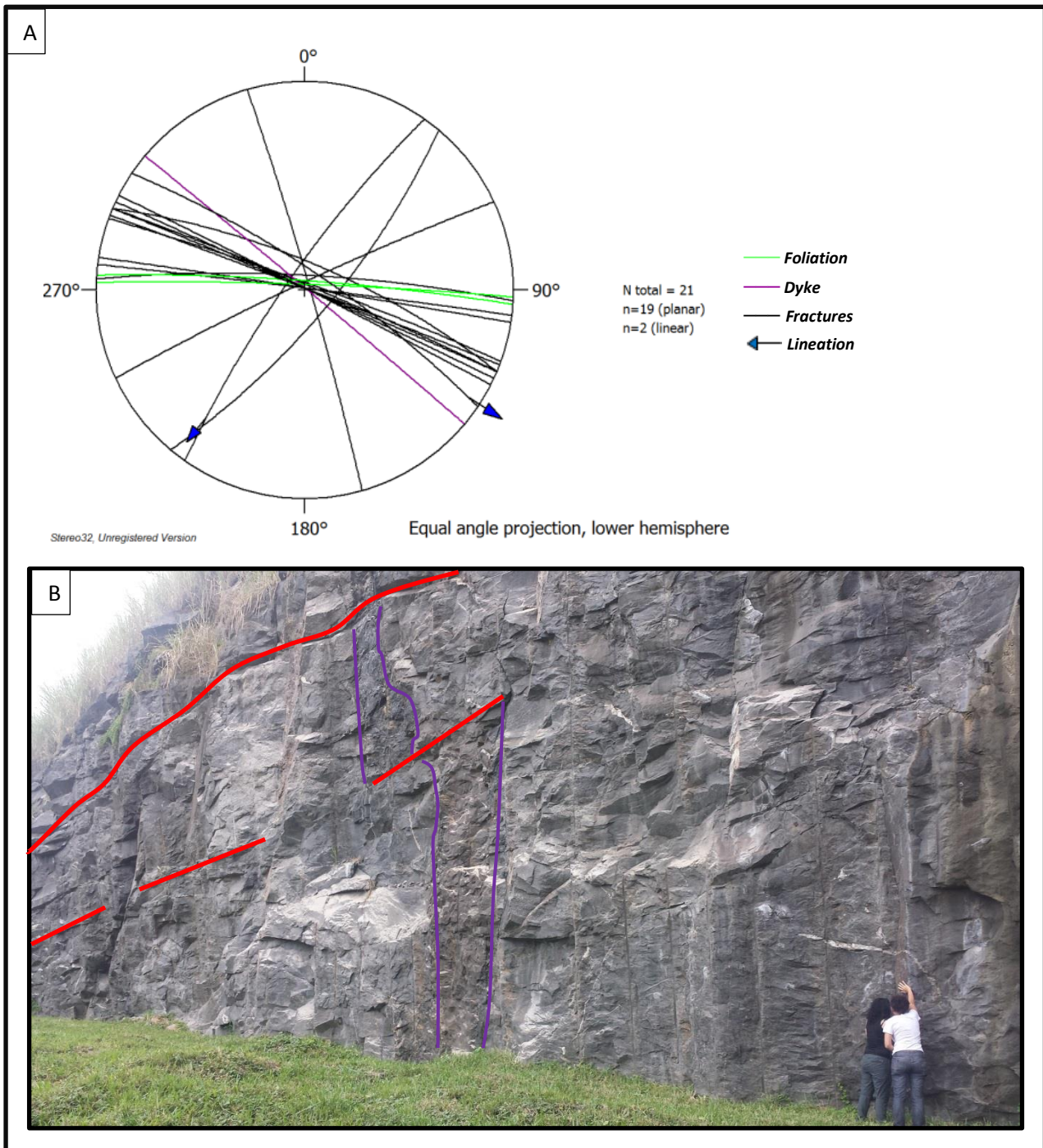


Figure 22: 22a stereographic projection showing parallel lines to the foliation and possible reactivation fractures E-W orientated (black.) The vectors represent the transport direction. Fig. 22b the dyke intrusion is offset by the NNW-SSE fracture.

Outcrop description:

Near the BR116 (Rodovia Presidente Dutra) highway an outcrop some 60m width by 20m of height is comprised of granodioritic gneiss with a porphyritic basalt dyke intrusion showing 1cm biotite lens and possible tourmaline crystals.

Outcrop-scale structures:

The main foliation dips north and trends E-W. The main set of fractures shows a preferential NW-SE orientation. The dyke has been offset by the NNW-SSE-striking sinistral strike slip fracture (Fig. 22b), however at the tip of the dike, displacement is minor or nonexistent, if there was any, it was possibly was erased by erosive processes. A faint lineation is imprinted in the zeolite infilling of the fracture in the outcrop.

Interpretation:

The E-W trending foliation has parallel fractures that might have been influenced by the basement; the dyke (Fig. 22b in purple colour) has an orientation WNW-ESE roughly following the foliation trend of the area and the dyke at location 2. The igneous intrusion follows the foliation anisotropy and considering the parallelism to the other fractures trending E-W this could be indicative of basement influence. The offset of the dyke by a NNW-SSE fracture could have been caused by a new event that post-dated the implied reactivation. The slickenlines in Fig. 16a indicating two different orientations, dextral and sinistral strike slip adding to the indication that the outcrop enjoyed at least two events under different paleostresses. Based on the stereographic projection these structures could be associated with two transtensional events of the area, the first during the Earlier Paleocene, a Transcurrent NE-SW as suggested by Cogné, Cobbold et al. (2013) and the second as per Riccomini, Sant'Anna et al. (2004) who suggested a NNW-SSE transtensional paleostress for the regional area during the Eocene.

4.3 Resende Basin

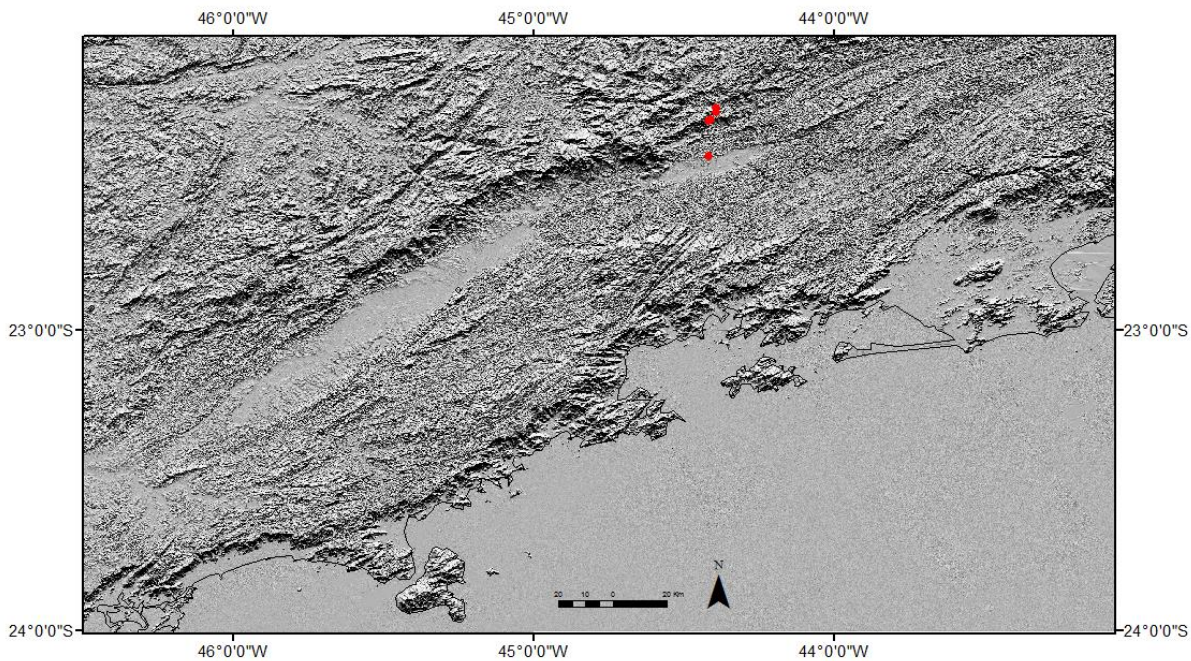


Figure 23: Map showing the points visited within the Resende Basin. Locations 9, 10, 11, 13. Location 12 was too close to location 13 and no relevant information was observed to justify its inclusion in the final report. Location 9 is seen at the hangwall of one of the main faults in the west side of the basin, whereas the other three outcrops are located on the footwall of the fault.

The Resende Basin is situated approximately 20km further west of the Volta Redonda basin (Fig. 1). The basin is orientated ENE-WSW and is 47km in length (Ramos, Mello et al. 2003). It is a half-graben with Eocene-Oligocene sediments which consist of rudites, arenites and lutites (Ramos, Mello et al. 2006). Ramos, Mello et al. (2006) proposed a revision of the basin stratigraphy, in which he described six different sedimentary facies, divided into three stratigraphic units: Ribeirão dos Quatis Formation, Resende Formation, and Floriano Formation. These formations correlate with the Volta Redonda formations described above, with exception to the Floriano Formation, which represents the last stage of fill of the basin through a meandering fluvial system (Ramos, Mello et al. 2006).

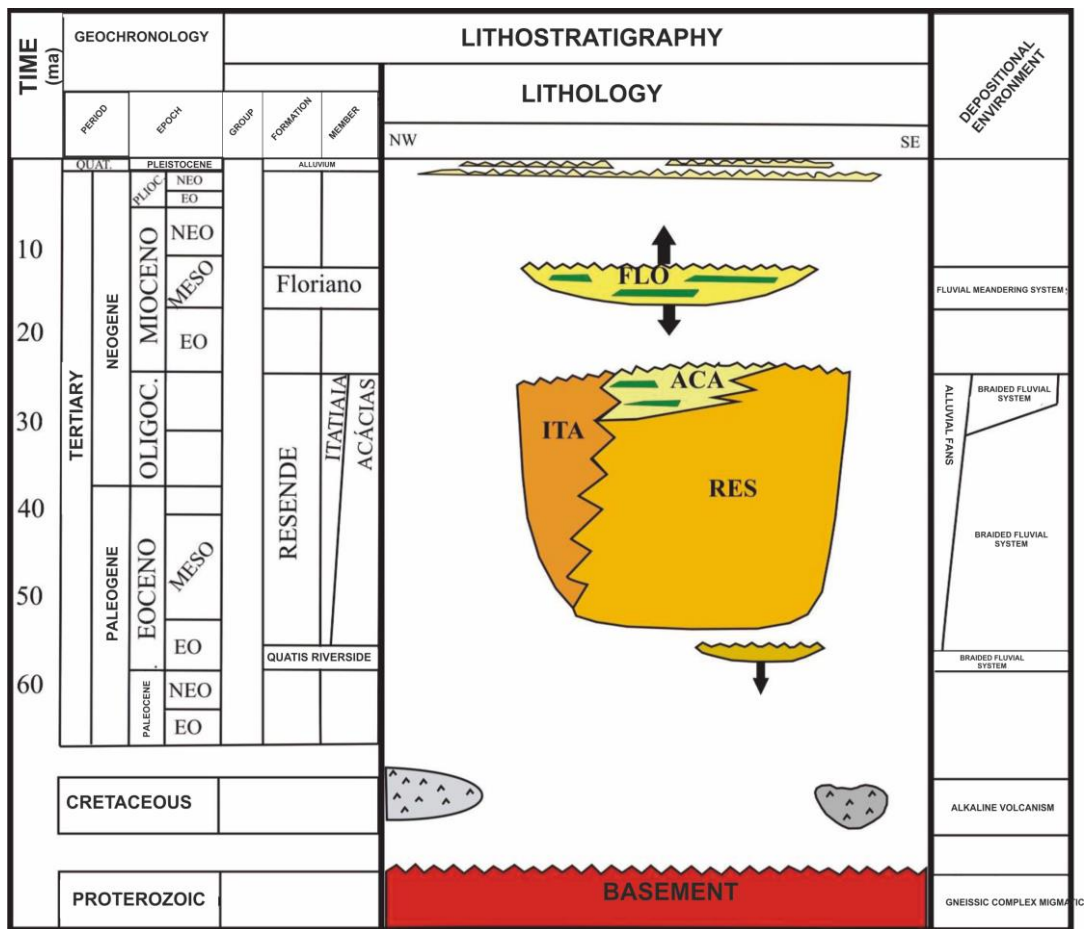
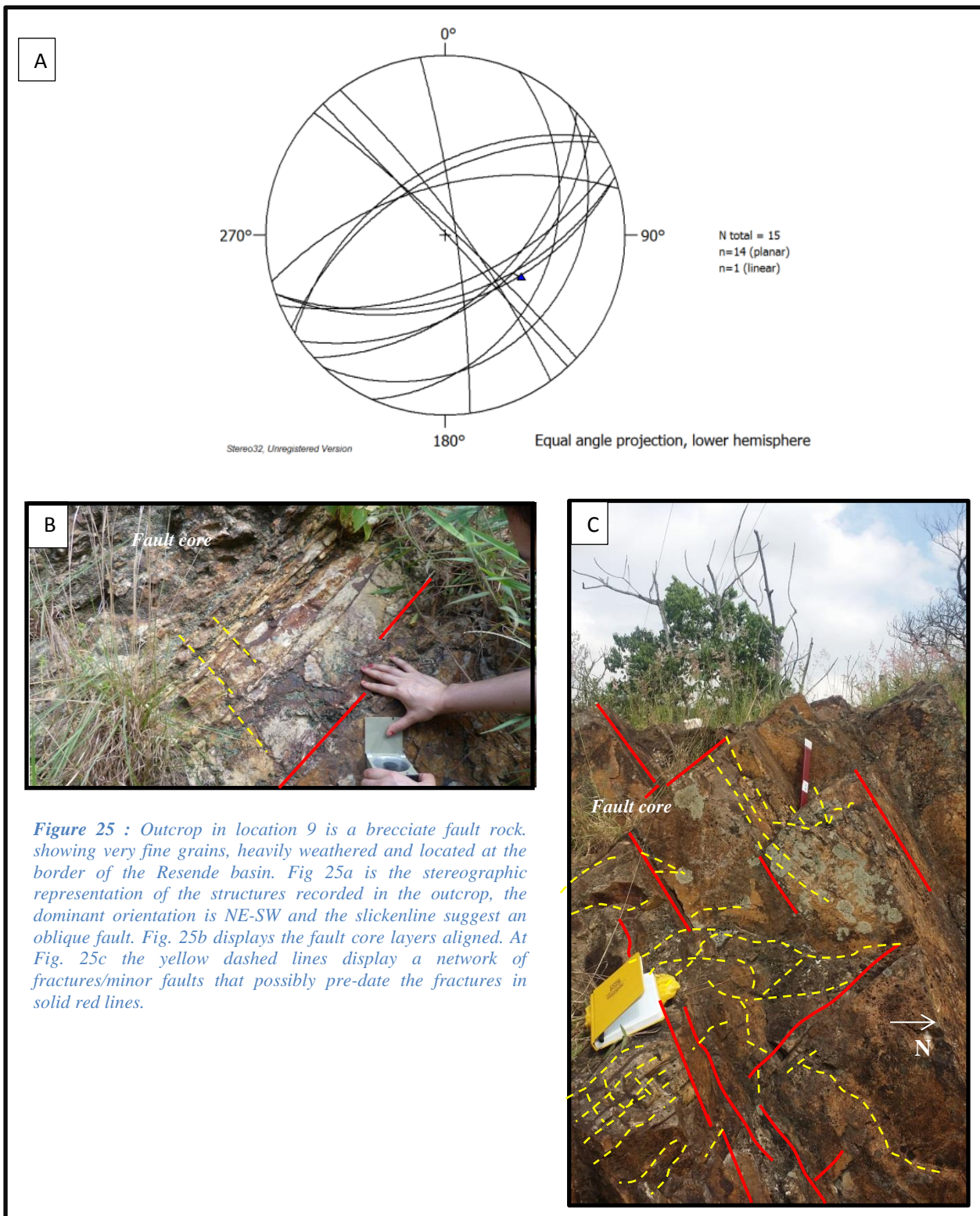


Figure 24: Chronostratigraphy for the Resende Basin (Ramos, Mello et al. 2006)

4.3.1 Location 9 (UTM: 23K 559770.2 7520585.9)



Outcrop description:

Location 9 in the Resende basin is by the highway RJ-161 on the south side of the *Paraíba do Sul* River. The lithology is an 8m high breccia, probably belonging to *Quirino* formation which is composed of facies of biotite-hornblende orthogneisses. The outcrop is heavily weathered, by phreatic water that has penetrates in a network of fractures. The orientation of the main fracture set plan is ENE-WSW.

Outcrop-scale structures:

This outcrop is a breccia that contains layers that vary in thickness from 1cm up to 30 cm (Fig. 19b) and fractures in three different orientations (Fig. 25c). Also presented in Fig. 25c are fractures that appear to link the main fault sets ENE-WSW, NW-SE and NE-SW.

The transport direction defined by slickenlines, suggest an oblique fault at a high angle (60° E) sense of movement (dextral) close to the intersection between NW-SE and ENE-WSW fractures as seen in the stereographic projection.

Microscale structures:

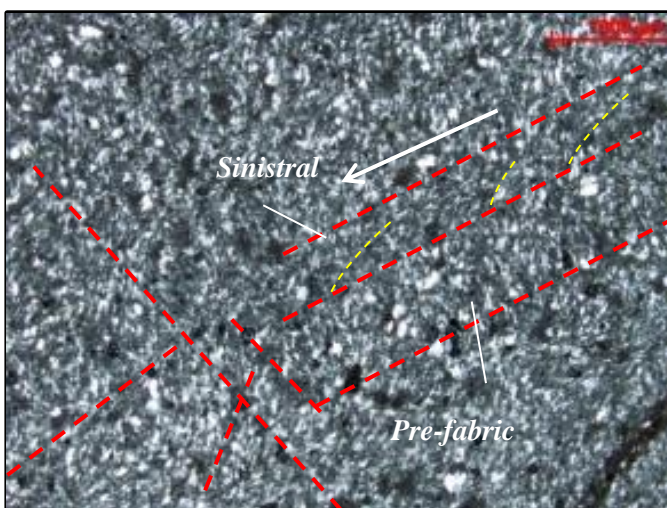


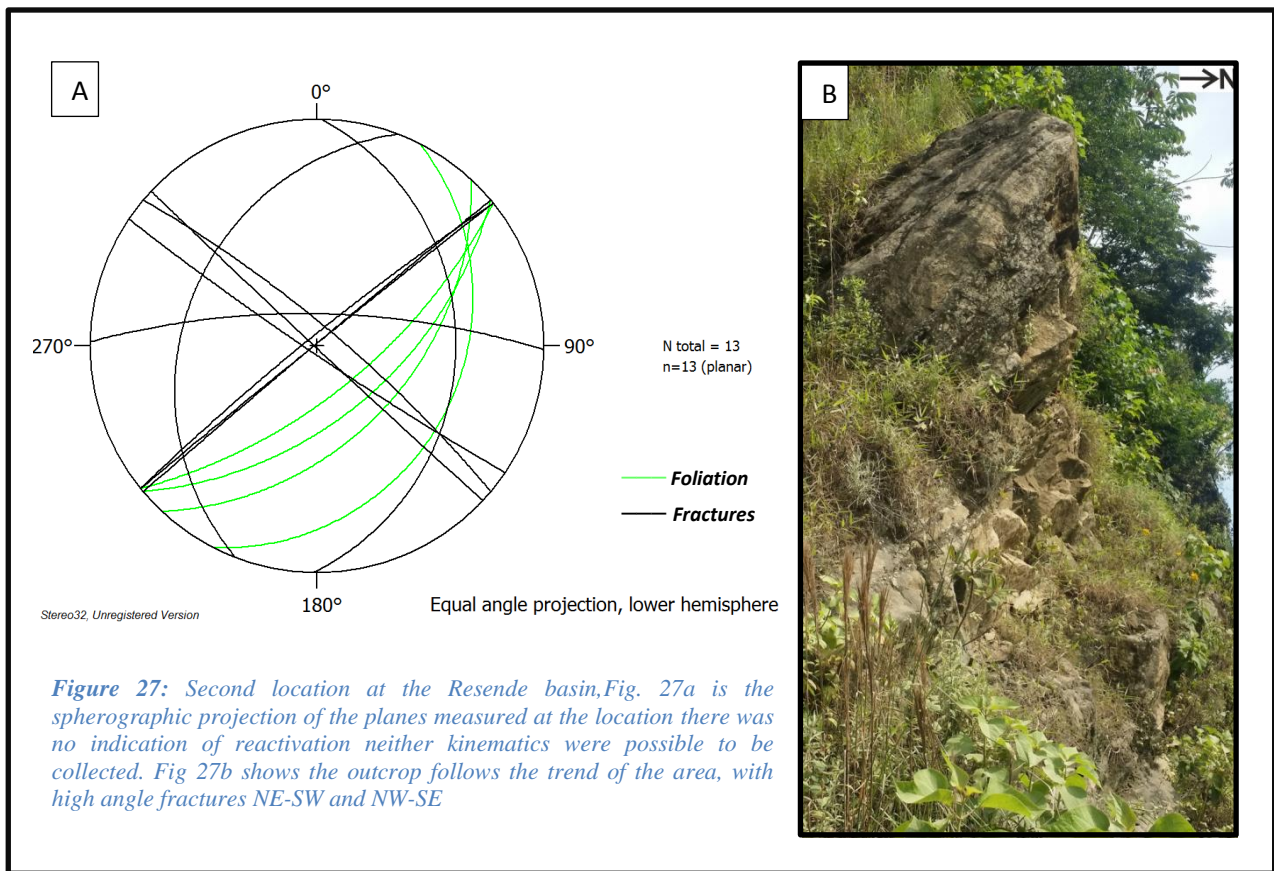
Figure 26: Thin section of sample showing field of view 1000µm , the red lines represent possible micro-structures for this outcrop. Quartz veins, shear zone and brittle micro-fractures. The quartz vein seems to have been offset by a microfracture, and the shear zone stops at an intersect point. The yellow dashed lines here are indicating a possible sinistral shear movement.

The thin section taken from a sample from this outcrop did not show strong evidence for brittle deformation; however faint lines (in red Fig. 26) suggest some previous fracture and what resembles a quartz vein showing recrystallized fine-grained quartz. The arrow in white indicates a possible sinistral shear movement. Lineations were observed (Fig. 25a) suggesting reactivation of the fault rock. The composition of the rock is quite difficult to identify, but considering the possible parent rock for this breccia (*Quirino* Formation) it is likely to contain mica and quartz.

Interpretation:

The layers were aligned possibly due to the mica minerals being re-oriented during the shear movements. The breccia displays, in the microscale, faint shearing bands and recrystallized quartz veins and is crosscut by the conjugate fractures, evidence for at least two events affecting the area, implying at least one to be tectonic reactivation. The first event possibly dating from early Cretaceous and the second event related to CRSB during the Paleogene (Riccomini 1989). The yellow dashed lines in Fig. 19c appears to link these main fault sets as secondary faults R and R', thus developing an anastomosing network. The shear component in the kinematic can corroborate to this interpretation. The lineation orientation suggests a normal fault with an oblique component to it, indicating a transtensional regime for this reactivation and it is possibly related to a deformation event under an extensional NW-SE regime, possibly post-dating the formation of CRSB during the Upper Cretaceous since it is possibly reactivating a fault rock structure.

4.3.2 Location 10 (UTM: 23K 559924.5 7533609.9)



Outcrop description:

Paragneiss outcrops at 808m elevation in the Serra da Mantiqueira mountain range, at km 54 on the RJ-161 highway by the *Corrego do Eme*, a stream belonging to the Paraiba do Sul River.

Outcrop-scale structures:

The paragneiss displays a foliation that strikes NE-SW and dips at a maximum angle of 66 to the SE, Two obvious fracture sets of fractures are orientated orthogonal to each other and are steep NE-SW and NW-SE striking structures. The other two fracture sets dip moderately to the E-W and the N-S.

Interpretation:

The NE-SW striking fractures that trend parallel to the foliation along with the NW-SE fractures were the most frequently recorded, there was no indication of reactivation and assigning an age for this event is problematic as no displacement has been observed. It could be suggest that the similiarities between structures at this outcrop and those at location 9 would imply that the outcrops have been affected by the same events referred previously as Upper Cretaceous and during the Paleocene.

4.3.4 Location 13 (UTM: 23K 562514.9 7538179.2)

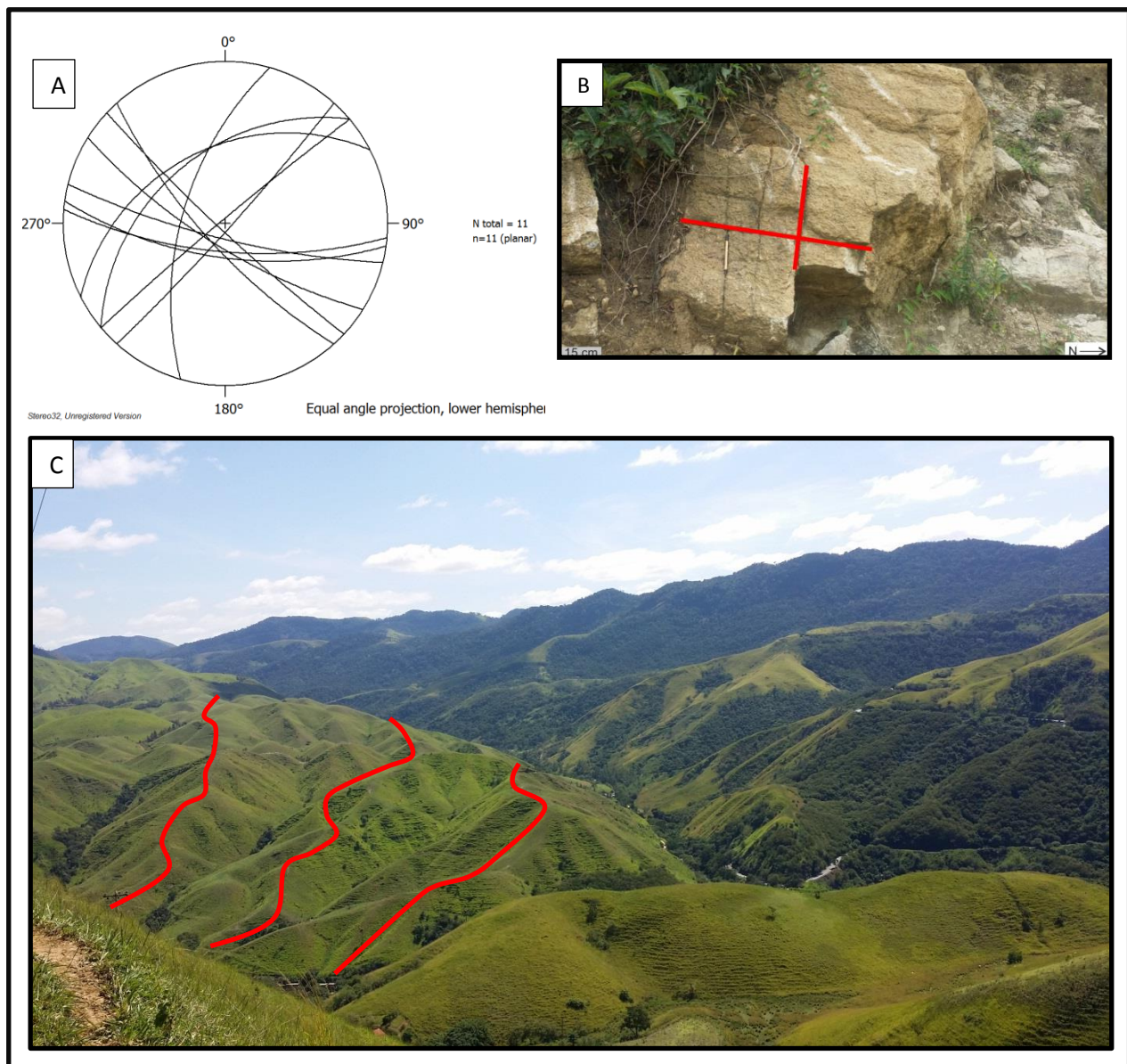


Figure 29: Another outcrop at high elevation, granitoid showing fabric showing preferential orientation and displaying joints. Fig. 29a is the spherographic projection of the fractures measured, Fig. 29b is showing two different sets of joints typical of uplifted areas and Fig. 29c is a panoramic view of the location looking towards N-NE, the scarp swarm orientation is marked by the red lines.

Outcrop description:

This outcrop was observed at km 28 on the RJ-16 highway at 958m elevation and comprised weakly foliated granitoid rocks that are heavily weathered.

Outcrop-scale structures:

The outcrop has a wide range of fracture orientations with NE-SW and NW-SE being the most prominent trends with mostly dips towards the NW direction (Fig. 29), these fractures also show no displacement, suggesting a rather tensile mechanism. From this location it is possible to see a swarm of scarps (Fig. 29c) showing a N-S preferential orientation.

Interpretation:

To the south of this area at regional scale, the N-S fractures become more common, however at outcrop scale it still not significant, and despite the number of fractures measure no clear evidence of offset or displacement as been observed. The set of NE-SW, NW-SE and E-W fractures could be classified as joints as per figure 12 a and b (also fig. 29b) demonstration, these joints could have been created during one of the uplifts events previously dated and can be part of the same set of joints as the previous location.

4.4 Taubate Basin

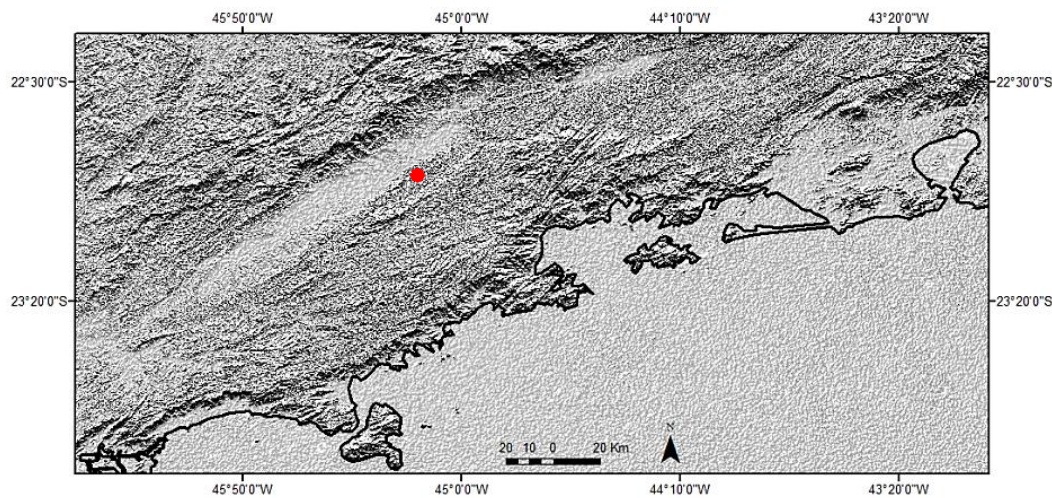
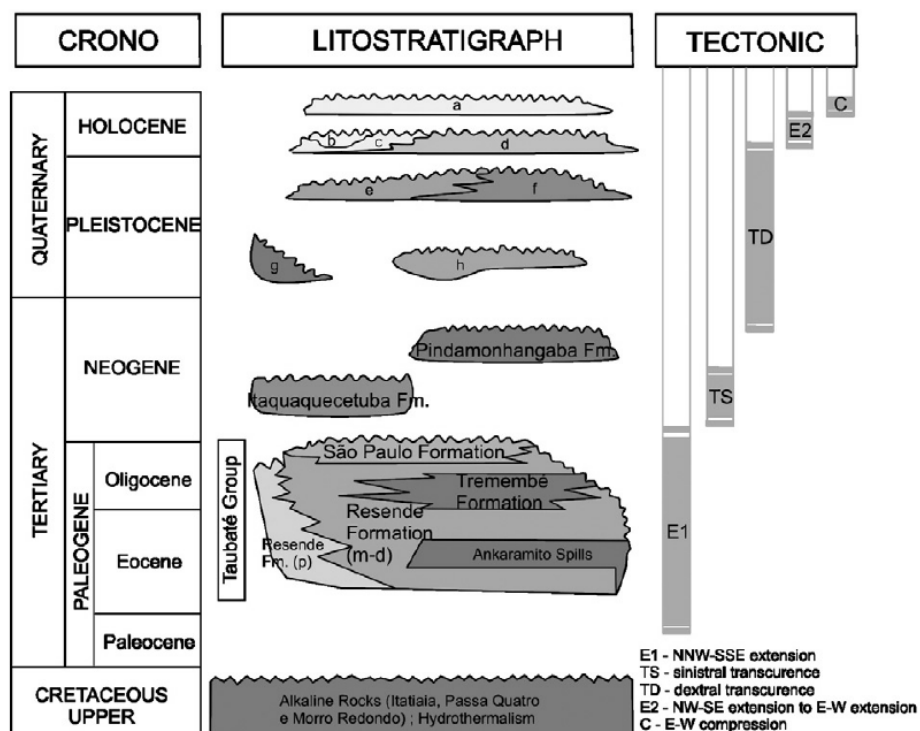


Figure 30: Map location of the outcrop visited at Taubate Basin, it is an active quarry at the border of the east side of the basin.

Taubate basin is the largest and most studied of the Tertiary basins in SE Brazil. It is 170km long and 20 km wide (Cogne, Cobbold et al. 2013), according to Riccomini (1989) the basin is divided into two sequences: syn-rift (sedimentary rocks) and post-rift (colluvial/alluvial) infills, they are underlain by the crystalline basement. Cogne, Cobbold et al. (2013) suggested that the basin formed under left-lateral transtension during the Palaeogene, but suffered right-lateral transpression during the Neogene.

Figure 31: Chronostratigraphic column of Taubaté basin (Torres-Ribeiro 2004)



4.4.1 Location 27 (Taubate basin) (UTM: 23K 474139 7470288)

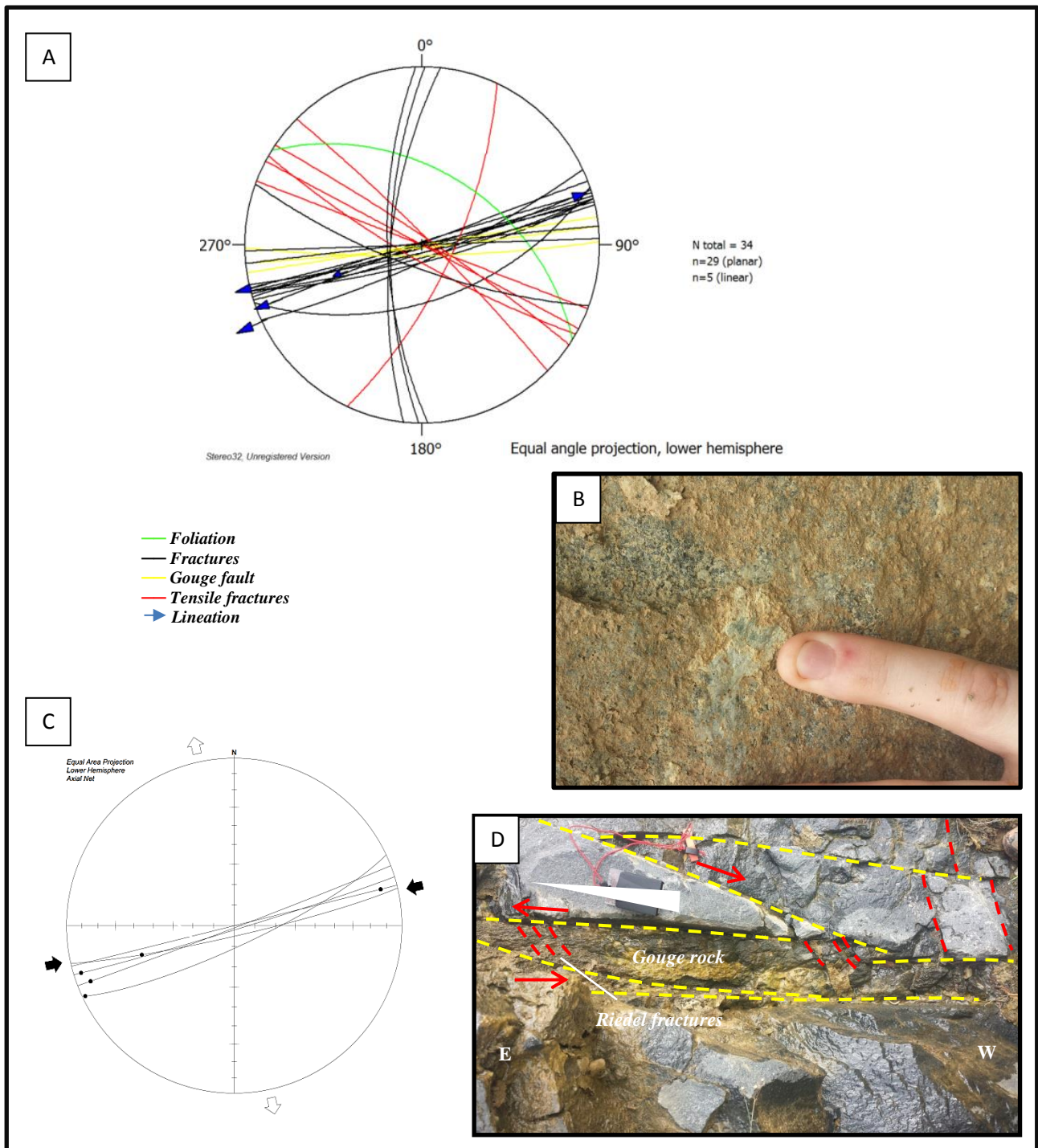


Figure 32: The stereonet displays its fractures in Fig 32a. The high angle dips faults cuts through the moderately dipping foliation (green line), the gouges trace an almost parallel with the deeply steep ENE-WSW fault sets. The slickensides imprinted in zeolite in the fracture wall (Fig. 32b).

Figure 32c is the result of an attempt to do a stress inversion with the data collected in this location. The result is not conclusive, probably due to the number of lineation recorded not being robust enough for the exercise. In red inside the fault rock (Fig. 32d) the tensile fractures indicate sinistral sense of movement. The white triangle indicates the change in grain size within the gouge and possible mylonite clasts. The lineation displayed in the stereonet suggest that dextral sense of movement is dominant in the outcrop's-S striking fractures are also recorded in red dashed lines.

Outcrop description:

Location 27 is at the border of Taubate basin in an active quarry at 567m of elevation, by the SP-060 highway (*Rodovia Dutra* cutting through the Sao Paulo estate) at exit 75. The outcrop type is a granoritic gneiss fault wall of approximately 30m height. It also displays fault rocks of small grains, yellowish in colour (probably due to weathering) and a fabric indicating preferential orientation.

Outcrop-scale structures:

The outcrop foliation trends NW-SE dipping moderately to the NE. The steeply SE dipping fractures orientated ENE-WSW are the dominant sets of faults in the locality (Fig. 32a). Secondary fractures trending NW-SE were also observed, and a less common NE-SW set was also recorded. Zeolite mineralization was also observed in the site within the fractures displaying strike-slip transport directions (Fig. 32b). A second set of fractures was observed with a steeply west-dipping N-S orientation, these are shorter structures that are perpendicular to the main set ENE-WSW faults. The gouges in the fault core fabric display preferential orientation as well as changes in its texture and fine upwards (Fig. 32d), possibly related to a change in the shearing intensity along the fault core. Fractures within the fault gouge show a small variation in its strike and crosscut the gouge fabric.

Interpretation:

The lack of fractures parallel to the foliation suggests that the brittle deformation was not influenced by the basement fabrics. Nevertheless gouge-bearing faults within the outcrop indicate reactivation of the E-W fracture set. The gouge internal fractures and the presence of mylonite clasts indicate a second event affected the structure by cutting through its body at the same E-W orientation. Riedel shears indicates sinistral strike slip for the fault gouge in Fig. 32d, but the general sense of motion to the outcrop is dextral, which could indicate reactivation of the

faults as suggested by variation in kinematics (Fig. 32a). According to the literature (Riccomini 1989, Riccomini, Sant'Anna et al. 2004, Cogné, Cobbold et al. 2013) the shear zone fractures enjoyed at least two reactivation events during the Paleogene (transtensional left-lateral when the basin was formed) and during the Neogene at right-lateral transpression. The N-S set of faults are the youngest set, and have a perpendicular relationship with the older E-W set. They appear to be discontinuous due to an abutting relationship to the longer and older faults, .

The tensile fractures recorded in the basement show a NW-SE direction implying that the minimum principal stress responsible for this set would be perpendicular to this direction working at NE-SW orientation. According to MyFault™ software which provided the stress inversion for this outcrop, the minimum principal stress was formed under a compressional regime (32d), however it would be necessary to collect a more robust data set to confirm this result; therefore this analysis should be considered a preliminary result.

4.5 Tamoios Highway: Embu Domain and Coastal Complex

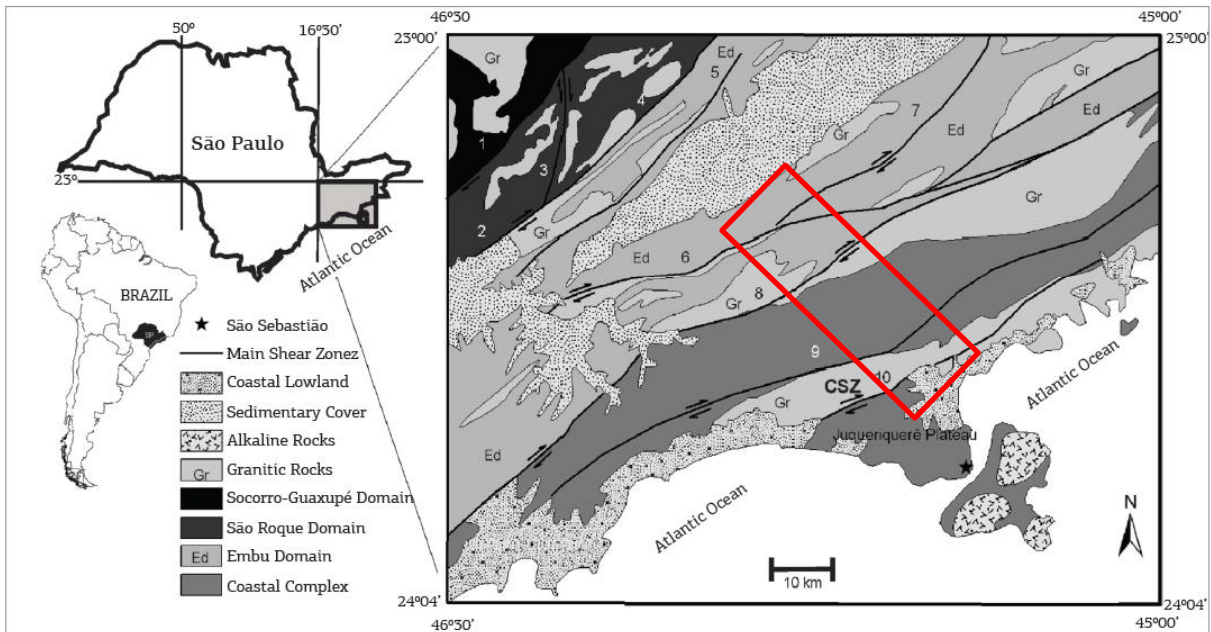


Figure 33: Geological sketch of the northern coast of the São Paulo state. The Camburu Shear Zone (CSZ) limiting at north the Juqueriquerê plateau. Modified from (Mora, Campanha et al. 2013)

The area covered by the Tamoios highway (SP-99) crosses several of the main shear zones of the Ribeira belt (Fig. 33). The Camburu Shear Zone is a NE-SW dextral transcurrent fault dividing two lithologies of the Coastal Domain: the Pico do Papagaio Granite (a hornblende monzogranite with a well-developed foliation) to the NW of the fault and the Juquei Augen Gneiss (biotite granite with blastomylonitic structure) to the SE of the Precambrian structure (Mora, Campanha et al. 2013). Along SP-99, it is possible to observe evidence of reactivation of the foliation (igneous intrusions in the outcrop, displacement of the plane of the foliation) in the large scale outcrops in the roads cuts but only a few could be analysed due to the traffic on the highway and the quality of the outcrops.

4.5.1 Location 22 (UTM: 23K 0422175 7421654)

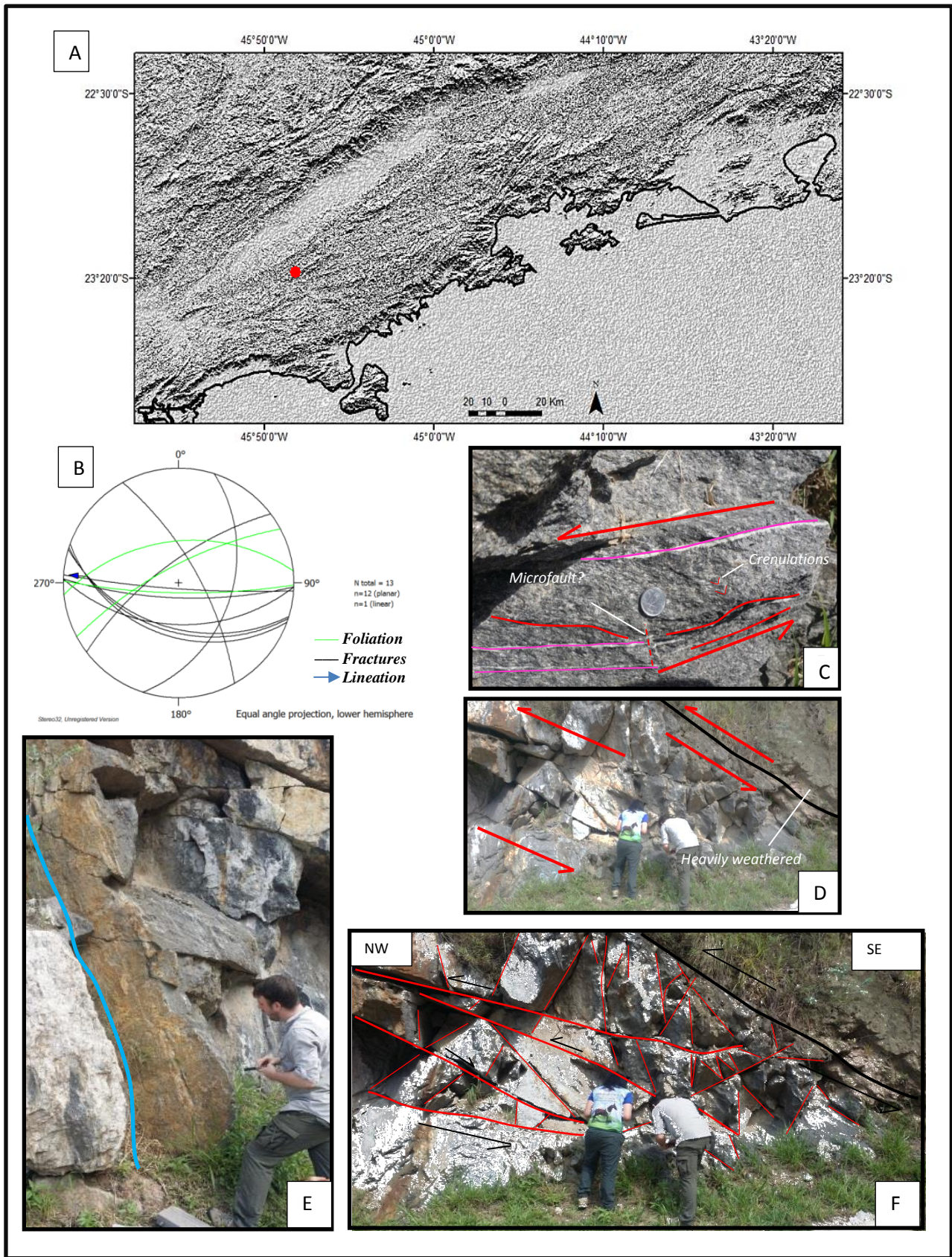


Figure 34: Location of the outcrop in Fig. 34a. Stereographic projection is shown in Fig. 34b. Figure 34c shows an inset of the sinistral sense of movement (red arrows) imprinted in the fabric with quartzo feldspathic veins (pink), cohesive corridor marked in red plain lines, and in dashed line a small possible microfault offsetting the red lines and veins. Still in Fig 34c crenulations displaying the Figure 34d displays the different sets of fractures/faults within the outcrop in Fig 34e.

Outcrop description:

The first point in this outcrop at SP-99 (Rodovia dos Tamoios) (Fig. 34c) is at 677m elevation and is a NW-SE orientated 8m high road cut that exposes a 125m wide section of quartzo-feldspathic banded light grey gneiss. The rounded grains are possibly due to granulite to migmatite grade metamorphism with minor pegmatite containing tourmaline formed parallel to the foliation.

Outcrop-scale structures:

The outcrop foliation recorded strikes in the range ENE-WSW to E-W with NW-N dips (Fig. 34b). A set (1) of brittle shorter faults forms a network of younger faults, striking NE-SW dipping N, SE-NW dipping NE and NNE-SSW dipping E. A visible E-W and WNW-ESE striking moderately dipping south fault set are the longer structures (2) that cut through the outcrop (Fig. 34b and Fig. 34c). A small offset on the fault plane along a transport direction of 20°W indicated a dextral strike slip fault.

Interpretation:

The two different sets of fractures in this outcrop suggest that at least two brittle deformation events affected this area. According to the stereographic projection the foliation enjoyed a clockwise rotation until it reached a steeply S dipping orientation. The fabric shows a sinistral sense of movement (Fig. 34c), a crenulation cleavage displayed in the fabric is very subtle but supports the idea that a compressional palaeostress was applied to the rock prior to brittle deformation. The two different sets of fractures in this outcrop suggest that at least two brittle deformation events affected this area. Set 1 fractures show a conjugate like geometry which is often associated with strike slip regimes. A dextral sense of movement has been inferred, through slickensides recorded in Fig. 34b and through the secondary fractures recorded. The parallelism between the foliation and the older faults suggests a possible basement reactivation.

4.5.2 Location 23 (UTM: 23K 427548 7417600)

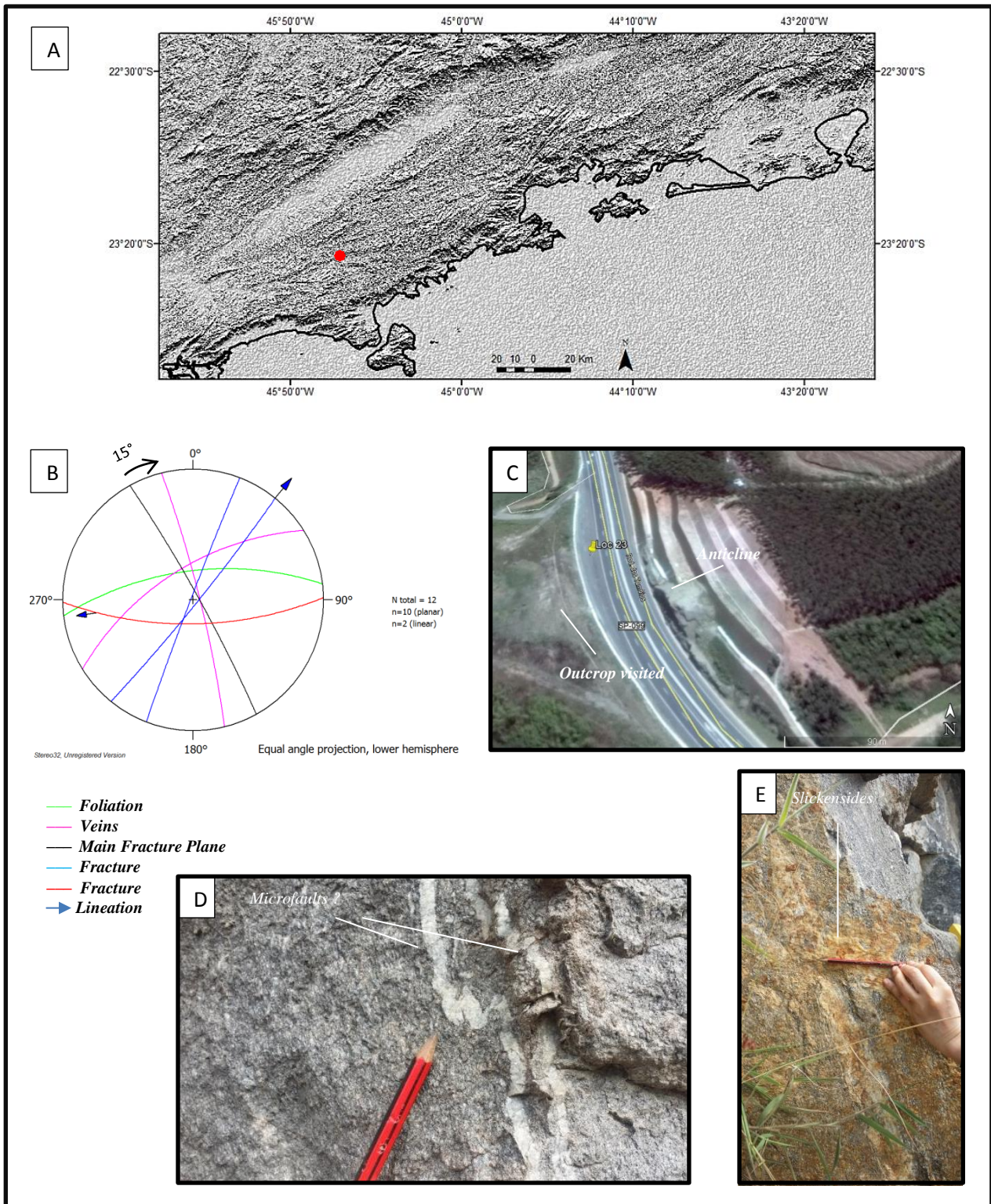


Figure 35: Fig. 35a is the location of the outcrop, 35b is the stereographic projection of the data recorded. Fig. 35c is the Google image of the anticline structure at the location of the outcrop, the measurement were taken from the opposite hand side of the highway. In 35d if a close insight of pegmatite veins, showing W microfold and possibly microfaults striking E-W cutting through these veins. Fig 35e the slickensides imprinted in one of the the NE-SW fault plane outcrop. In Fig 36 a close up of the outcrop striking NW- SE.

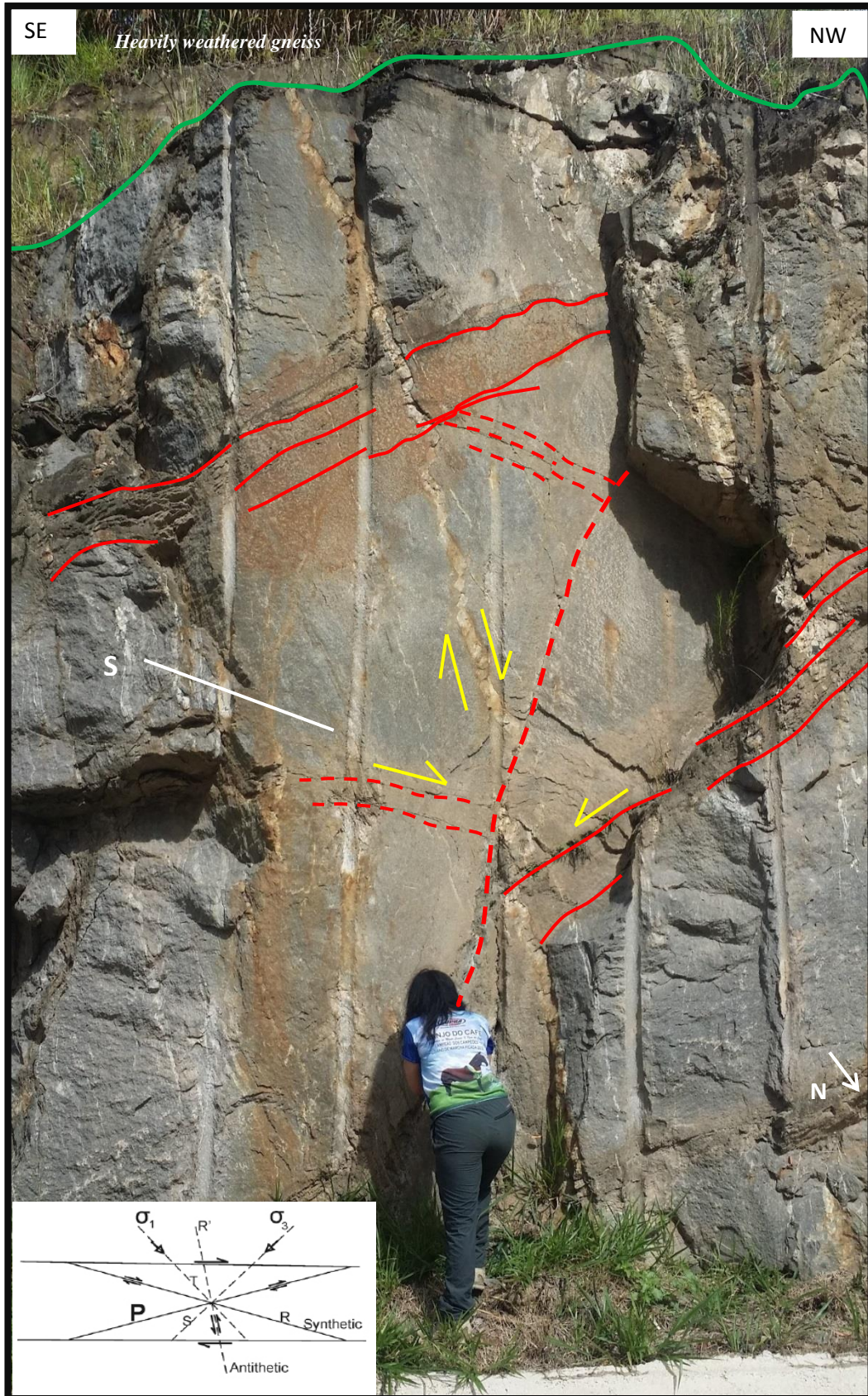


Figure 36: Fig 36 shows part of the anticline pictured in Fig 35c, the vein striking SSE-NNW has perfect left-lateral strike lip fault and cut through cleavage of the structure. The dashed red lines are striking E-W, layers displaying a fabric showing preferential orientation but with hollow space in between the beddings probably resulting of dissolution of minerals. On the left corner the riedel diagram for dextral strike slip

Outcrop description:

Further to the east from the previous locality, location 23 is situated beside the SP-99 highway at 657m elevation. The outcrop is on a wide curve, striking NE-SW and has the same lithology as location 22.

Outcrop-scale structures:

The outcrop shows an E-W foliation dipping N, and preserves a faint SC fabric with shear planes that show a dextral sense of movement. The fabric is crosscut by a set of veins of pegmatite striking NW-SE steeply dipping E and NE-SW steeply dipping E respectively. These veins show a right-stepping structure. The main fracture plane infill contained a horizontal lineation (Fig. 35e) suggesting the NE-SW-trending fracture set was a perfect strike slip structure. Another fracture strikes E-W steeply dipping to the S and recorded slickenside plunging 17° to the west. The main fault plane in this outcrop is a dextral strike slip structure orientated NW-SE steeply dipping E.

Interpretation:

The outcrop is an anticline that has been mechanically altered for the highway. The faint SC fabric recorded indicates dextral kinematics in the main foliation plane (Fig. 36), the foliation at this location follows the same E-W (E83W 65N, Fig. 35b) orientation as the foliation in the previous outcrop (E84W 50N, Fig. 35c), suggesting that both outcrop enjoyed similar clockwise rotational movement. The E-W striking fault dipping S, is shown in the field in red solid lines (Fig. 36) and suggests shear planes have been displaced by the NE-SW fault set in a possibly local compressional regime, given the reverse nature of the displacement. The pegmatite vein orientating at NW-SE steeply dipping E is at a 15° clockwise rotation away from the main plane fault (Fig. 35b). The acute angle between them could suggest contemporaneous formation with the vein being classified as R fracture. The NE-SW faults are in accordance with the regional

trend of the Ribeira Belt shear zones. The data suggest these faults to behave in a dextral transcurrent system (Fig. 36 diagram).

4.5.3 Location 24 (UTM: 23K 443030 7400035)

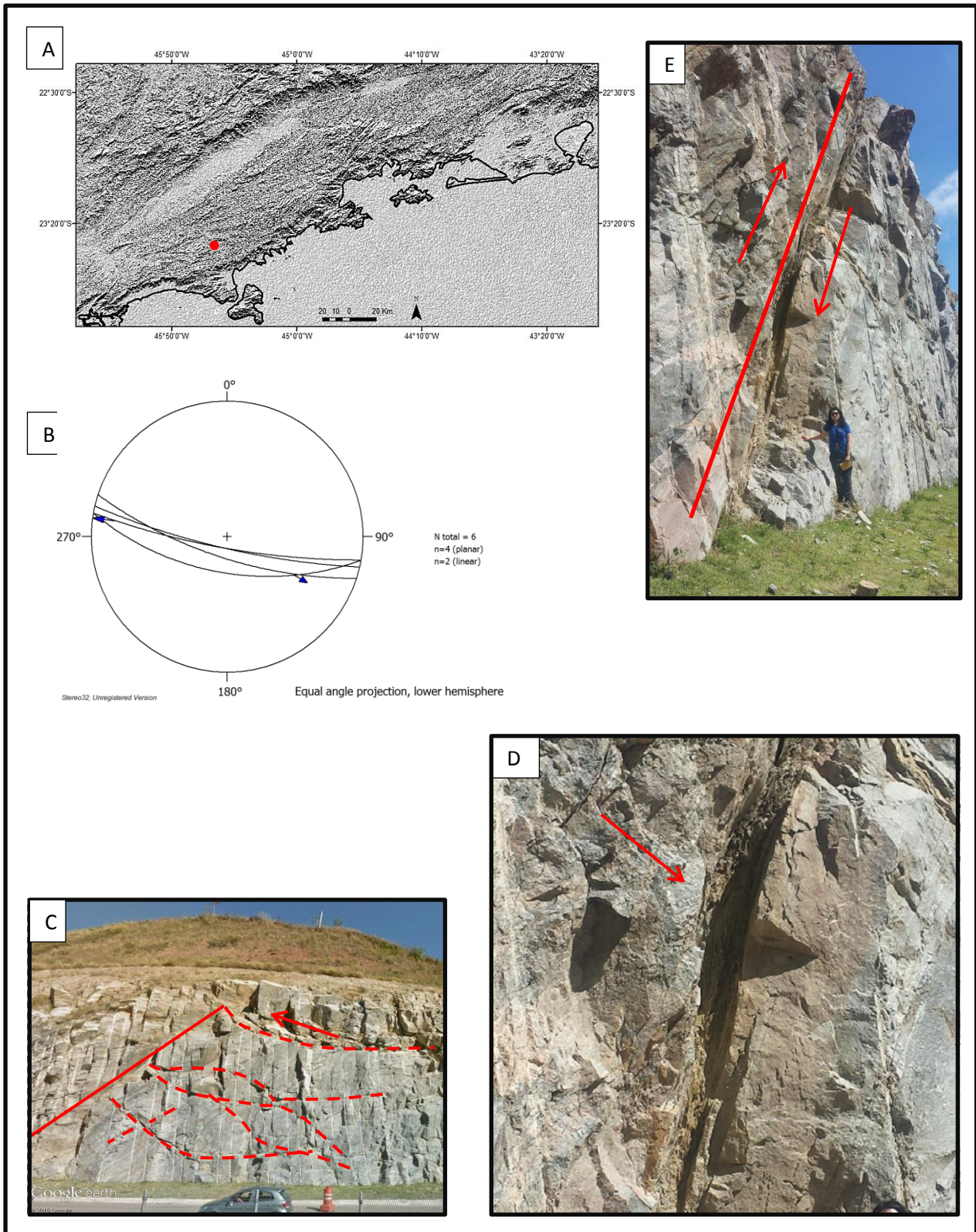


Figure 37 (anticlockwise): Fig. 37a is the map location of the outcrop, while Fig 37b stereographic projection; Fig. 37c displays the listric fault in the outcrop being cut-off by the E-W predominant fault set in the outcrop. Fig 37d pictures the fault gouge, and the fig 37e is an inset of the fault gouge in the reactivated foliation dipping south.

Outcrop description:

The outcrop, measuring 25m height and 80m width, at location 24 is at 787m elevation adjacent to highway SP-99 and is comprised of a heavily altered garnet gneiss. Due to the lack of place to park the car we were unable to take more measurements for this location other than the one here provided.

Outcrop-scale structures:

From a distance the geometry of layers in the outcrop which strikes NW-SE shows sinistral kinematics based on the geometry of secondary fractures present within the layers, especially towards the top. The layers have similar thickness and their arrangement suggests the minor faults have a listric geometry. A set of E-W orientated fractures dipping steeply S include a gouge-bearing fault (Fig. 37d and Fig. 37e). The listric faults have a sinistral shear sense whereas a dextral orientation is recorded by the E-W fracture set (Fig. 37b). Zeolite mineralization was also present. The pair of lineations in the stereographic representation (Fig. 37b) suggest a strike slip fault for one event and an oblique faulting for the other event. The E-W faults set are possibly the youngest of the events.

Micro-scale structures:

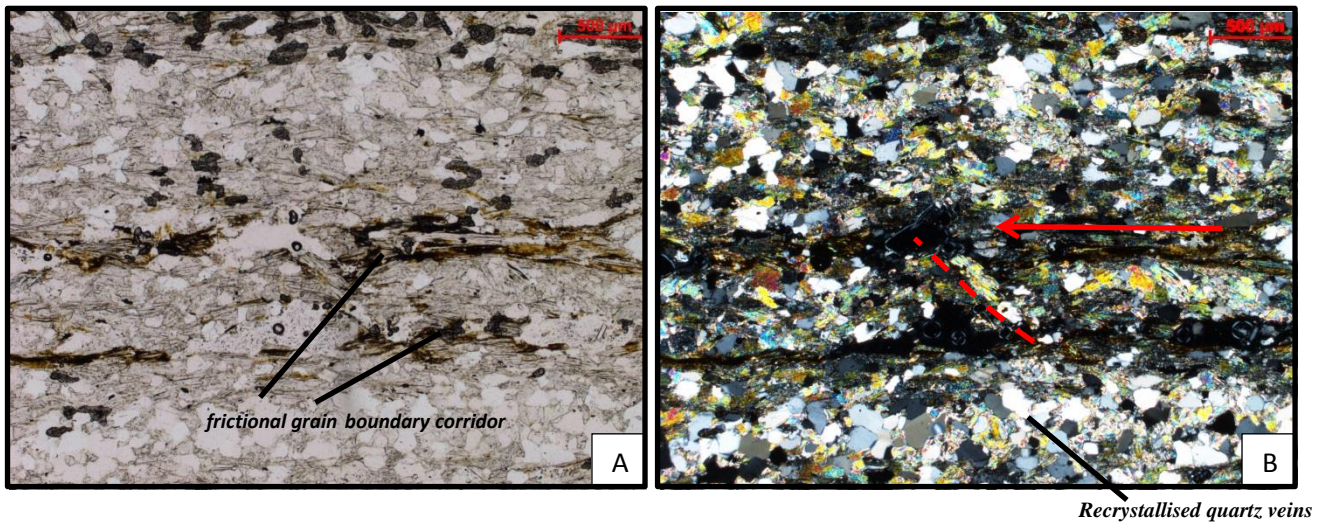


Figure 38: Thin section of the fault gouge sample taken from the location. Fig 38a is in PPL (plain polarized light). In Recrystallized quartz veins and frictional grain boundary corridor can be observed . Possible microfaults in dashed red lines.

In Figure 38 the gouge-bearing fault at microstructure scale shows evidence for reactivation. The phyllosilicates minerals follow the preferential orientation of the foliation. The recrystallized quartz vein appears to pre-date the slip surface (corridor) that accommodates the fracture in its centre, where an imbricated crystal of muscovite (biotite altered into muscovite) can be observed.

Interpretation:

Location 24 has the same NW-SE orientated ductile fabrics as the previous locations. The data suggest that at least two brittle deformation events have affected the outcrop. The lower angle listric faults of the set 2 secondary fractures form geometric structures that resemble an anastomosing linked system reminiscent of a strike slip faults where the faults are joined into segmented faults. The reactivation of the foliation is confirmed by the E-W fault set which are younger than the listric faults set, not very far from this outcrop a beautiful reverse fault has been observed (fig. 13) giving clear evidence of a reactivation event in the area. This might have been the responsible for the propagation of the E-W faulting set. The presence of slickenlines imprinted in zeolite veins imply that reactivation of the faults during the latest event happened at

a shallow depth in the crust. The major events in the area postulated by the literature happened during the Upper Cretaceous and Paleogene and concur with the orientation of the main structures in this locality. The gouge fault provided slickenlines indicating its reactivation, the fault of orientation E100W 60S has an oblique component to it plunging at 36°E, nevertheless a strike slip regime was the predominant regime in the area indicated by the results from the previous localities.

4.6 Sao Paulo Basin

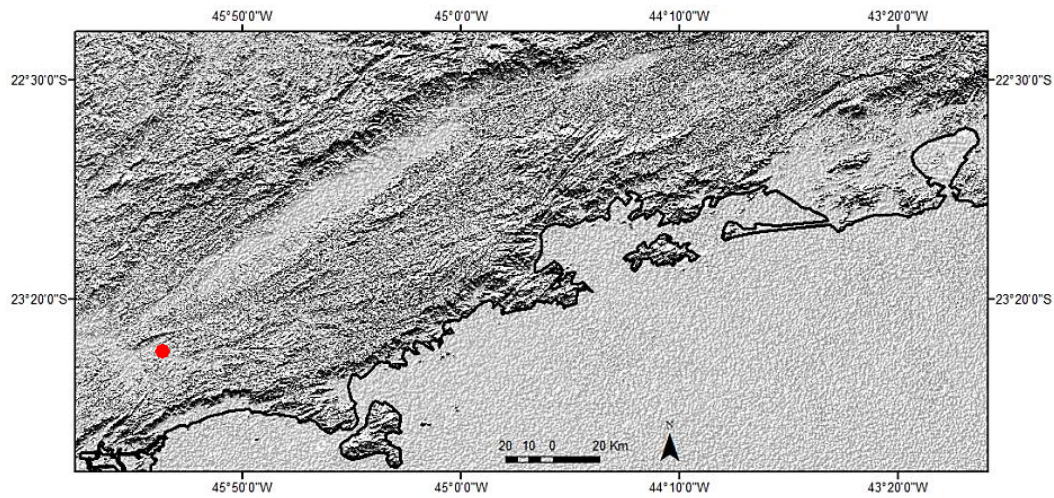


Figure 39: The quarry visited at São Paulo basin is marked with the red dot.

The São Paulo basin underlies the Greater São Paulo region and occupies an area of approximate 1000km². To the north, the basin is delimited by the Taxaquara-Jaquari fault zone and to the south is defined by irregular contacts with the Precambrian basement (Zanão, Castro et al. 2006). The Sao Paulo basin is the most southerly basin from the Central Segment of the Ribeira Belt included in the CRSB and is separate from the Taubate basin by a transform fault and sits in the junction between the Taxaquara and the Cacauiá Shear Zones.

The lithostratigraphic units recorded in the Sao Paulo Basin comprises the Resende Formation, Tremembe, Sao Paulo and Itaquaquecetuba Formations, overlain by alluvium and colluviums fed by the Alto Tiete Hydrographic Basin (Biagolini, Bernardes-de-Oliveira et al. 2013) (Fig. 39). Suguio, Riccomini et al. (2010) postulate the depositional age for the Itaquaquecetuba Formation might be $47,000 \pm 6,000$ and $89,000 \pm 12,000$ y.o. based on OSL (Optically Stimulated Luminescence) from samples.

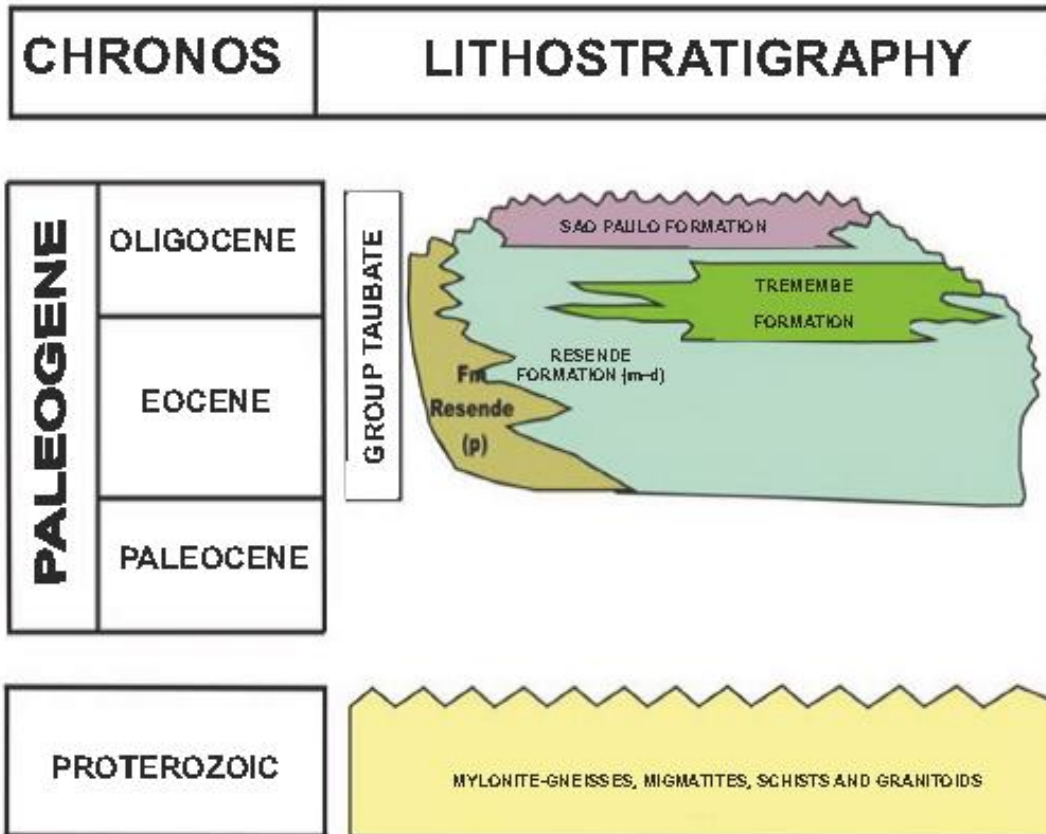


Figure 40: Chronostratigraphy column of São Paulo basin.. Modified from Riccomini et al. (2004).

4.6.1 Location 0 (UTM: 23K 362778 7403387)

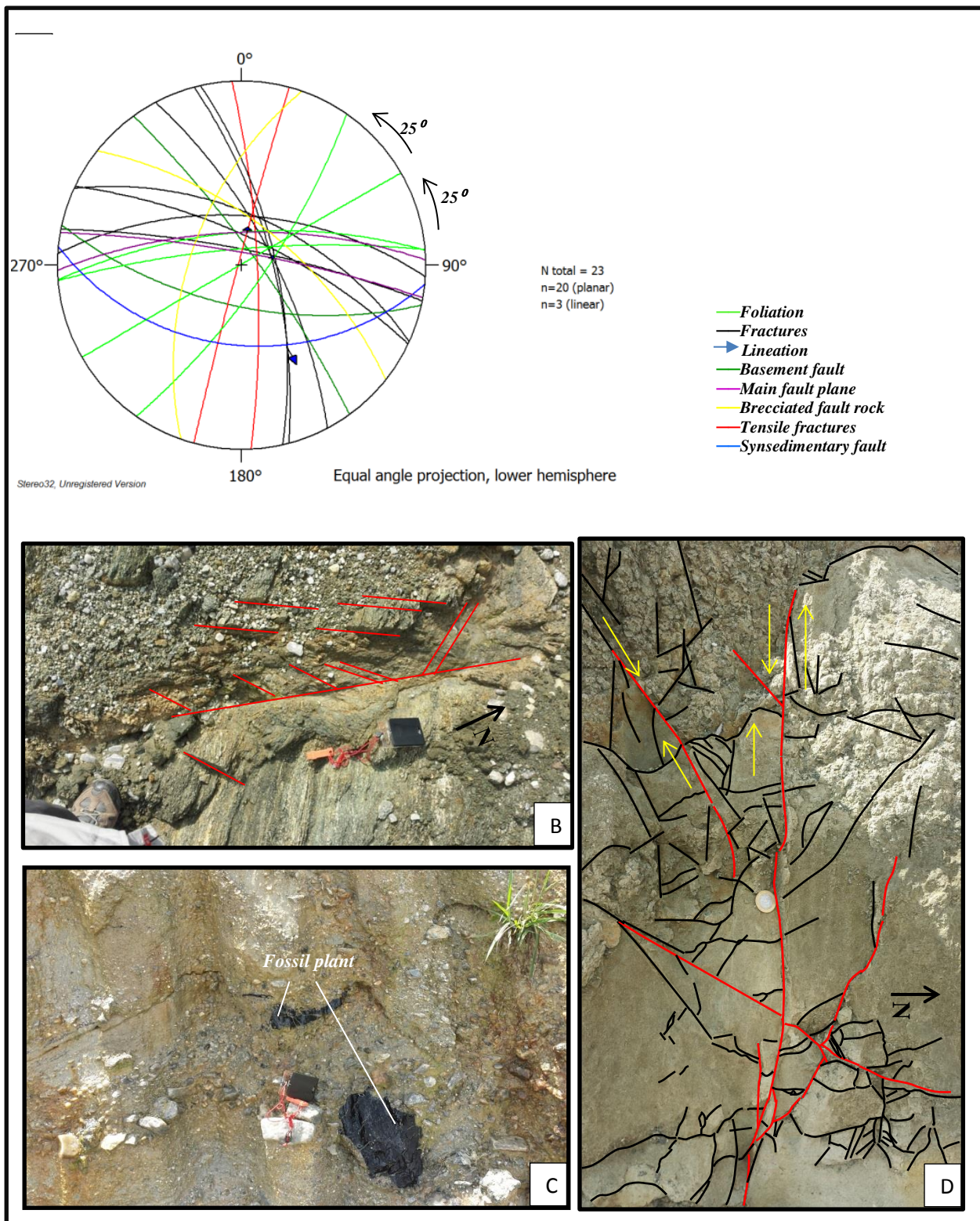


Figure 41: Fig 41a is the stereographic projection of its linear/plane structures, the lineation recorded here shows oblique to dip slip fault, the foliation rotated anti-clockwise in apparently two stages, 25° each, adding up to a 50° change in its strike. Fig. 41b is the basement gouge displaying secondary fractures. Fig 41c is an example of fossil plants which are very common within the Itaquaquecetuba formation of the Sao Paulo basin. These fossils have been dated back to Pleistocene, the fine upwards is characteristic of fluvial deposits. Fig. 41d is a picture of a flower structure displayed on the outcrop, the red lines are represent the original shape of the structure while the black lines represent the secondary that developed as faulting progressed under different stresses regimes locally.

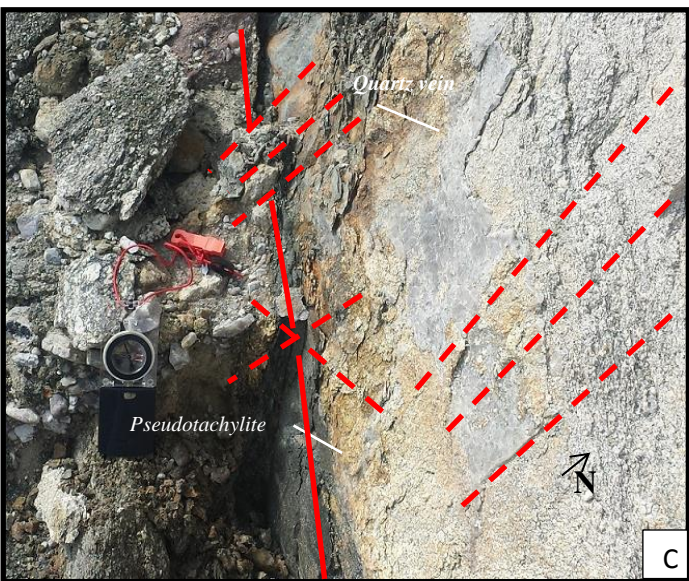
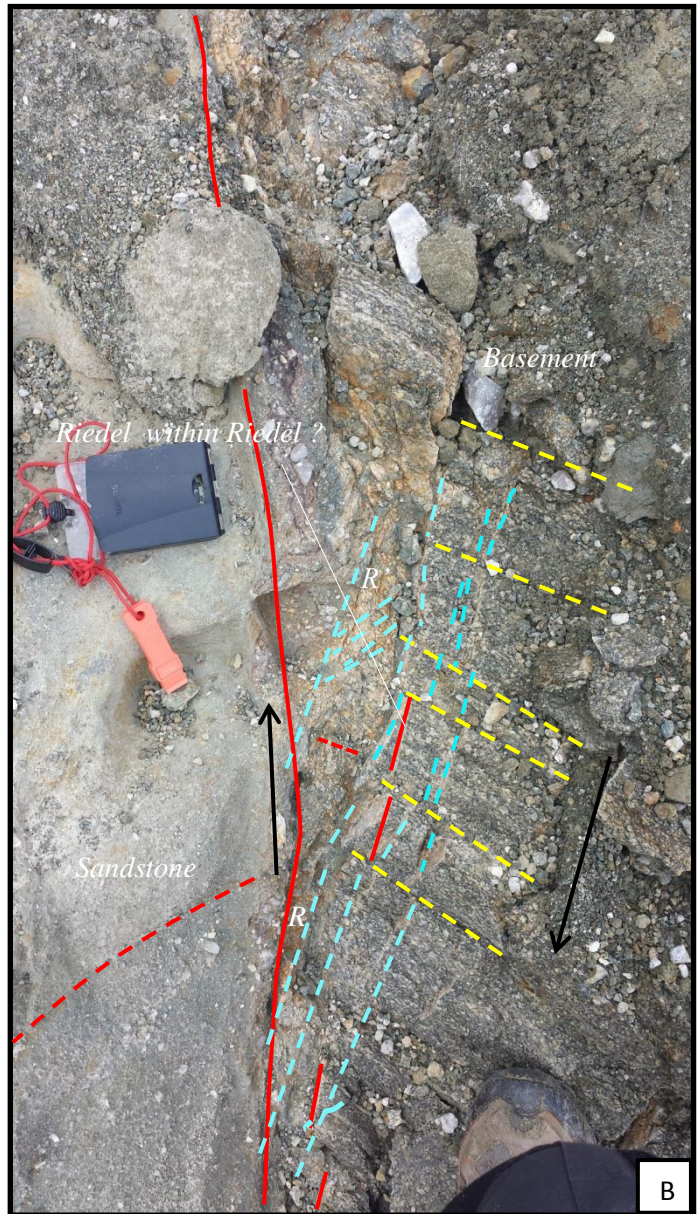
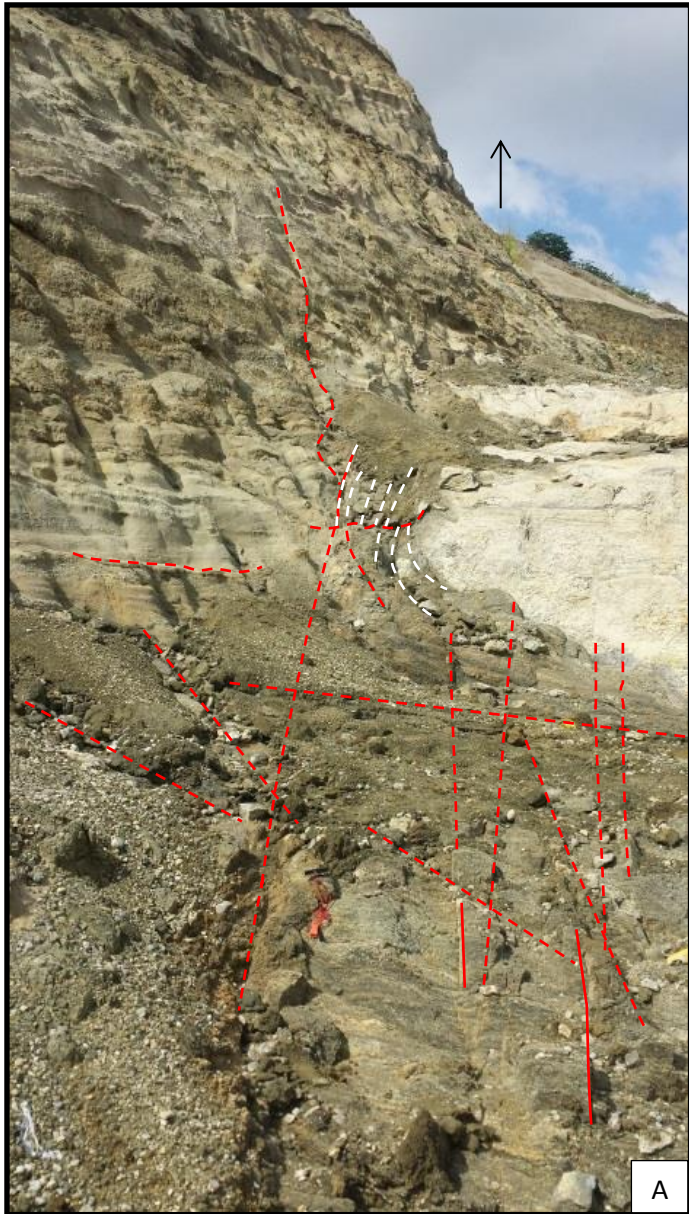


Figure 42(clockwise): Fig. 42a display the fault bending in the outcrop that occurred when the NW-SE fault joined the NNE basement fault. Fig. 42b is the inset of the structure marked with the red square in Fig. 42a. The riedel fractures are marked in blue (R and R'), the yellow dashed lines are possibly reactivated foliation which offset the fault line of the fault wedge. The solid red lines represent the fault line NW-SE. The basement rocks are augen gneiss (the dark one get its colour due to the contact with the running water from the quarry and Sandstone consistent of fluvial sediments). Red arrows indicating sense of movement. The solid yellow lines suggest a possible secondary fractures relationship that seems to repeat across the basement plan. Dashed white lines displaying the curvature of the faults.

Fig. 42c is the inset of the brecciated fault (basement/basement), the foliation at this location is striking E-W. It is possible to identify small indications of the fractures that cut through the faulted area, pseudotachylite is also present within the fault suggesting shallow tectonic activity. Reminiscent quartz material is also observed on the wall of the fault.



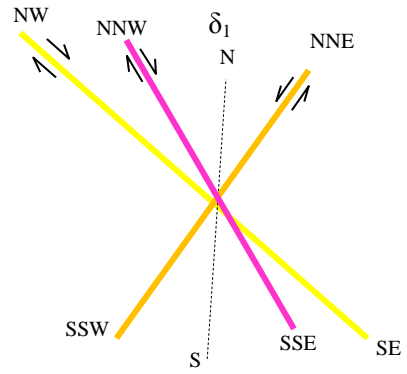
Unconformity - - - *Beddings* ——— *Fractures* - - - *Faults* ———



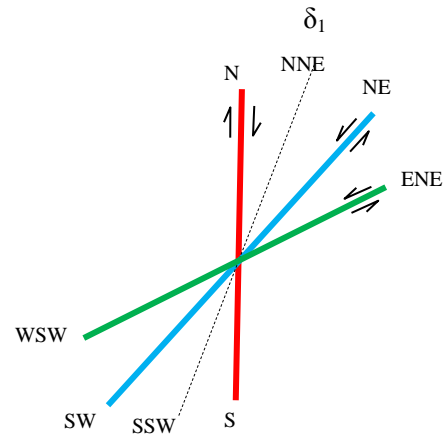
Figure 43: Fig. 43a and b shows a panoramic view of the outcrop with its different beddings within the Pleistocene sandstone. The black lines separate the beddings showing distinctive structures and textures, these beddings are following a NE-SW orientation, similar to the deflected foliation of the basement. A small angular unconformity is also marked with a purple dashed line. At the base of the outcrop gravel and some parts of the basement are still exposed. The red dashed lines are indicating fractures and red lines are faults where displacement is observed.



Figure 44: In this figure a better exposure of the outcrop beddings, sedimentary structures indicate a fluvial environment. The solid black lines are contact between the beddings whether they are discontinued or fractured. The solid red lines are faults recorded in the sediment and the red dashed lines are possible fractures.



Stress N-S dextral



Stress NNE-SSW Sinistral

Figure 45: *Inferred paleostress based on remote sensing lineaments inferred on the fault wall of the Pleistocene sandstone, according to Riedel diagram.*



Figure 46: Another point of the same outcrop in Fig. 46a, a negative flower structure indicates that the structures enjoyed a transtensional regime. Here is possible to observe water responsible for heavily weathered and reduced basement directly. The water also causes the erosion within the beddings leaving karstic like cavities structures cut across the beddings, which are marked by the solid black lines. The solid red lines are fault lines, and the dashed lines are used suggest fractures. The throw between unit A and B, suggests a syn-sedimentary process that might have been influenced by pre-existing basement structures, and the stream (blue) (Fig. 46b) running down the outcrop seems to follow the direction to the heavily weathered basement slope towards S.



Figure 47: The flower structure from Fig. 41c seen from another angle emphasizing the main fault planes. It shows the contact between the basement and sandstone, in red dashed lines infer tensile faults showing sinistral vergence.

Outcrop description:

This location is an active quarry on the margin of the Tiete River at the town of Itaquaquecetuba, on the SE side of the *São Paulo* basin. It is accessible via the Rua Rio Negro (Rio Negro Road) crossing through to the Av. Vereador Almiro Dias de Oliveira. The outcrop is about 10m high, 40m wide. An unconformity between the Pleistocene (sandstone) and the Precambrian (augen gneiss) basement is observed (Fig. 43a). The outcrop is heavily weathered, and the difference in colour between the white crystalline gneiss and the dark, greenish crystalline gneiss can be seen at Fig. 43c. The sandstone sedimentary structures (cross-lamination) suggest fluvial (meandering) depositional environment. Zanão, Castro et al. (2006) proposed that the Itaquaquecetuba formation is a system of alluvial fans. The sediments shows load structures, flame structures, dish structures and ribbon channels, with evidence of gravity-loading and a persistent lateral passage of water. Looking at the topography of the site, a rapid change in elevation from higher in the N to lower towards the S marks the location where E-W normal faults form scarps and have influenced the small streams of water that run down from the main fault plan in the outcrop (Fig. 46b).

Outcrop-scale structures:

The main foliation in the augen gneiss is orientated 85°E steeply dipping 80N and displays a dextral sense of movement. A deflection by faulting event has bent the foliation in an anti-clockwise sense to $\text{NE}035^{\circ} 75^{\circ}\text{S}$ and $\text{NE}060^{\circ}$ steeply dipping (90°) (Fig. 41a and Fig. 42b). The contact between the basement and the sandstone is inferred to be an unconformity (Fig. 37a in purple) covered by gravel. Secondary faults indicate sinistral oblique motion as suggested by the steeply plunging slickenside on the fault plane of the fault $\text{SE}165^{\circ}$ which steeply dips 70°E (Fig. 41a). Riedel faults (R) orientating $\text{S}177^{\circ}$ dipping 79°E indicates sinistral movement to the fault gouge $\text{SE}128^{\circ}$ dipping 63°NE . On a smaller fault wall beside

the outcrop, small fractures were inferred remotely (Fig. 44). These fractures display different orientations and sense of movement, here inferred trigonometrically, using a riedel shear model to infer the paeleostress, determined according to the relationship of the inferred conjugate fractures to the main fault planes (Fig. 44 and 45). Vertical displacement indicates that the main synsedimentary fault strikes $E097^{\circ}$ dipping $43^{\circ}S$ (Fig. 47). The syn-sedimentary faults orientated E-W within the outcrop displays the lowest dip angle in the area, which differs from the steeply dipping E-W set recorded in the basement.

Interpretation:

The data analysed from the outcrop may be interpreted to suggest at least two major events happened in the Sao Paulo basin area. These are a sinistral transcurrent (ST) and a dextral transcurrent (DT) deformation that possibly reactivated the basement.

The main fault planes striking E-W and NW-SE in the Neoproterozoic basement represent a change in the stress, possibly a rotational stress, indicated by the change in orientations recorded in the field from dextral to sinistral. These faults are in line with the fractures formed under the paleostresses determined by Riccomini 1989. They are believed to have been reactivated based upon indication produced by the field analyses, because associated fractures crosscut the Itaquaquecetuba formation which is of younger age than the Pleistocene. The foliation has dextral kinematics superimposed on the ductile deformation, an augen lens displaying dextral sense of direction, in line with the transcurrent dextral period from the Pleistocene. The parallelism suggested by the E-W set of faults to the initial foliation orientating at $E88W^{\circ} 70^{\circ}N$ and $E85^{\circ} 70^{\circ}N$ respectively, also indicates a possible basement reactivation (Fig. 14, Fig. 41a), with the E-W fault vertically offsets the foliation which subsequently has been deflected by a sinistral faulting event that rotated and tilted the foliation anticlockwise from $E88W^{\circ} 70^{\circ}N$ into $NE60^{\circ}$ and later to $NE35^{\circ}$ orientation (Fig. 46a), changing its dip direction from N to S. This process can be associated with a sinistral

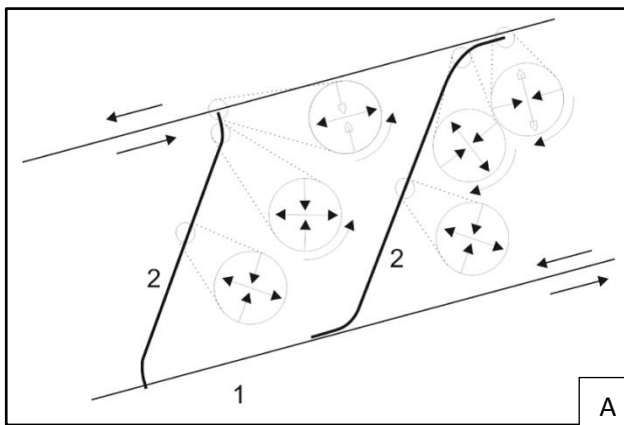
transtensional system, which is in accordance with the left-lateral E-W transcurrent regime with NW-SE extension suggested by Riccomini (1989) for the CRSB in the Neogene. Also according to Riccomini (1989), the asymmetry of the rift suggests listric fault behaviour in some border areas of the basin prior to its separation from Taubate basin, where the tilting of the blocks would be responsible to the changes on the orientation of the dips from N to S. Two of the tectonic processes listed in table 3 is present here, Transcurrent sinistral and Transcurrent dextral. The sandstone (Itaquaquecetuba Formation) in the outcrop is dated to have been deposited in the Late Pleistocene-Holocene (Suguio, Riccomini et al. 2010) under an E-W right-lateral transcurrent regime at this time, therefore the faults cutting through the outcrop are from Early to Late Holocene. The blind syn-sedimentary faults orientating E-W within the outcrop display the lowest angle in the area dipping 42°S which differ from the up to 80° steeply dipping E-W set recorded in the basement, it cuts through the Pleistocene material suggesting a extensional regime post-dating that period, therefore it is not impossible to suggest a local extensional stress orientating at N-S.

Bend of the fault

In Fig. 42b a bend is observed at the contact between the basement and the sandstone, it was caused due to the 165°NNW-SSE fault curved into and abutting against the 019°NNE-SSW basement fault and bends along it. The relationship between these faults points to a dextral sense of movement indicating a local principal horizontal stress (δ_1) orientation of N-S, creating a right-stepping *en-echelon* structure (yellow dashed lines in Fig. 42b). In order to explain the curved development of fractures and/or faults, Dyer (1988) proposed a model (Fig. 48a) where the younger fractures propagates towards the perturbed stress field in the vicinity and suggests the consistent change in the stress field is due to the presence of the older fault.

In Figure 48b, a similar curving-into-parallelism relationship between the faults is shown, the green dashed line represents the NNW-SSE fault and the pink dashed lines represents the older basement fault. It is possible to observe how the NNW-SSE fault curves towards the NNE-SSW older fault

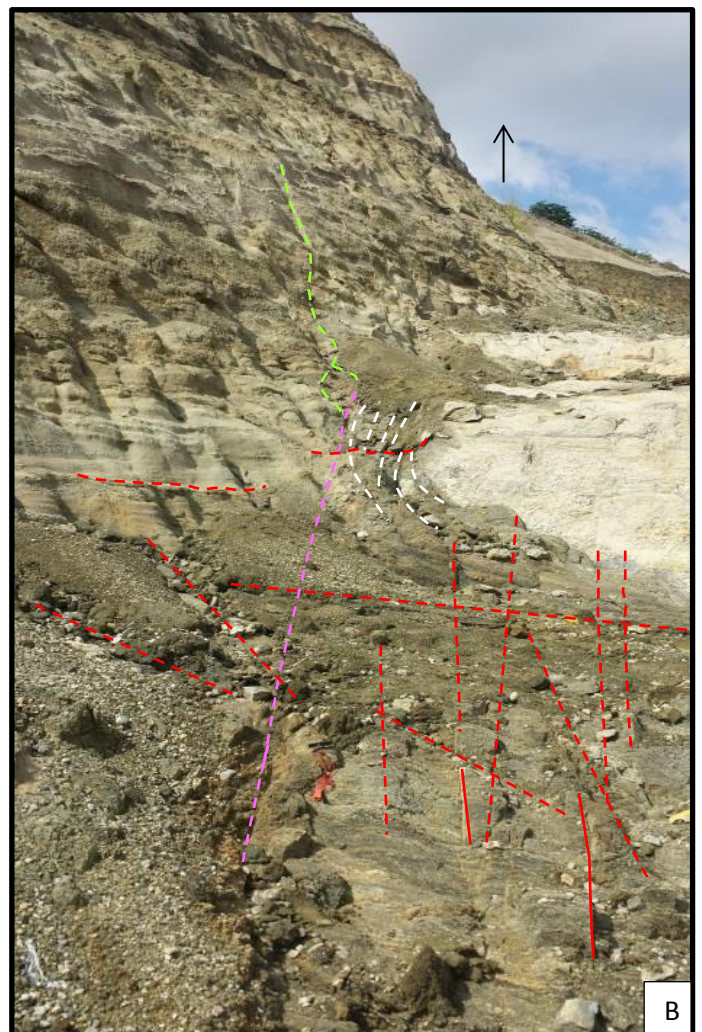
The white dashed lines are part of the NNE-SSW fault set, and seem to curve into and abut against the older E-W fault (red dashed lines Fig.48). These fractures display the same curvature process as the NNW-SSE fault, however some of them curve and stop perpendicular to another NNE-SSW, instead of running parallel to the fault as the NNW-SSE. This is indicative that the white dashed lines set is younger and that both cases fit to the models proposed by the diagram.



1 Oldest fracture 2 Youngest fracture. The black arrows show the rotation of the principal stresses near the older fractures, they are responsible for the sigmoidal geometry of the younger fractures.

Model modified from Hansen and Bergh (2012) modified from Dyer (1988)

Figure 48: Figure 48a the diagram suggests that the youngest fractures propagate towards the stress perturbations. Figure 48b The pink dashed lines in the picture on the left represents the fault NNE-SSW and the green dashed lines represents the NNW-SSE. White dashed lines represent faults from the NNE-SSW set going through the same dynamic with the older E-W fault set.



4.7 Lineaments Analysis (Comparison of Remote Sensing and Fieldwork data)

In this section, the remotely sensed lineaments and their relationship to the field observations are discussed. The lineaments are likely to represent zones of weakness formed by faults and fractures that have followed the anisotropy of rock foliation. The data plotted in Figure 49 were first analysed with the GEOrient software to enable the regional scale patterns to be established. The Figure 49a and 49b shows the results for the azimuth of the lineaments selected from aerial image. Figure 49b suggest that the longer lineaments have a preferential orientation that is aligned NE-SW (Fig. 5). Figures 50 and 51 show lineaments that represent brittle and ductile linear structures respectively.

As expected the ductile set represents the main NE-SW orientation (Fig. 49b and Fig. 51) as postulated by many authors (Riccomini 1989, Heilbron, Valeriano et al. 2008, Cogné, Gallagher et al. 2011). NE-SW was the pattern most visible throughout the area, whereas N-S orientations became more common in the southern region of the area of study from the mid- Taubate basin to the Sao Paulo basin.

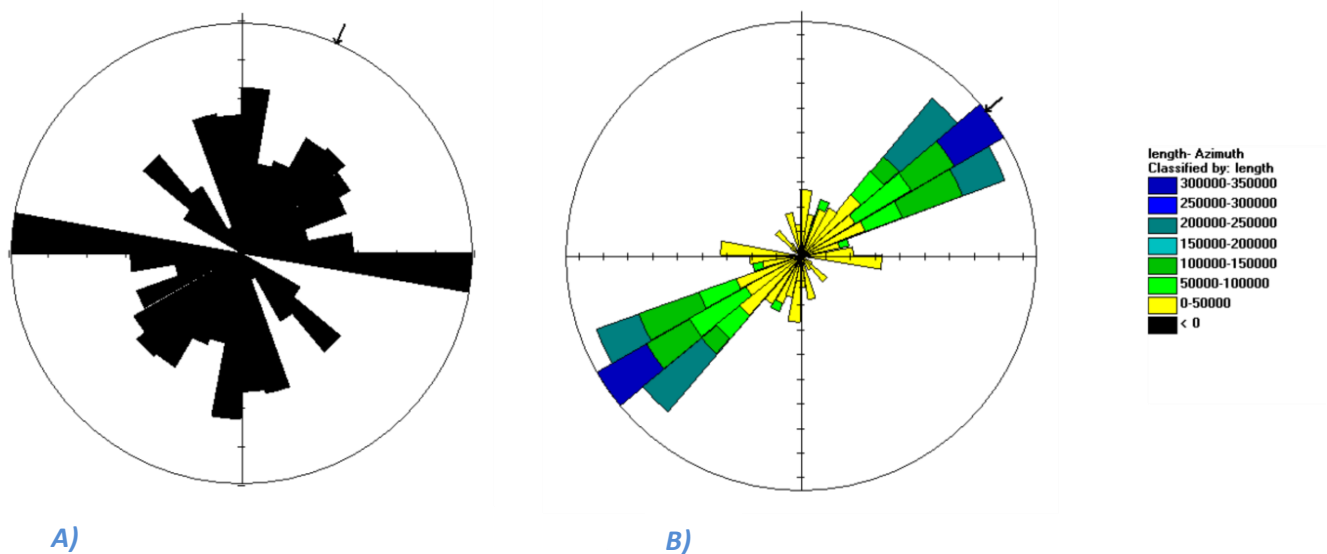


Figure 49: Figures A represent the azimuth of the structural lineaments and B has been separated by length. The colours are representing the different sets of the lineaments by orientation; the longer fractures are orientating NE-SW and are the ductiles lineaments reactivated at late cretaceous. The shorter yellow lines, representing the brittle fractures E-W and N-S, likely to have been created under different tectonic regime.

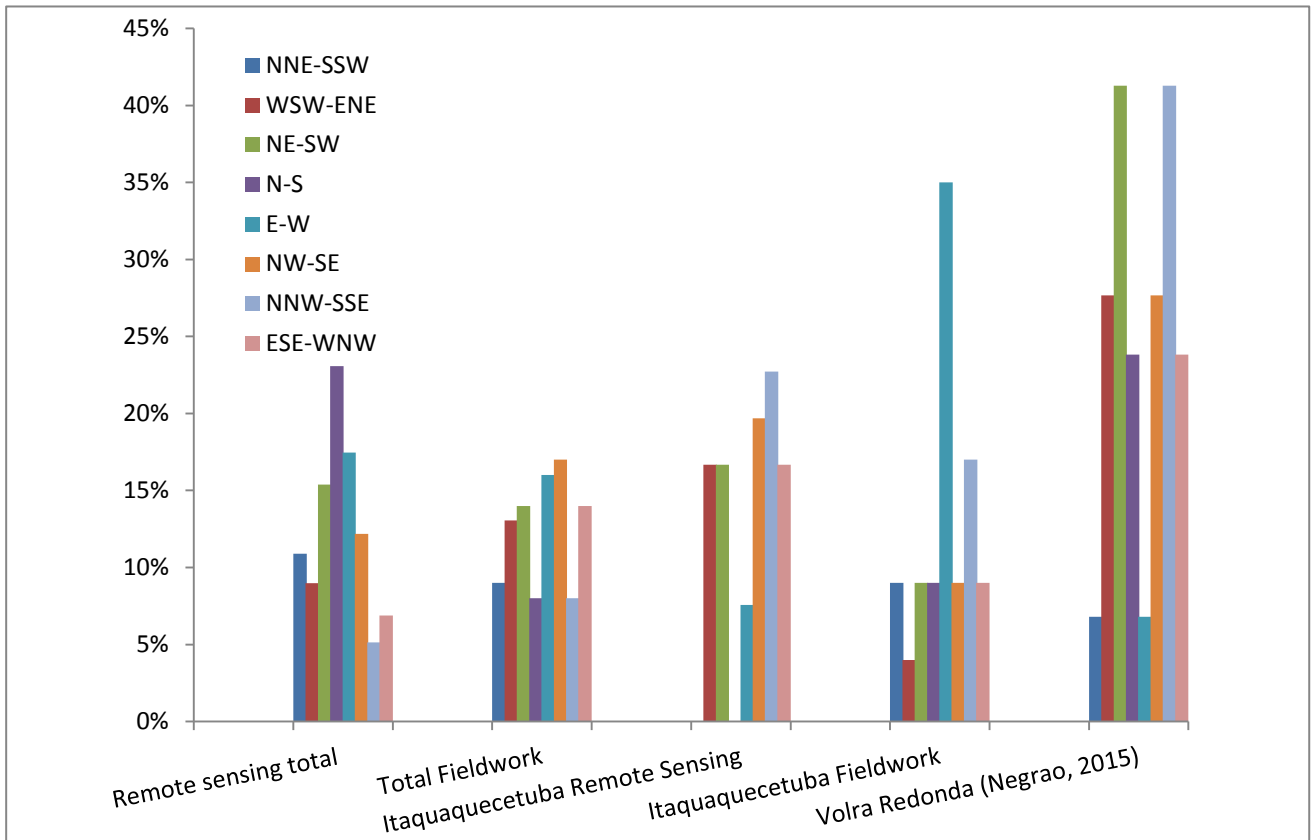


Chart 1: This shows the occurrences of the different fractures orientations captured by this work to the total of the area at outcrop scale and regional scale (remote sensing map of the DEM image).

Throughout the area between Rio de Janeiro and Sao Paulo the lineaments recorded, showed that mostly structures associated with the Serra do Mar and Serra da Mantiqueira regions have NE-SW trending fractures, which reflects the orientation of the ductile structures (Fig. 51).

The data recorded onshore presented is consistent with the overall NE-SW trend following the strong foliation in the area, and reactivation of these ductile fabrics and structures as faults has been postulated by many studies in the area. (Riccomini 1989, Zalán and Oliveira 2005, Cogné, Gallagher et al. 2011).

The data in chart 1 displays the number of fractures recorded in the field and the lineaments remotely inferred highlighting the areas of Sao Paulo basin (Itaquaquetuba) and Volta Redonda basin (dataset for Volta Redonda has been added from (Negrão 2014) (Negrão, Ramos et al. 2015)Negrão (2014)). The initial model created for this area from remote sensing

suggested a predominantly N-S orientation, although these structures are more prominent in the southern part of the area of study. The fieldwork pointed to fractures of orientations NW-SE/E-W to be more prominent in the field. This result can be attributed to the fact that these structures are associated with an event prior to the development of the Tertiary basins and are better exposed due to the denudation processes that have exposed the crystalline basement and depleted the area of younger sediments. This set of faults can be observed relatively consistently throughout the data in the chart. Locally the Itaquaquecetuba outcrop showed predominantly E-W/NNW-SSE orientation, according to Riccomini, Sant'Anna et al. (2004) the later structures controls the sedimentation in the area, associated with the formation of basin. The NNW-SSE set is also consistently present in the small data set remotely acquired within the Pleistocene sandstone strata of the Itaquaquecetuba location, in contrast, the E-W set is considerable smaller in comparison with the field collection at the same location. This example shows that a common theme that emerges when comparing the remote sensed data to the local fracture distributions. At Volta Redonda the lineament datasets show predominantly NNW-SSE and NE-SW orientations and display a similar profile to the Itaquaquecetuba remote sensing results but there is considerable discrepancy for the number of E-W structures between the basins compared to the field datasets.

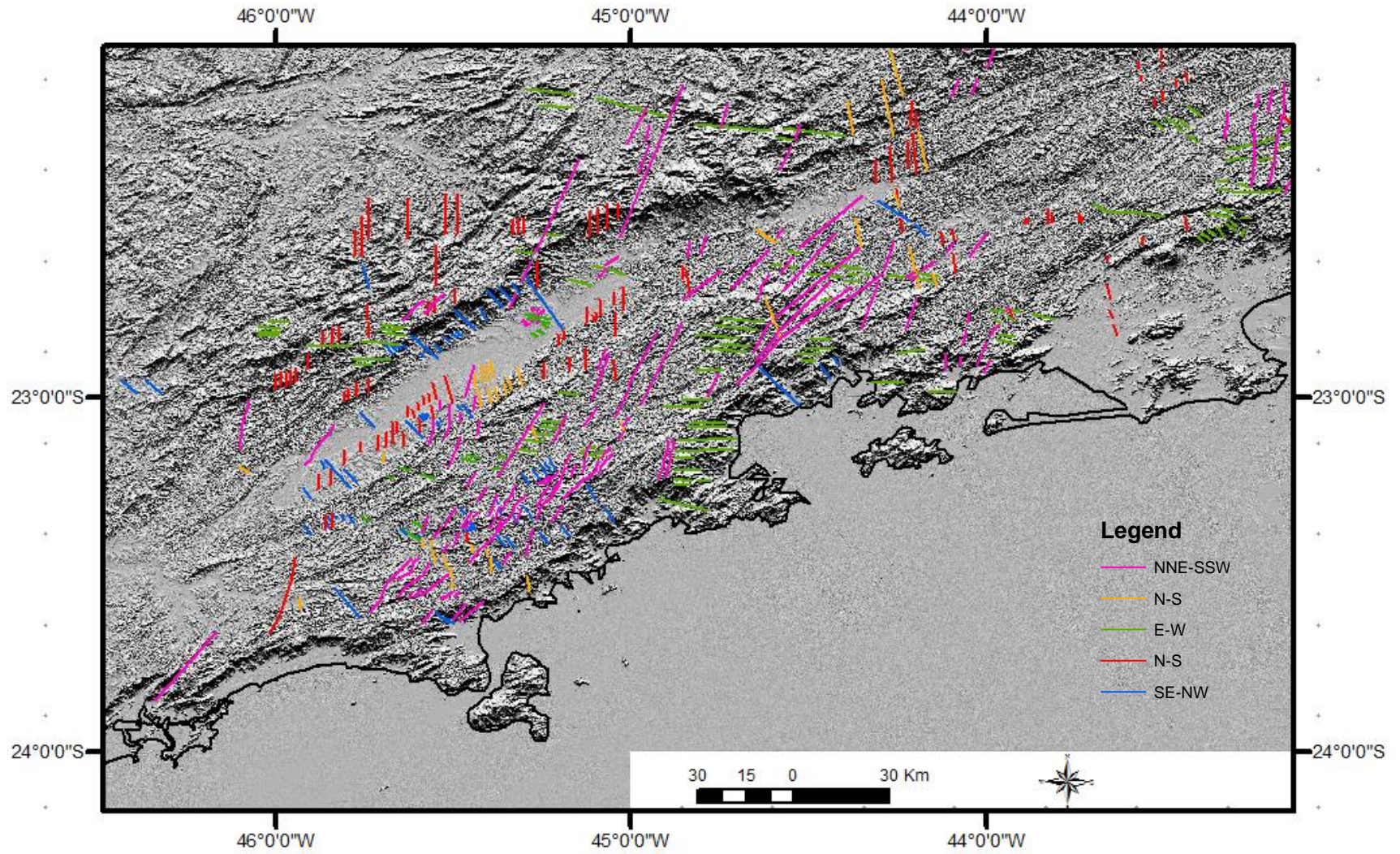


Figure 50: The lines in this map represent the brittle structures in the area, E-W and N-S orientations.

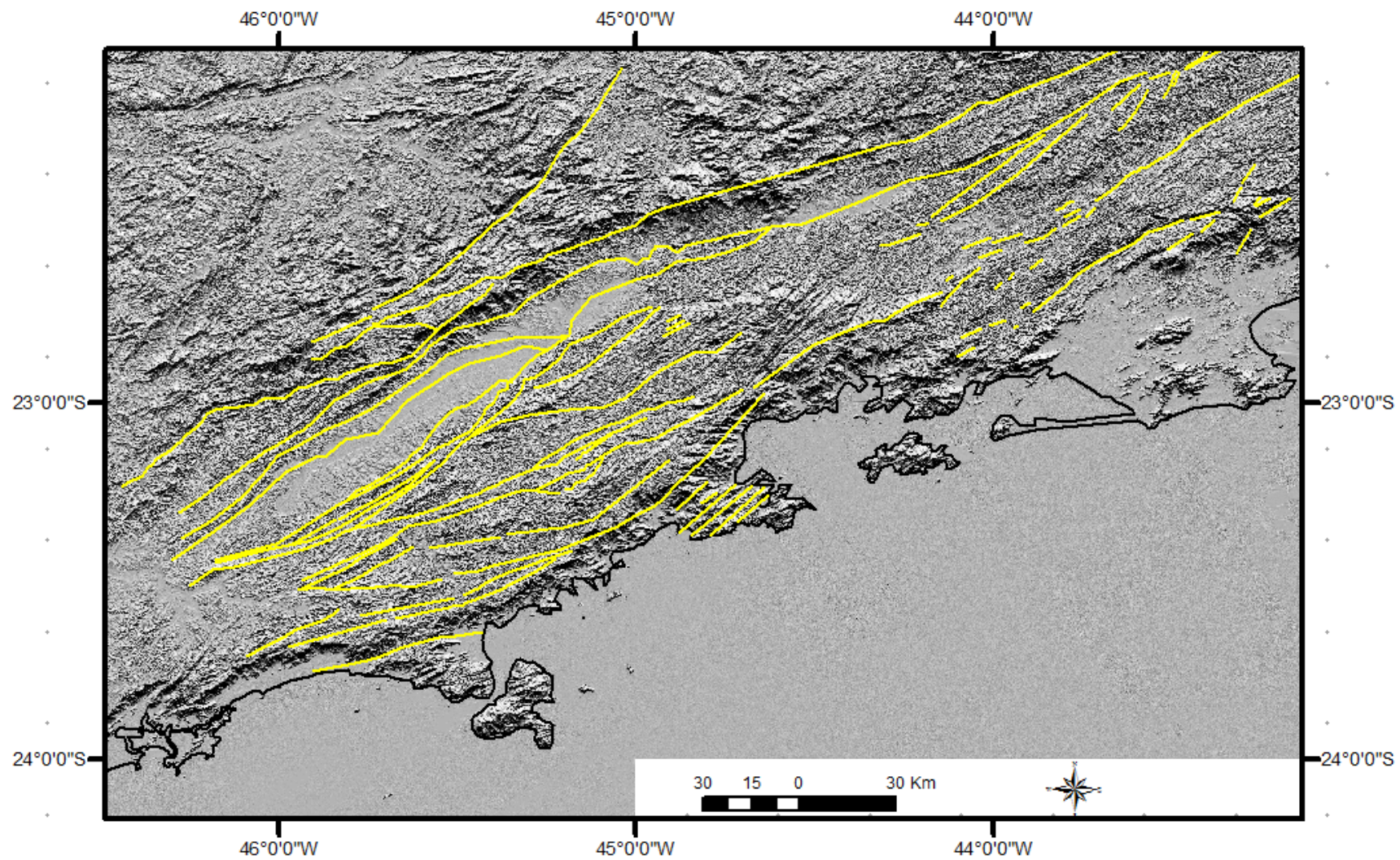


Figure 51: The yellow lines are ductile features, primarily formed during the amalgamation of Ribeira belt during the Neo-Proterozoic.

5 Control of the local structures – Discussion

The data collected during this study were expected to reflect the recent geological events that deformed the SE Brazilian rifted margin. The locations here, for example locations 1, 2 and 9 display good expressions of these events, and evidence for reactivation and/or basement influence is examined in this discussion. According to (Gontijo-Pascutti, Bezerra et al. 2010), the Santana Graben should be included in the CRSB system, because its graben features can be correlated with other basins belonging to this system. The table below displays the orientation both of the foliation and fractures that could support either reactivation of the foliation or/and basement inheritance. Each foliation has a correspondent fracture set in each location, and whether it follows the foliation trend. It can be indicative of the fractures following the basement anisotropy caused by pre-existing structures (i.e. strong foliation and pre-existing faults/fractures) and consequently reactivating said structures or having its orientations influenced by the pre-existing features. The basement foliation shows a clockwise rotation from NE-SW in the northern area of the study area to E-W in the southern part of the study area. Although the sense of movement of the faults is not specified with the exception of those in the Santana Graben and the Sao Paulo localities, many of the other locations display, through stereographic analysis, structures that are parallel to those expected to have been created by the regional events, which according to Riccomini (1989) are due to a change of the subduction and mid Atlantic-ridge forces, when one overcomes the other.

The Central Segment of the CRSB (Volta Redonda, Resend, Taubate and Sao Paulo basins) are located in a structurally complex area. Many papers have addressed the uplift of these regions

(Hackspacher, Juliani et al. 2001, Hackspacher, Ribeiro et al. 2004, Tello Saenz, Hadler Neto et al. 2005, Hiruma, Riccomini et al. 2010, Franco-Magalhaes, Cuglieri et al. 2013, Karl, Glasmacher et al. 2013) have postulated rapid exhumation events correlating with the Upper Cretaceous and Paleogene periods. These periods are associated with the major recent seismic events that formed and deformed the CRSB. The E-W and NW-SE fault sets of the CRSB in the Neoproterozoic basement have been reactivated first as normal faults during the Paleogene and later as strike slip (Riccomini, Sant'Anna et al. 2004). In the Neogene the stress regime changed from extensional regime to strike slip regime with local compression NE-SW (Riccomini 1989, Zalán and Oliveira 2005, Cogné, Gallagher et al. 2011). Still according to Riccomini, the CRSB was under NW-SE compressive stress throughout the Late Pleistocene-Holocene, changing to E-W/NW-SE extension during the Holocene and finally E-W compression at the present day (Fig. 52).

In the field what was noticed is that the structures geometrically suggested the inheritance of the basement as per the definition of Misra and Mukherjee (2015) and Vauchez, Tommasi et al. (1998). This work was unable to provide paleostresses data due to the lack of information needs to execute stress inversion for the areas visited. Nevertheless the geometrical relationship of the faults suggested an initial assessment to inheritance of the basement in the modern architecture of SE Brazil that would fit to a model of reactivation of pre-existing structures of a passive margin.

The table 3 displays the tectonic events that possibly reactivated the pre-existing structures during the CRSB resume the events and most of the authors agree with the events postulated by Riccomini (1989). All the structures and their orientations correlate with a model of an oblique strike slip basins. The authors above all agree that the tectonic evolution of the CRSB occurred in four events throughout the Cretaceous until the present day.

The orientations recorded during the fieldwork for this project are believed to be correlated with these events. The tables below synthesises these structures in order to compare the structures recorded in the field with the structures orientations postulated by Riccomini (1989) however to correlate them is difficult given the difference in scale. Table 1 is regional-scale whereas table 2 display mostly local structures. Riccomini (1989) using the Right dihedral method determined the orientations for the structures, the method is not reliable to stablish age relationship between structures. Not much fieldwork has been done focusing on the local brittle reactivation and its control of the onshore of the continental margin, hence it is possible that an update for these structures are long overdue. Table 2 is more representative of local structures which can justify its more diverse strikes, it differs from table 1 in the sense that table 2 has structures not only relevant to the CRSB regional deformation but also structures pre-dating the Cenozoic at local scale. For example at location 6/7 (Fig. 21a) a low angle N-S structure has been recorded that follows the Neoproterozoic foliation orientation, but it is cross-cut by a NE-SW fault, this N-S data set correlates with extensional regime and diagnostic characteristics as boudinage are also recorded within the foliation. This fault NE-SW could be a by product of the Upper Cretaceous extensional regime. Between these two tables what can be noted is the consistent presence of the NE-SW/NW-SE faulting sets. These are the main sets which controlled the deformation of the CRSB at regional scale and represents the pre-existing zones of the Ribeira belt and they are key to understanding the controls of the recurring and new structures in the area.

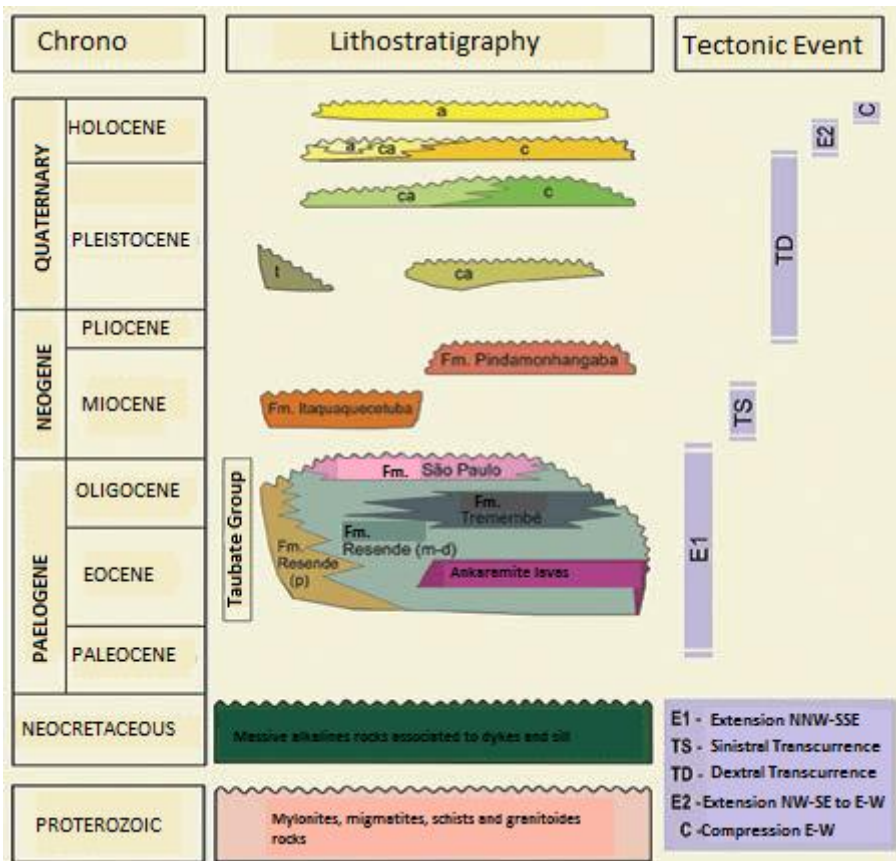


Figure 52: Stratigraphic column for the CRSB with tectonic regime according to Riccomini, Sant'Anna et al. (2004)

| <i>Period</i> | <i>Stresses</i> | <i>Faults associated with</i> |
|------------------|-------------------------------|-----------------------------------------------------------|
| Eocene-Oligocene | NNW-SSE (Extensional) | ENE/NE (Normal) |
| Neogene | E-W (Transcurrent sinistral), | NE-SW (Normal) NW-SE (Reverse) WNW-ESE(Strike-slip) |
| Pleistocene | E-W (Transcurrent dextral) | NE-SW (Reverse) NW-SE (Normal) |
| Early Holocene | NW (WNW)-SE (ESE) (Extension) | N/A |
| Late Holocene | E-W (Compression) | |

Table 1 and Table 2: Table 1 is a synthesis of the paleostress suggested by Riccomini (1989) with the faults associated with these stresses based upon Angelier and Mechler (1977) method. Table 2 is a synthesis of the main structures recorded within the area of study for this project.

Fo – Foliation

Fr – Fracture

| <i>Locations</i> | <i>Basin/Graben</i> | <i>Orientation Fo</i> | <i>Orientation Fr Relative age</i> | | <i>Inferred stress directions</i> |
|------------------|---------------------|-----------------------|-------------------------------------|-------------------------------------------------------------------------------------------------------------------------------------------------------------------------------------------------------------------------|-----------------------------------------|
| Location 2 | Santana Graben | NE-SW | NW-SE/NE-SW | NW-SE fractures terminates at the NE-SW fractures | Unknown |
| Location 6/7 | Volta Redonda Basin | N-S | N-S/NE-SW | N-S fault is a basement low angle fault, NE-SW fault cuts through the basement | Transtensional dextral Regime |
| Location 28 | Volta Redonda Basin | E-W | NW-SE/ NE-SW / WNW-ESE/ NNW-SSE | The dyke NW-SE crosscut the foliation E-W and is offset by NE-SW fault. | NNE-SSW and NE-SW Transtensional Regime |
| Location 9 | Resende Basin | Breccia | ENE-WSW/ NW-SE/NE-SW/N-S | The breccia has a E-W orientation and is crosscut E-NE-WSW oblique fault. An N-S fault is also seen abutting against the fault core. | NW-SE Extensional Regime |
| Location 27 | Taubate Basin | NW-ENE-SW | ENE-WSW/ NW-SE/NE-SWNW-SE/NE-SW/N-S | E-W gouge bearing fault is the oldest structure in relation to NW-SE. A second set E-W is truncated by the NW-SE fault. The N-S set abut against the second E-W set, and becomes the youngest structure in the outcrop. | NNW-SSE Transtensional Regime |
| Location 0 | Sao Paulo Basin | E-W/NE-SW | NW-SEsn/E-W/N-S/NNW-SSE/NNE-SSW | E-W set is the oldest set in these relationships, parallel to the basement it is truncated by the NW-SE faults set, the NNW-SSE is a basement fault that propagates into the Upper Pleistocene sandstone. | N-S Extensional Regime |

| TIME (ma) | Geochronology | | Volta Redonda Basin | TE according to Negrão, 2015 based upon Sanson (2006). | Resende Basin | TE according to Albuquerque (2004) | Taubaté Basin | TE according to Cogné, Cobbold et al. (2013) | São Paulo Basin | TE according to Riccomini (2004) | This work (Based upon literature and fieldwork) No tectonic event have been recorded | | | | | |
|--------------------------|------------------|-------------|---------------------|--------------------------------------------------------|--------------------------|------------------------------------|----------------------------|---------------------------------------------------|-------------------|----------------------------------|--------------------------------------------------------------------------------------|---------------------------|----------------------|-------------------|--------------------|-------------------|
| | Period | Epoch | | | | | | | | | | | | | | |
| Lithostratigraphy | | | | | | | | | | | | | | | | |
| 10 | Quaternary | Holocene | Alluvium | Extension NW-SE | Alluvium | Extension NW-SE | Alluvium | E-W Compression (based upon the world stress map) | Alluvium | E-W Compression | Alluvium | | | | | |
| | | Pleistocene | | | | | | | | | | Transcurrent Dextral E-W | Transcurrent Dextral | | | |
| | Tertiary | Neogene | Pliocene | Pindamonhangaba Formation | Transcurrent Dextral E-W | Florianópolis Formation | Transcurrent sinistral E-W | Transpressional E-W | Quiescence Period | Itaquaquecetuba Formation | Transcurrent sinistral | Pindamonhangaba Formation | | | | |
| | | | Miocene | | | | | | | | | | São Paulo Formation | Resende Formation | | |
| | | | Oligocene | | | | | | | | | | | | Tremembé Formation | Resende Formation |
| | | | Eocene | | | | | | | | | | | | | |
| | | Paleogene | Quatis Riverside | Quatis Riverside | | | | | | | | | | | | |
| | | | | | Paleocene | Alkaline Volcanic rocks | Guanabara Graben | | | | | | | | | |
| | | | | | | | | CRETACEOUS | Basement | Guanabara Graben | | | | | | |
| | | | | | | | | | | | PROTEROZOIC | Basement | Guanabara Graben | | | |
| Basement | Guanabara Graben | | | | | | | | | | | | | | | |
| | | Basement | Guanabara Graben | | | | | | | | | | | | | |
| | | | | Basement | Guanabara Graben | | | | | | | | | | | |

Table 3: Summary of previous authors and the lithostratigraphy examined in this body of work

TE – Tectonic Events

The Santana Graben is not in the table as it is not part of the CRSB, but according to Gontijo-Pascutti, Bezerra et al. (2010) it should be added to the Continental Rift of Southeast Brazil system of Zalan (2004) given its tectonic evolution characteristics. The faults controlling its genesis followed the basement fabric (e.g. locations 1 and 2) NE-SW with younger faults NW-SE abutting against them. The outcrops in this location yielded data in line with Gontijo-Pascutti (2010) studies within the Santana Graben and displacements of at least 7m were recorded following the same trend of the supposedly first event during the Palaeogene that created the Graben. The change in the regional stress documented by the table 2 is possibly represented in this case by the faults measured in the NE-SW/NW-SE conjugate structures.

A similar pattern was observed in the Volta Redonda basin, which according to Negrão, Ramos et al. (2015) went through more phases of deformation and display both reactivation of the basement in bimodal NW-SE/ENE-WSW striking faults which is in accordance with the findings of location 28 (Table 2). The faults recorded this location display shallow angles and follow the anisotropy of the pervasive fabric and are parallel to pre-existing structures. This location is a good candidate to assess the reactivation of the basement using a more sophisticated and robust dataset i.e. subsurface images and seismic data. At location 6/7 the fault is a dip-slip structure with a strike-slip component to it, showing a more oblique angle to the main trend of the CRSB, this fault cross-cut the foliation, it is possible that this fault is part of a setting of conjugate faults, possibly a consequence of the regional strike slip regime. The sediment it cuts is part of the Pinheiral Formation of Palaeogene age (Fig 21), which according to the authors on the table undergone effects of a transcurrent sinistral E-W deformation.

The Resende Basin follows the NE-SW trending main fault set, and it is where the first site of reactivation was observed in this project. A breccia at location 9 displayed polymodal fractures, and microstructures showed evidence of reactivation of a breccia fault rock (Fig. 25

and Fig. 26). All the locations of Resende basin displayed fracture orientations that are consistent with the CRSB main orientations. In the Taubate basin, there was only one location representative of its structures, nevertheless it still offered useful data for this study. The quarry visited provided information on the depth of its structural development as well as possible basement influence. The foliation at this point changes its orientation from NE-SW to NW-SE and a set of fractures with the same strike has been recorded at location 27. This change in orientation indicates a change in stress as per the table 2 aforementioned for the paleostresses from Extension NW-SE in the Palaeogene to NE-SW in the Holocene. The presence of lineation imprinted within zeolite infill in pre-existing fractures suggested that the tectonic event happening at shallow depth, considering that zeolite can be formed at 200°C (Coombs, Ellis et al. 1959). To the east of the Taubate basin, the area that is part of Embu Terrain and Coastal complex showcased interesting features along the Tamoios Highway. Here the foliation changes again this time to E-W orientation and again E-W faults are recorded in the outcrop as per location 27. Also along the Tamoios highway, a reverse fault is at display where it is possible to identify the reactivation of a pre-existing fault at the area of the Cubatao shear zone (Fig. 14).

The Itaquaquecetuba site in the Sao Paulo basin displayed the best outcrop-scale structure and lithologic exposure at location 0, an active quarry by the Tiete River (Fig.42a), the structures shows a strong geometric display for basement inheritance and has been postulated by Riccomini (1989) to be a pull-apart basin as part of the CRSB. In this location the main foliation has an E-W orientation, although it has been deflected during faulting causing an anticlockwise rotation, from E-W into NE-SW. The Sao Paulo basin displays Late Pleistocene–Holocene sediments and Quaternary faults that imply that these structures are possibly still active; a network of small structures forming around a negative flower feature implies strain is building around the Quaternary structures. Many aspects have to be taken

into consideration, especially when dealing with an area that demonstrates several features that might influence its tectonic activity and the control of its structures. At the Itaquaquecetuba site, Holocene sediments displayed a buried syn-sedimentary fault striking E-W, it is prominent in the outcrop and basement fault rocks have been recorded, suggesting this fault could be a segment of a basement fault. The fault rocks crosscutting the basement show possible evidence that support the influence of pre-existing faults/fractures in the basement on the orientation of the newly developed faults, these younger faults in the basement follow the same orientation as the pre-existing ones, and many of them are seen propagating from the basement to the Pleistocene formation. The gouges display mylonitic texture and contain mylonite clasts, with differences in grain sizes implying different degrees of shearing. The parallelism of the synsedimentary E-W faults with the basement fault rock foliation indicates the influence of the foliation anisotropy. It is possible that the anisotropy of the foliation contributed to the development of new fractures, causing reactivation of these gouges, small fractures are observed within the gouge, some of which demonstrate Riedel shear geometry in effect Riedel within Riedel. Following the structures from the basement into the Itaquaquecetuba formation it is easy to recognize the negative flower structures branching out from the main E-W fault, this is probably a Riedel fracture that propagated during a period of local deformation, as suggested by the analyses of the damage zone (Fig. 41d), which displays a sinistral sense of movement. These structures do not represent the transpressional modern stress attributed to SE Brazil, these could be a product of local extensional stress from the early Holocene as postulated by Riccomini 2004. The parallelism of the synsedimentary E-W faults with the basement foliation, that is itself moderately dipping S, and is a branch of a negative flower structure (Fig.47). This is probably a Riedel fracture that propagated during a period of local deformation, as suggested by the analyses of the damage zone (Fig. 41), which displays a sinistral sense of movement,

even though the flower structure display a negative profile. Along the E-W fault set, the NNW-SSE/NNE-SSW faults in the basement propagates towards the Pleistocene sediments, and are consistent with the modern transpressional stress attributed to the SE Brazil. Despite not having recorded many N-S faults in the area as expected considering the stress regime, the NNW-SSE/NNE-SSW are consistent with these expectations. It is possible to suggest that some of these fractures/faults have been reworked as gouges (Fig. 41b), which display sinistral kinematics and show water escape sedimentary structure, consistent with a compressional (transpressional in this case) setting with Principal Horizontal stress orientating E-W according to Anderson's theory.

As noted before, in the north of the area of study a NE-SW orientation for the foliation and fractures prevail, whereas E-W orientations for both are dominant in the mid to southern parts of the area of study. Whilst this is no confirmation that the pre-existing foliation is reactivated and only circumstantial evidence for influence of the basement has been observed it does display geometric relationships that demonstrate possible pre-existing structural reactivation on the brittle deformation processes within the crystalline basement which can be termed 'tectonic inheritance'. In similar exposed continental basement areas, for example NW Scotland and NE Brazil the influence of the basement has been researched and demonstrated through quantitatively methods (Beacom, Holdsworth et al. 2001, Kirkpatrick, Bezerra et al. 2013). Salomon (Salomon, Koehn et al. 2015) in his paper made a comparison between the NE and SE Brazil, and cited the work of (Bezerra, do Nascimento et al. 2011) who postulated strike slip faulting with an E-W compressional axis based on boreholes and breakouts in the NE Brazil; and Assumpção (Assumpção, Dourado et al. 2011) suggested the same flexural bending process would apply in the SE Brazil. According to the (Salomon, Koehn et al. 2015) it is not possible to have the same pattern in the SE Brazil due to the extra

compressional force necessary to trigger strike-slip faulting. Solomon also suggested that whilst the south Brazil would display almost no seismicity, the SE Brazil - especially in the central segment of the CRSB - is unusually seismic and recognised the reactivation of part of pre-existing fractures in the central area. The Central segment of the Ribeira belt is located within several shear zones, where the crust is thinner than its surroundings (Assumpção, Feng et al. 2013). To the north, the region is underlain by the Sao Francisco craton and in the southwest by the Parana basin which has a thicker crust. According to (Assumpção, Feng et al. 2013), a compilation of the crustal thickness of Brazil suggested that the area around the central segment of the Ribeira belt is between 31 km to 36.5 km, with an uncertainty between 2-5km depending of which model it is being used to infer the crustal thickness. This could be one of the factors influencing the higher seismicity of the central segment of the Ribeira Belt as pointed out by Salomon et al. (2015).

Under a more local consideration with regard to the structures, Negrao 2015 (Negrao, Ramos et al. 2015) suggested that the paleostresses responsible for the origin and development of the Volta Redonda basin were in accordance with the paleostresses postulated by (Riccomini 1989), with extensional NNW-SSE, transcurrent sinistral E-W, transcurrent dextral E-W and extensional NW (WNW)-SE (ESE) faults formed. Negrao 2015 focused on regional stress influencing the basin deformation and has not studied a local control to the basin fractures. It is mentioned that the structures (local or regional) might be associated with various controls from igneous intrusions, transcurrent fault system striking NW-SE and pre-Cenozoic to tectonic reactivations. The data recorded by this project within this area unfortunately is not enough to establish what could locally control these structures. The Sao Paulo basin has an interesting location; it sits on top of the intersection point between the Taxaquara fault and Caucaia fault (Fig. 50), it is separated from the Taubate basin by a transform fault and at south it is limited by a structural high in the form of a sill, emplaced there during the

Paleogene during the latest major tectonic event in the area (Riccomini 1989). Based on the complexity of the fault network displayed by the stereographic projection (Fig. 41a) a local control of faults should be considered in this situation, given the stress perturbations along the faults and the rheology in the area. De Paola 2005 (De Paola, Holdsworth et al. 2005) analysing partitioned strain, reactivation and lithological control that formed complex faulting patterns associated with transtensional rift zones at reservoir scale, suggesting that the heterogeneities under that apparent stress that traditionally would be interpreted as being due to polyphase deformation did not fit with the field observations. In a similar scenario, the data recorded in the field for the Sao Paulo basin suggests an oblique regime for the younger faults, although the most of the history of events points to the regional strike slip regime.

On the basement influence for the new structures, Bezerra et al 2011 (Bezerra, do Nascimento et al. 2011) described that in the seismically active zone of the Borborema Province in NE Brazil, the ductile-fabric controls the seismic anisotropy, presenting two case studies where it was concluded that the fast shear wave runs parallel to the Precambrian foliation instead of stress aligned fluid-filled cracks or the direction of minimum stress. The seismic data used by them showed three different patterns for the faults relationships with the pre-existing faults. These are pre-existing reactivated faults, parallelism of the faults with the foliation or quartz veins and faults that cut across pre-existing structures, all of these patterns were observed within the Itaquaquecetuba quarry. Bezerra also points out that there is a misfit between the predictions for several areas in the Borborema Province made by numerical models and the field data, the author attributes the data misfit to local factors such as density contrast and sedimentation discrepancy between oceanic and continental crusts, in agreement with other publications (Assumpcao 1992, Ferreira, Oliveira et al. 1998) that these local factors play a role to the present day tectonic stresses. Another publication that support the need to a more focused research in the local constraints for fault reactivation is the

(Kirkpatrick, Bezerra et al. 2013) paper, where the authors analysed the scale dependence of the influence of pre-existing basement shear zones. Their suggestion was that at small scale the basement has little influence on faults path, as shown by structures formed in a NE orientation that postulate that basement influence is scale dependent. At rift system scale, however, the rift faults are concordant with the shear-zones orientations even when the rocks are not mylonitic due to the seismic anisotropy leading to a broadly distributed low strain. Fractures at outcrop scale are weakly influenced by the basement pre-existing strained rocks, crosscutting the foliations and displaying several orientations with only few parallel to the shear zone.

Another aspect in the area that might locally influence how the fractures respond to the basement influence is the groundwater in the area. Dewatering structures were observed in location 0 (Fig. 41b). The quarry itself is near the unconfined part of the Guarani aquifer, which is one of the largest reservoirs of ground water in the world with 1.2 M km² total surface and can reach depths of up to 1800 m. The unconfined part of the aquifer is due to the uplift of the Serra do Mar coastal range in the Late Cretaceous (Hirata, Gesicki et al. 2011), combining these factors with the network of fractures which favours the fluid flow and content of clay in the area it could be a potential topic to explain the local stress and seismic perturbations even if transient. Neuzil (2015) investigated highs and lows of pore fluids potential in shallow (< ~ 1 km depth) argillaceous formations in intraplate settings, the author focus on the pressure anomalies and factors controlling the formation permeability in otherwise stable scenario. Neuzil (2015) attribute the pressure anomalies to geological disturbance of flow in water-saturated argillaceous formations. This factor is beyond the scope of this dissertation due to the limited dataset available to make inferences on this aspect. Nonetheless there are strong indications for basement influence as suggested in this chapter. Based on Anderson's theory, the principal horizontal stresses that worked upon the

Itaquaquecetuba area have been stipulated to be consistent with the events that occurred on the continental margin of the SE Brazil, as suggested by the authors displayed in the Table 3. Based on their findings these paleostresses have been recognized in the field and have postulated reactivation of the shear zone. This study suggests that the present day architecture has been influenced by the inheritance of the basement pre-existing structures based upon findings within the four basins visited, which display fractures within sediments that span from Neoproterozoic to Quaternary, making it possible to assess their development throughout the geological time.

For future work: The structural relationship between the offshore with onshore continental margin of Brazil would be benefit from future works focused on the onshore fractures at local scale. One of the biggest challenges in this project was to find clear crosscutting relationship between the structures to establish age relationship, cases like this can be aided by the use of Potts and Reddy (2000) younging table to construct relative deformation histories for the area of studies.

The factors influencing these structures could also affect offshore structures based upon basement influence. The Figure 49 displays the combination of magnetic map of the Santos basin with the geologic map of the Mantiqueira Province by (Zalán and Oliveira 2005) suggesting that Cenozoic grabens within the Santos basin with onshore faults could be extrapolated offshore and form border faults to the main grabens within that area, implying the influence of the offshore faults to the formation of the Tertiary basins.

This topic could be investigated further using a combination of near-shore geophysical techniques such as shallow-reflection seismology and bathymetric profiling.

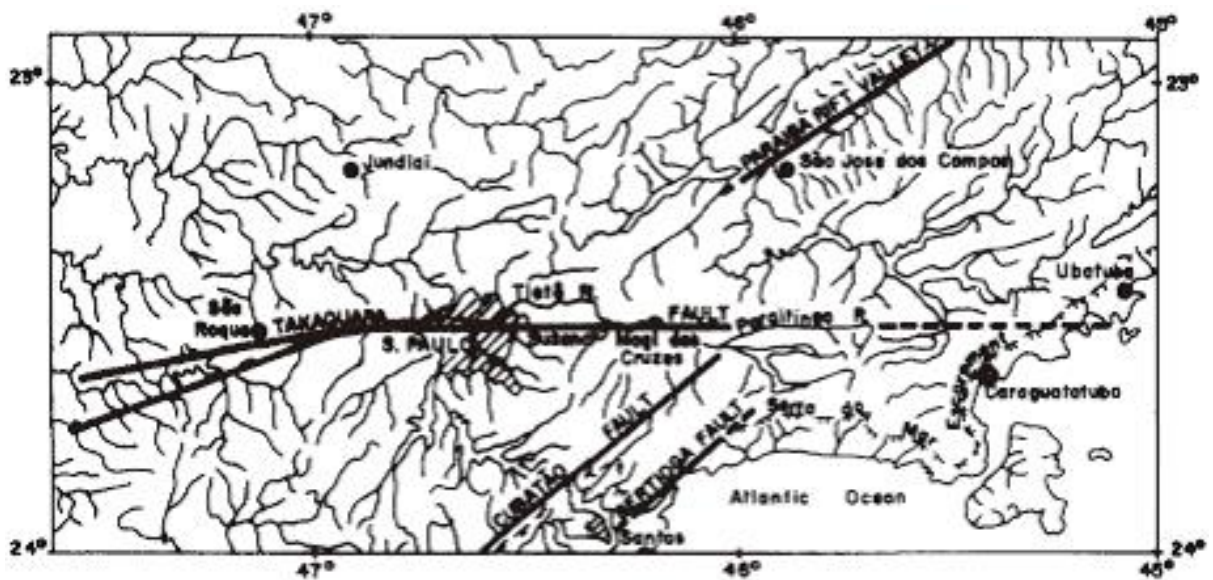


Figure 53: Taxaquara fault cross cutting the São Paulo basin, the dashed line inferring that the fault disappears towards the Santos basin

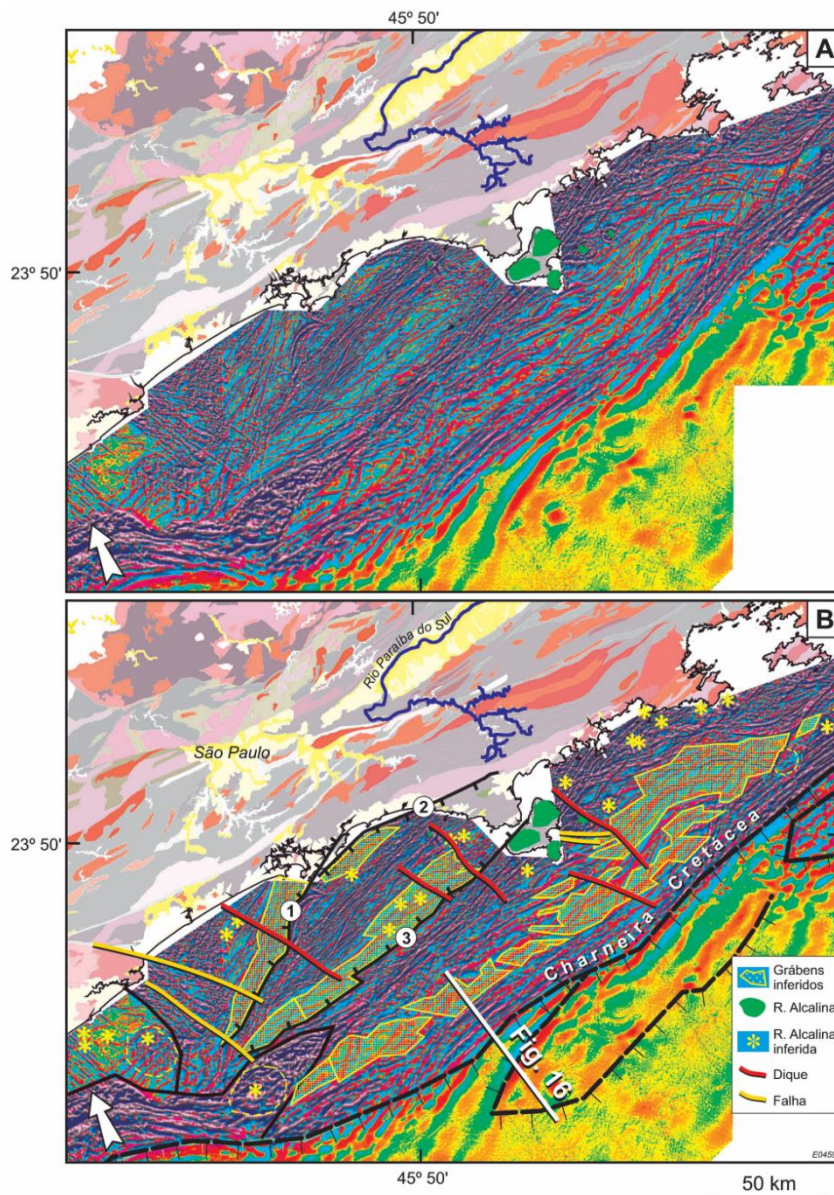


Figure 54: Zalan 2005 inferred grabens within the shallow part of the Santos basin area. Implying them to be from Cenozoic age, reflecting the same geometry of the onshore rift system and the basement anisotropy influence in the formation of new structures. Dykes and faults are cross cutting these grabens, suggesting tectonic activities that reactivate transfer zones, possibly during the Paleogene. Modified from Zalan and Oliveira (2005)

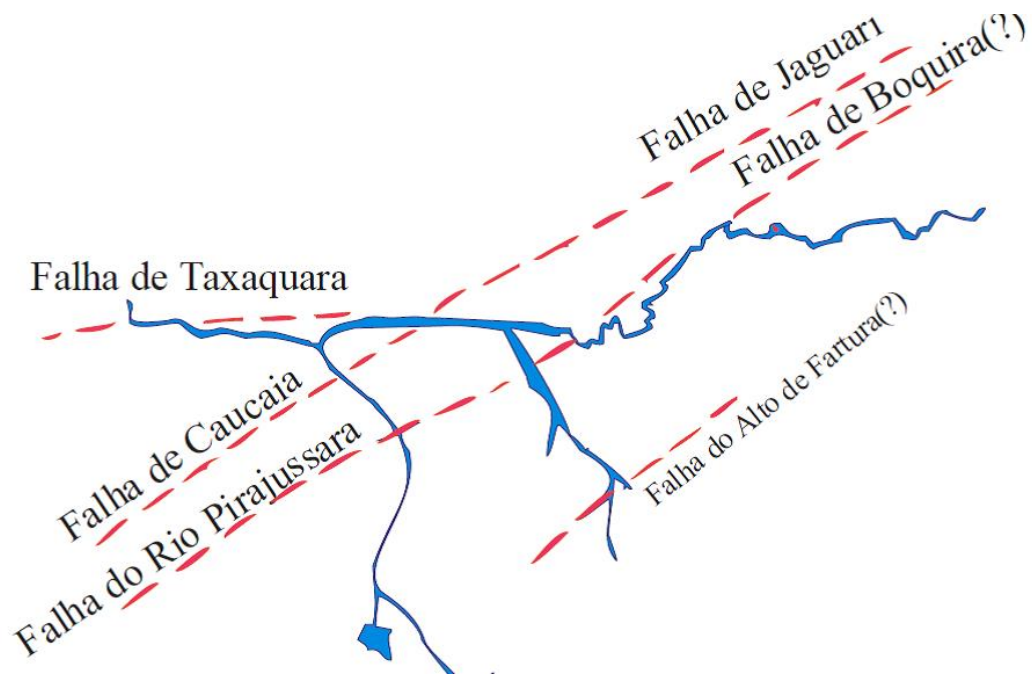


Figure 56: sketch based on the faults crosscutting the Sao Paulo basin from Rodriguez (1998)

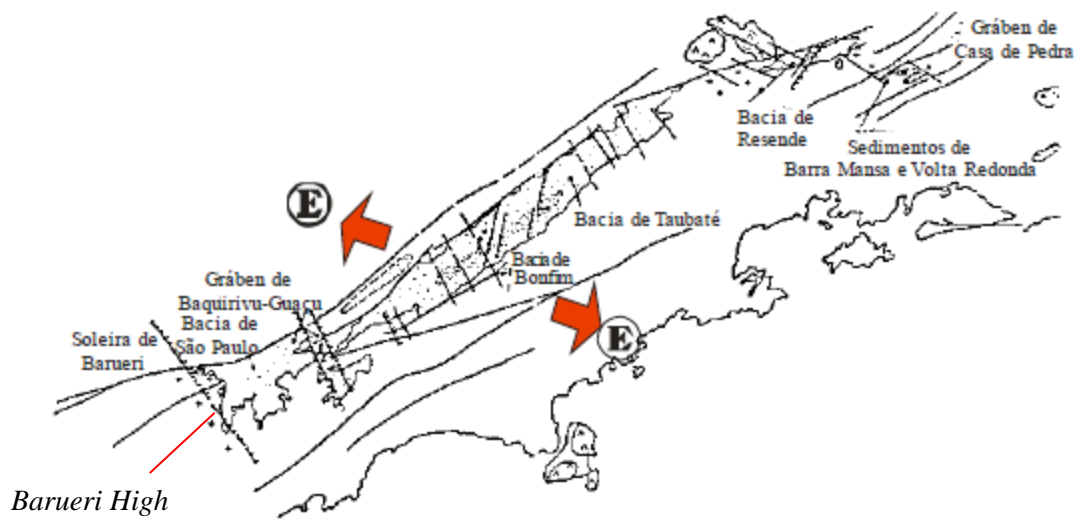


Figure 55: Sketch taken from (Rodriguez 1998) modified from (Riccomini 1989)

6 Conclusion

To understand how the basement influences the neotectonics/ present day tectonics in SE Brazil it is vital to understand how faults have evolved passive margin setting. Many authors already postulate reactivation during these periods in SE Brazil (Ricomini 1989), while reactivation was not the main initial aim of this work, basement inheritance became a topic while the project developed. Throughout the study area the outcrops visited were mostly found in neoproterozoic basement, and the structures recorded within them were associated with deformation events from the Upper Cretaceous to Paleogene, suggesting basement influence controls these structures and the architecture of the region, and it seems to still play a role for active tectonic in the area.

The relationship between present day stress with the geological structures is not known, but looking back to features in Pleistocene sediments in the Sao Paulo basin it was possible to have a better analyses of the relationship younger structures with the basement. It is not impossible to suggest that a basement influence plays a role in the control of these features in this site based upon this exercise. The array of fractures NW-SE /E-W dominates the area. These fractures orientations are reminiscent of the period of deformation of sinistral and dextral transpression (NE-SW). An extensional profile is easily observed in the area and they have been recorded both in the fault wall of the sandstone strata and in the basement, synsedimentary faults also have been recorded suggesting the influence of pre-existing fractures to its geometry. It would be feasible to suggest that these pre-existing faults and the strong fabric foliation acting upon the site fractures network in this site could be indication for basement influence in the process.

Appendix 1

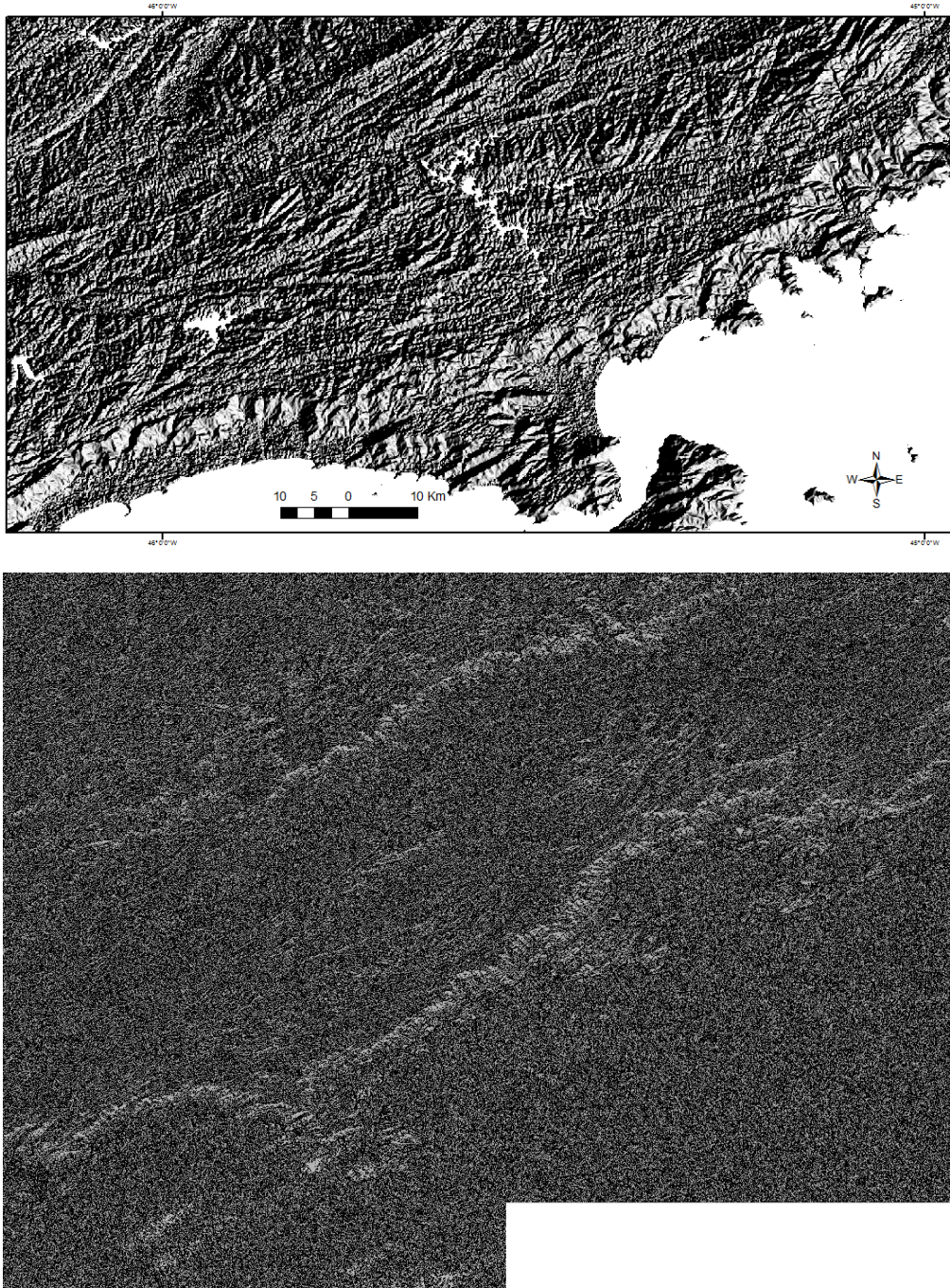


Figure 57: First attempt to create different angles through hillshade of the DEM map of 30m resolution. Because of the poor quality of the results as above it was decided to use the results for the 90m resolution.(picture on the top displaying hillshade process on 90m resolution)

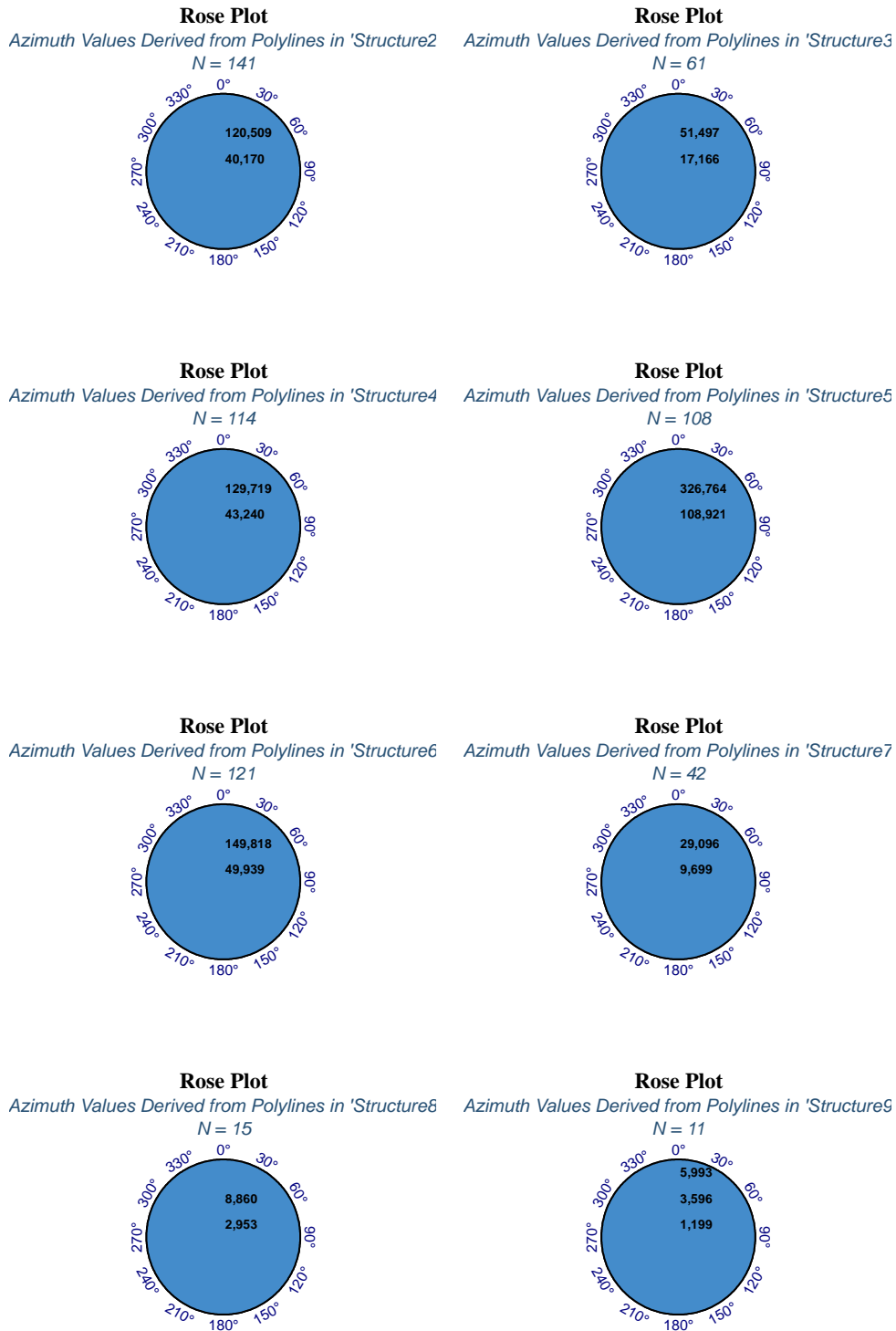
Appendix 2

Table 4: The colours are not correlating with the colours in the map and are for use in the exercise only

| E-W | | | NE-SW | | | NW-SE | | | NNE-SSW | | | ENE-WSW | | | ESE-WNW | | | NNW-SSE | | |
|---------|---------|---------|---------|----------|---------|----------|---------|----------|---------|-----------|---------|------------|---------|-----------|---------|-----------|---------|---------|---------|--------|
| Length | Azimuth | Length | Azimuth | Length | Azimuth | Length | Azimuth | Length | Azimuth | Length | Azimuth | Length | Azimuth | Length | Azimuth | Length | Azimuth | Length | Azimuth | Length |
| 1142 W | 95 | 13867 E | 232 | 3263 SW | 41 | 4337 NE | 128 | 4137 SE | 213 | 4761 SSW | 248 | 5200 WSW | 123 | 7191 ESE | 162 | 46366 SSE | | | | |
| 1013 W | 95 | 9398 E | 223 | 2339 SW | 230 | 22047 SW | 126 | 5137 SE | 199 | 7229 SSW | 255 | 5816 WSW | 123 | 3584 ESE | 167 | 2720 SSE | | | | |
| 780 W | 96 | 6150 E | 232 | 1839 SW | 227 | 21636 SW | 138 | 6187 SE | 211 | 6387 SSW | 244 | 9655 WSW | 117 | 794 ESE | 167 | 2720 SSE | | | | |
| 952 W | 96 | 6150 E | 220 | 1849 SW | 231 | 23176 SW | 129 | 4111 SE | 215 | 20602 SSW | 67 | 142481 ENE | 83 | 895 E | 164 | 4948 SSE | | | | |
| 750 W | 88 | 17030 E | 229 | 2226 SW | 42 | 1089 NE | 128 | 4266 SE | 212 | 2230 SSW | 60 | 141251 ENE | 115 | 5610 ESE | 167 | 2046 SSE | | | | |
| 806 W | 92 | 17009 E | 233 | 5103 SW | 53 | 50007 NE | 127 | 1825 SE | 200 | 15654 SSW | 67 | 71704 ENE | 113 | 4053 ESE | 169 | 2412 SSE | | | | |
| 926 E | 92 | 16506 E | 234 | 1056 SW | 52 | 53706 NE | 127 | 1791 SE | 213 | 26284 SSW | 66 | 246646 ENE | 106 | 10058 ESE | 166 | 3146 SSE | | | | |
| 1001 W | 88 | 16832 E | 224 | 1282 SW | 55 | 73482 NE | 127 | 1790 SE | 205 | 9181 SSW | 75 | 8636 ENE | 104 | 14977 ESE | 161 | 4607 SSE | | | | |
| 666 W | 92 | 8151 E | 232 | 718 SW | | | 129 | 5956 SE | 198 | 5850 SSW | 61 | 12761 ENE | 104 | 21937 ESE | 154 | 2581 SSE | | | | |
| 3224 E | 85 | 3448 E | 217 | 3316 SW | | | 124 | 2646 SE | 193 | 5090 SSW | 67 | 63048 ENE | 106 | 6915 ESE | 163 | 3399 SSE | | | | |
| 3268 E | 96 | 6137 E | 50 | 24793 NE | | | 124 | 3575 SE | 203 | 6889 SSW | 64 | 8763 ENE | 105 | 3422 ESE | 168 | 1866 SSE | | | | |
| 6818 E | 96 | 6135 E | 221 | 4118 SW | | | 125 | 3731 SE | 202 | 50671 SSW | 62 | 4630 ENE | 112 | 5966 ESE | 168 | 3632 SSE | | | | |
| 6897 E | 96 | 6137 E | 215 | 10883 SW | | | 131 | 3461 SE | 196 | 10640 SSW | 63 | 5829 ENE | 105 | 2940 ESE | 168 | 2216 SSE | | | | |
| 6056 W | 94 | 3692 E | 217 | 3668 SW | | | 134 | 3638 SE | 202 | 10040 SSW | 72 | 3353 ENE | 102 | 5192 ESE | 164 | 1679 SSE | | | | |
| 5974 E | 99 | 4147 E | 216 | 9252 SW | | | 135 | 7489 SE | 199 | 15745 SSW | 71 | 12634 ENE | 107 | 3621 ESE | 166 | 3170 SSE | | | | |
| 8767 W | 97 | 4600 E | 233 | 17289 SW | | | 125 | 990 SE | 223 | 4021 SSW | 63 | 16478 ENE | 283 | 6217 WNW | 166 | 1999 SSE | | | | |
| 2587 E | 98 | 2444 E | 236 | 5042 SW | | | 128 | 2954 SE | 209 | 18801 SSW | 64 | 6557 ENE | 290 | 2803 WNW | 168 | 3813 SSE | | | | |
| 7716 W | 96 | 5695 E | 223 | 3952 SW | | | 128 | 2541 SE | 195 | 4240 SSW | 72 | 4958 ENE | 104 | 12571 ESE | 149 | 3519 SSE | | | | |
| 21632 E | 98 | 1732 E | 232 | 2702 SW | | | 134 | 7406 SE | 208 | 7590 SSW | 64 | 3394 ENE | 104 | 15 ESE | 153 | 2478 SSE | | | | |
| 1722 W | 100 | 6876 E | 223 | 33257 SW | | | 144 | 5211 SE | 205 | 32400 SSW | 61 | 5979 ENE | 110 | 19164 ESE | 153 | 234 SSE | | | | |
| 2827 W | 94 | 7646 E | 226 | 45071 SW | | | 143 | 4318 SE | 198 | 8543 SSW | 73 | 5768 ENE | 121 | 11340 ESE | 164 | 7534 SSE | | | | |
| 3083 W | 93 | 3566 E | 215 | 6908 SW | | | 131 | 10389 SE | 194 | 12416 SSW | 70 | 8260 ENE | 119 | 2220 ESE | 149 | 4172 SSE | | | | |
| 6824 E | | | 222 | 23691 SW | | | 137 | 11261 SE | 196 | 12104 SSW | 69 | 6067 ENE | 124 | 2174 ESE | 150 | 3477 SSE | | | | |
| 3508 E | | | 218 | 2888 SW | | | 136 | 6547 SE | 213 | 4761 SSW | 76 | 5067 ENE | 113 | 1009 ESE | 156 | 3997 SSE | | | | |
| 8270 E | | | 219 | 5604 SW | | | 138 | 5868 SE | 205 | 5015 SSW | 76 | 5067 ENE | 113 | 1841 ESE | 152 | 5752 SSE | | | | |
| 9359 E | | | 225 | 15406 SW | | | 130 | 3502 SE | 205 | 6685 SSW | 259 | 27098 WSW | 113 | 1854 ESE | 149 | 1695 SSE | | | | |
| 6736 E | | | 218 | 6835 SW | | | 138 | 4362 SE | 198 | 3685 SSW | 243 | 33112 WSW | 113 | 1172 ESE | 158 | 1477 SSE | | | | |
| 6143 E | | | 222 | 8695 SW | | | 131 | 1888 SE | 208 | 3923 SSW | 243 | 26146 WSW | 109 | 1925 ESE | 153 | 1219 SSE | | | | |
| 11419 E | | | 233 | 4456 SW | | | 131 | 1888 SE | 205 | 7826 SSW | 250 | 31962 WSW | 106 | 3171 ESE | 148 | 869 SSE | | | | |
| 11414 E | | | 233 | 10132 SW | | | 131 | 1888 SE | 202 | 5061 SSW | 252 | 16650 WSW | 104 | 4340 ESE | 148 | 1600 SSE | | | | |
| 8602 E | | | 218 | 3176 SW | | | 138 | 4355 SE | 206 | 7592 SSW | 243 | 86815 WSW | 123 | 7162 ESE | 151 | 2051 SSE | | | | |
| 5021 E | | | 215 | 5353 SW | | | 138 | 4355 SE | 197 | 7153 SSW | 237 | 313032 WSW | 117 | 4118 ESE | | | | | | |
| 4091 E | | | 223 | 3533 SW | | | 138 | 4355 SE | 200 | 6502 SSW | 245 | 105857 WSW | 123 | 3582 ESE | | | | | | |
| 5536 E | | | 219 | 5338 SW | | | 138 | 4355 SE | 200 | 5012 SSW | 255 | 45822 WSW | 108 | 4324 ESE | | | | | | |
| 6151 E | | | 225 | 6088 SW | | | 138 | 4354 SE | 203 | 8837 SSW | 242 | 14606 WSW | 109 | 3406 ESE | | | | | | |
| 6163 E | | | 231 | 9593 SW | | | 127 | 3334 SE | 204 | 5665 SSW | 240 | 132019 WSW | 103 | 4012 ESE | | | | | | |
| 5040 W | | | 225 | 9824 SW | | | 131 | 4756 SE | 208 | 8815 SSW | 246 | 27017 WSW | 103 | 7469 ESE | | | | | | |
| 12751 W | | | 223 | 4021 SW | | | 135 | 17132 SE | 200 | 9772 SSW | 246 | 32410 WSW | 104 | 6819 ESE | | | | | | |
| 10549 W | | | 222 | 27949 SW | | | 138 | 5542 SE | 193 | 5298 SSW | 250 | 45151 WSW | 117 | 2375 ESE | | | | | | |
| 5277 W | | | 218 | 3176 SW | | | 143 | 3924 SE | 210 | 12767 SSW | 251 | 18919 WSW | 117 | 2375 ESE | | | | | | |
| 5884 E | | | 221 | 4475 SW | | | 133 | 8391 SE | 199 | 9653 SSW | 241 | 101111 WSW | 117 | 2375 ESE | | | | | | |
| 1274 E | | | 229 | 20782 SW | | | 132 | 2340 SE | 199 | 9653 SSW | 239 | 34061 WSW | 117 | 664 ESE | | | | | | |
| 1756 E | | | 228 | 4493 SW | | | 135 | 2328 SE | 205 | 4723 SSW | 252 | 9124 WSW | | | | | | | | |
| 1386 E | | | 226 | 15862 SW | | | 138 | 7512 SE | 205 | 7795 SSW | 248 | 9171 WSW | | | | | | | | |
| 1386 E | | | 54 | 14168 NE | | | 144 | 20026 SE | 212 | 609 SSW | 252 | 7001 WSW | | | | | | | | |
| 6151 E | | | 36 | 27997 NE | | | 131 | 1887 SE | 213 | 1018 SSW | 238 | 6167 WSW | | | | | | | | |
| 6152 E | | | 54 | 1706 NE | | | 136 | 2293 SE | 195 | 32197 SSW | 237 | 9087 WSW | | | | | | | | |
| 6151 E | | | 225 | 63021 SW | | | 139 | 1267 SE | 198 | 3230 SSW | 239 | 10716 WSW | | | | | | | | |
| 6150 E | | | 228 | 15584 SW | | | 142 | 2044 SE | 207 | 28280 SSW | 242 | 4972 WSW | | | | | | | | |
| 6149 E | | | 221 | 4307 SW | | | 135 | 1346 SE | 199 | 16163 SSW | 243 | 22101 WSW | | | | | | | | |
| 17842 E | | | 217 | 5203 SW | | | 132 | 1724 SE | 197 | 4812 SSW | 242 | 5380 WSW | | | | | | | | |
| 14552 E | | | 229 | 5811 SW | | | 145 | 5538 SE | 198 | 1409 SSW | 247 | 5940 WSW | | | | | | | | |
| 6138 E | | | 223 | 3007 SW | | | 132 | 3084 SE | 193 | 2701 SSW | 255 | 9035 WSW | | | | | | | | |
| 6139 E | | | 215 | 16600 SW | | | 139 | 12158 SE | 213 | 1768 SSW | 241 | 11477 WSW | | | | | | | | |
| 1386 E | | | 232 | 2558 SW | | | 135 | 2997 SE | 207 | 3995 SSW | 254 | 15242 WSW | | | | | | | | |
| 1386 E | | | 216 | 2798 SW | | | 135 | 1586 SE | 206 | 27834 SSW | | | | | | | | | | |
| 1386 E | | | 226 | 2943 SW | | | 130 | 6427 SE | 206 | 9471 SSW | | | | | | | | | | |
| 1386 E | | | 234 | 4463 SW | | | 130 | 6427 SE | 21 | 3563 NNE | | | | | | | | | | |
| 12682 E | | | 233 | 4514 SW | | | 142 | 3127 SE | 209 | 9181 SSW | | | | | | | | | | |
| 17809 E | | | 228 | 11714 SW | | | 145 | 2087 SE | 202 | 4664 SSW | | | | | | | | | | |
| 5067 E | | | 231 | 30413 SW | | | 145 | 2087 SE | 210 | 8817 SSW | | | | | | | | | | |
| 9394 E | | | 50 | 54078 NE | | | 136 | 2680 SE | 34 | 10133 NNE | | | | | | | | | | |
| 6411 E | | | 56 | 41468 NE | | | 145 | 2087 SE | 207 | 5901 SSW | | | | | | | | | | |
| 8251 E | | | 37 | 3630 NE | | | 135 | 3640 SE | 209 | 7497 SSW | | | | | | | | | | |
| 7142 E | | | 40 | 3405 NE | | | 137 | 3580 SE | 215 | 15762 SSW | | | | | | | | | | |
| 4394 E | | | 40 | 3405 NE | | | 138 | 4113 SE | 213 | 13489 SSW | | | | | | | | | | |
| 4766 E | | | 41 | 10485 NE | | | 145 | 4010 SE | | | | | | | | | | | | |
| 16836 E | | | 51 | 30346 NE | | | 146 | 5709 SE | | | | | | | | | | | | |
| 10012 E | | | 53 | 50007 NE | | | 144 | 2586 SE | | | | | | | | | | | | |
| 8991 E | | | 52 | 53706 NE | | | 144 | 855 SE | | | | | | | | | | | | |
| 12626 E | | | 55 | 73482 NE | | | 144 | 1817 SE | | | | | | | | | | | | |
| 12631 E | | | 48 | 20914 NE | | | 146 | 2612 SE | | | | | | | | | | | | |
| 12633 E | | | 36 | 27997 NE | | | 128 | 859 SE | | | | | | | | | | | | |
| 12629 E | | | 54 | 1706 NE | | | 127 | 1075 SE | | | | | | | | | | | | |
| 20411 E | | | 50 | 54078 NE | | | | | | | | | | | | | | | | |
| 33200 E | | | 56 | 41468 NE | | | | | | | | | | | | | | | | |
| 6979 E | | | 37 | 3630 NE | | | | | | | | | | | | | | | | |
| 20867 W | | | 40 | 3405 NE | | | | | | | | | | | | | | | | |
| 50365 W | | | 40 | 3405 NE | | | | | | | | | | | | | | | | |
| 239 E | | | 41 | 10485 NE | | | | | | | | | | | | | | | | |
| 3019 E | | | 51 | 30346 NE | | | | | | | | | | | | | | | | |
| 5594 E | | | 216 | 20238 SW | | | | | | | | | | | | | | | | |
| 4567 E | | | 44 | 16348 NE | | | | | | | | | | | | | | | | |
| 7914 E | | | 38 | 6849 NE | | | | | | | | | | | | | | | | |
| 14728 E | | | 51 | 32957 NE | | | | | | | | | | | | | | | | |
| 3262 E | | | 49 | 10998 NE | | | | | | | | | | | | | | | | |

Appendix 3

Figure 58: Rose diagrams representing the different orientations of the area, separated the structures in group based on their azimuth.



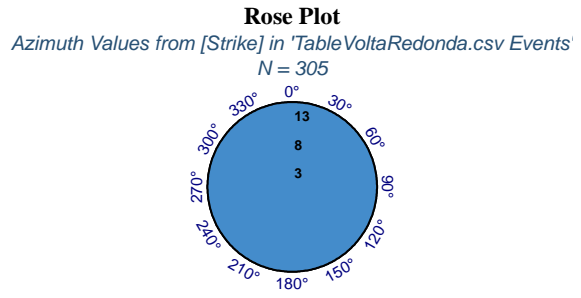
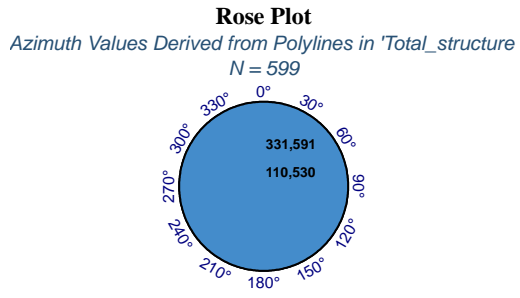


Figure 59: Rose diagrams comparing regional to local structures orientations

References

- Almeida, F. F. D. and C. D. R. Carneiro (1998). "Origem E Evolução Da Serra Do Mar." Revista Brasileira de Geociências **28**(2): 135-150.
- Almeida, F. F. M., Y. Hasui, B. B. De Brito Neves and R. A. Fuck (1981). "Brazilian Structural Provinces An Introduction." Earth Sciences Review **17**: 1-29.
- Angelier, J. and P. Mechler (1977). "A graphic method applied to the localization of principal stresses for fault tectonics and seismology: the right dihedral method." Bull Soc Geol Fr **19**: 1309-1318.
- Ashby, D. E. (2013). "Influences on continental margin development: a case study from the Santos Basin, South-eastern Brazil." <http://theses.dur.ac.uk/6989/>.
- Assumpcao, M. (1992). "The regional intraplate stress field in South America." Journal of Geophysical Research **97**(B8): 11889.
- Assumpção, M., J. R. Barbosa, J. Berrocal, A. M. Bassini, J. A. V. Veloso, V. I. Mârza, M. G. Huelsen and L. C. Ribotta (1997). "Seismicity patterns and focal mechanisms in southeastern Brazil." Revista Brasileira de Geofísica **15**: 119-132.
- Assumpção, M., J. Dourado, L. Ribotta, W. Mohriak, F. L. Dias and J. Barbosa (2011). "The São Vicente earthquake of 2008 April and seismicity in the continental shelf off SE Brazil: further evidence for flexural stresses." Geophysical Journal International **187**(3): 1076-1088.
- Assumpção, M., M. Feng, A. Tassara and J. Julià (2013). "Models of crustal thickness for South America from seismic refraction, receiver functions and surface wave tomography." Tectonophysics **609**: 82-96.
- Assumpção, M., L. C. Ribotta, C. Chimplignond, M. V. Huelsen and G. S. França (2008). "Update of the RIS of Brazil 2008." ICOLD (International Comission of Large Dam) Conference 2008.
- Assumpcao, M., M. Schimmel, C. Escalante, J. R. Barbosa, M. Rocha and L. V. Barros (2004). "Intraplate seismicity in SE Brazil: stress concentration in lithospheric thin spots." Geophysical Journal International **159**(1): 390-399.
- Beacom, L. E., R. E. Holdsworth, K. J. W. McCaffrey and T. B. Anderson (2001). A quantitative study of the influence of pre-existing compositional and fabric heterogeneities upon fracture-zone development during basement reactivation. Nature and Tectonic Significance of Fault Zone Weakening. R. E. Holdsworth, R. A. Strachan, J. F. Magloughlin and R. J. Knipe. Bath, Geological Soc Publishing House. **186**: 195-211.
- Bezerra, F. H. R., A. F. do Nascimento, J. M. Ferreira, F. C. Nogueira, R. A. Fuck, B. B. B. Neves and M. O. L. Sousa (2011). "Review of active faults in the Borborema Province, Intraplate South America — Integration of seismological and paleoseismological data." Tectonophysics **510**(3-4): 269-290.
- Biagolini, C. H., M. E. C. Bernardes-de-Oliveira and A. G. Caramês (2013). "Itaquaquecetuba Formation, São Paulo basin, Brazil: new angiosperm components of Paleogene Taphoflora." Brazilian Journal of Geology **43**(4): 639-652.
- Cobbold, P. R., K. E. Meisling and V. S. Mount (2001). "Reactivation of an obliquely rifted margin, Campos and Santos basins, southeastern Brazil." AAPG bulletin **85**(11): 1925-1944.
- Cogne, N., P. R. Cobbold, C. Riccomini and K. Gallagher (2013). "Tectonic setting of the Taubate Basin (Southeastern Brazil): Insights from regional seismic profiles and outcrop data." Journal of South American Earth Sciences **42**: 194-204.
- Cogné, N., P. R. Cobbold, C. Riccomini and K. Gallagher (2013). "Tectonic setting of the Taubaté Basin (Southeastern Brazil): Insights from regional seismic profiles and outcrop data." Journal of South American Earth Sciences **42**: 194-204.

Cogné, N., K. Gallagher and P. R. Cobbold (2011). "Post-rift reactivation of the onshore margin of southeast Brazil: Evidence from apatite (U–Th)/He and fission-track data." Earth and Planetary Science Letters **309**(1-2): 118-130.

Coombs, D., A. Ellis, W. Fyfe and A. Taylor (1959). "The zeolite facies, with comments on the interpretation of hydrothermal syntheses." Geochimica et cosmochimica acta **17**(1-2): 53-107.

Curvo, E. A. C., C. A. Tello S, A. Carter, A. N. C. Dias, C. J. Soares, W. M. Nakasuga, R. S. Resende, M. R. Gomes, I. Alencar and J. C. Hadler (2013). "Zircon fission track and U–Pb dating methods applied to São Paulo and Taubaté Basins located in the southeast Brazil." Radiation Measurements **50**: 172-180.

De Paola, N., R. E. Holdsworth, K. J. W. McCaffrey and M. R. Barchi (2005). "Partitioned transtension: an alternative to basin inversion models." Journal of Structural Geology **27**(4): 607-625.

Dyer, R. (1988). "Using joint interactions to estimate paleostress ratios." Journal of Structural Geology **10**(7): 685-699.

Ferrari, A. L. (2001). "Evolução Tectônica Do Graben Da Guanabara."

Ferreira, J. M., T. Oliveira, M. K. Takeya and M. Assumpção (1998). "Superposition of local and regional stresses in northeast Brazil: evidence from focal mechanisms around the Potiguar marginal basin." Geophysical Journal International **134**(2): 341-355.

Franco-Magalhaes, A. O. B., M. A. A. Cuglieri, P. C. Hackspacher and A. R. Saad (2013). "Long-term landscape evolution and post-rift reactivation in the southeastern Brazilian passive continental margin: Taubaté basin." International Journal of Earth Sciences **103**(2): 441-453.

Gallagher, K., C. J. Hawkesworth and M. S. M. Mantovani (1994). "The denudation history of the onshore continental margin of SE Brazil inferred from apatite fission track data." Journal of Geophysical Research: Solid Earth **99**(B9): 18117-18145.

Gallagher, K., C. J. Hawkesworth and M. S. M. Mantovani (1994). "The denudation history of the onshore continental margin of SE Brazil inferred from apatite fission track data." Journal of Geophysical Research **99**(B9): 18117.

Gontijo-Pascutti, A., F. H. R. Bezerra, E. La Terra and J. C. H. Almeida (2010). "Brittle reactivation of mylonitic fabric and the origin of the Cenozoic Rio Santana Graben, southeastern Brazil." Journal of South American Earth Sciences **29**(2): 522-536.

Gontijo-Pascutti, A., F. H. R. Bezerra, E. L. Terra and J. C. H. Almeida (2010). "Brittle reactivation of mylonitic fabric and the origin of the Cenozoic Rio Santana Graben, southeastern Brazil." Journal of South American Earth Sciences **29**(2): 522-536.

Hackspacher, P. C., C. Juliani, A. Fetter and E. L. Dantas (2001). "Evolution of the Central Ribeira Belt, Brazil: Implications for the Assembly of West Gondwana." Gondwana Research **4**(4): 626-627.

Hackspacher, P. C., L. F. B. Ribeiro, M. C. S. Ribeiro, A. H. Fetter, J. C. H. Neto, C. E. S. Tello and E. L. Dantas (2004). "Consolidation and Break-up of the South American Platform in Southeastern Brazil: Tectonothermal and Denudation Histories." Gondwana Research **7**(1): 91-101.

Hansen, J.-A. and S. G. Bergh (2012). "Origin and reactivation of fracture systems adjacent to the Mid-Norwegian continental margin on Hamarøya, North Norway: use of digital geological mapping and morphotectonic lineament analysis." Norwegian Journal of Geology/Norsk Geologisk Forening **92**(4).

Heilbron, M., C. M. Valeriano, C. C. G. Tassinari, J. Almeida, M. Tupinamba, O. Siga and R. Trouw (2008). "Correlation of Neoproterozoic terranes between the Ribeira Belt, SE Brazil and its African counterpart: comparative tectonic evolution and open questions." Geological Society, London, Special Publications **294**(1): 211-237.

Hirata, R., A. Gesicki, O. Sracek, R. Bertolo, P. C. Giannini and R. Aravena (2011). "Relation between sedimentary framework and hydrogeology in the Guarani Aquifer System in São Paulo state, Brazil." Journal of South American Earth Sciences **31**(4): 444-456.

Hiruma, S. T., C. Riccomini, M. C. Modenesi-Gauttieri, P. C. Hackspacher, J. C. H. Neto and A. O. B. Franco-Magalhães (2010). "Denudation history of the Bocaina Plateau, Serra do Mar, southeastern Brazil: Relationships to Gondwana breakup and passive margin development." Gondwana Research **18**(4): 674-687.

Holdsworth, R. E., A. A. Butler and A. M. Roberts (1997). "The recognition of reactivation during continental deformation." *Journal of the Geological Society* **154**: 73–78.

Holdsworth, R. E., M. Hand, J. A. Miller and I. S. Buick (2001). "Continental reactivation and reworking: an introduction." *Geological Society, London, Special Publications*(184): 1-12.

Holdsworth, R. E., M. Stewart, J. Imber and R. A. Strachan (2001). "The structure and rheological evolution of reactivated continental fault zones: a review and case study." *Geological Society, London, Special Publications* **184**: 115-137.

Hudec, M. R. and M. P. A. Jackson (2004). "Regional restoration across the Kwanza Basin, Angola Salt tectonics triggered by repeated uplift of a metastable passive margin." *AAPG Bulletin* v. **88** (no. 7): 971–990.

Imber, J., R. E. Holdsworth, C. A. Butler and G. E. Lloyd (1997). "Fault-zone weakening processes along the reactivated Outer Hebrides Fault Zone, Scotland." *Journal of the Geological Society* **154**: 105-109.

Karl, M., U. A. Glasmacher, S. Kollenz, A. O. B. Franco-Magalhaes, D. F. Stockli and P. C. Hackspacher (2013). "Evolution of the South Atlantic passive continental margin in southern Brazil derived from zircon and apatite (U–Th–Sm)/He and fission-track data." *Tectonophysics* **604**: 224-244.

Kirkpatrick, J., F. Bezerra, Z. Shipton, A. Do Nascimento, S. Pytharouli, R. Lunn and A. Soden (2013). "Scale-dependent influence of pre-existing basement shear zones on rift faulting: a case study from NE Brazil." *Journal of the Geological Society* **170**(2): 237-247.

Kirkpatrick, J. D., F. H. R. Bezerra, Z. K. Shipton, A. F. Do Nascimento, S. I. Pytharouli, R. J. Lunn and A. M. Soden (2013). "Scale-dependent influence of pre-existing basement shear zones on rift faulting: a case study from NE Brazil." *Journal of the Geological Society* **170**(2): 237-247.

Lundin, E. and A. G. Dore (2002). "Mid-Cenozoic post-breakup deformation in the 'passive' margins bordering the Norwegian-Greenland Sea." *Marine and Petroleum Geology* **19**(1): 79-93.

McClay, K. R. (1991). "The mapping of geological structures."

Misra, A. A. and S. Mukherjee (2015). "Tectonic Inheritance in Continental Rifts and Passive Margins." *Springer*.

Mora, C. A. S., G. C. Campanha and K. Wemmer (2013). "Microstructures and K-Ar illite fine-fraction ages of the cataclastic rocks associated to the Camburu Shear Zone, Ribeira Belt, Southeastern Brazil." *Brazilian Journal of Geology* **43**(4): 607-622.

Negrão, A. (2014). *Evolução tectonossedimentar e deformação rúptil cenozoica da região da bacia sedimentar de Volta Redonda (Segmento Central do Rifte Continental do Sudeste do Brasil, RJ)*, PhD Thesis, Instituto de Geociências, Universidade Federal do Rio de Janeiro, Rio de Janeiro.

Negrão, A. P., C. L. Mello, R. R. C. Ramos and M. S. R. Sanson (2015). "Mapa geológico do cenozoico da região da bacia de Volta Redonda (RJ, segmento central do Rifte Continental do Sudeste do Brasil): identificação de novos grabens e ocorrências descontínuas, e caracterização de estágios tectonossedimentares." *Brazilian Journal of Geology*, **45**(2): 273-291.

Negrão, A. P., R. R. C. Ramos, C. L. Mello and M. d. S. R. Sanson (2015). "Mapa geológico do cenozoico da região da bacia de Volta Redonda (RJ, segmento central do Rifte Continental do Sudeste do Brasil): identificação de novos grabens e ocorrências descontínuas, e caracterização de estágios tectonossedimentares." *Brazilian Journal of Geology* **45**(2): 273.

Neuzil, C. E. (2015). "Interpreting fluid pressure anomalies in shallow intraplate argillaceous formations." Geophysical Research Letters **42**(12): 4801-4808.

Potts, G. J. and S. M. Reddy (2000). "Application of younging tables to the construction of relative deformation histories—1: fracture systems." Journal of Structural Geology **22**(10): 1473-1490.

Ramos, R. R. C., C. L. Mello and M. S. R. Sanson (2003). "Revisão Estratigráfica Da Bacia De Resende, Rift Continental Do Sudeste Do Brasil, Estado Do Rio De Janeiro."

Ramos, R. R. C., C. L. Mello and M. S. R. Sanson (2006). "Sistemas Aluviais Terciários Da Bacia De Resende, Estado Do Rio De Janeiro, Brasil: Análise De Fácies E Revisão Estratigráfica." São Paulo, UNESP, Geociências **25**(1): 59-69.

Ribeiro, L. F. B., P. C. Hackspacher, C. A. T. Saenz, J. C. H. Neto, P. J. Iunes and S. R. Paulo (2005). "Phanerozoic Brittle Tectonics In The South American Continental Platform, Southeast Brazil: New Insights From Fission Track Studies On Apatite In Reactivated Fault Zones." Revista Brasileira de Geociências **35**(2): 151-164.

Riccomini (1989). "O RIFT CONTINENTAL DO SUDESTE DO BRASIL."

Riccomini, C. (1989). "O Rift Continental do Sudeste do Brasil."

Riccomini, C. (1989). O rift continental do sudeste do Brasil, Universidade de São Paulo.

Riccomini, C., A. U. G. Peloggia, J. C. L. Saloni, M. W. Kohnke and R. M. Figueira (1989). "Neotectonic activity in the Serra do Mar rift system (southeastern Brazil)." Journal of South American Earth Sciences **Vol. 2**(2): 191-197.

Riccomini, C., L. G. Sant'Anna, A. L. Ferrari, V. Mantesso-Neto, A. Bartorelli, C. Carneiro and B. Brito-Neves (2004). "Evolução geológica do rift continental do sudeste do Brasil." Geologia do continente Sul-Americano: evolução da obra de Fernando Flávio Marques de Almeida: 383-405.

Rodriguez, S. K. (1998). Geologia urbana da região metropolitana de São Paulo, Universidade de São Paulo.

Saenz, C. A. T., P. C. Hackspacher, J. C. H. Neto, P. J. Iunes, S. Guedes, L. F. B. Ribeiro and S. R. Paulo (2003). "Recognition-of-cretaceous-paleocene-and-neogene-tectonic-reactivation-through-apatite-fission-track-analysis-in-precambrian-areas-of-southeast brazil." Journal of South American Earth Sciences(15): 765–774.

Salomon, E., D. Koehn, C. Passchier, P. C. Hackspacher and U. A. Glasmacher (2015). "Contrasting stress fields on correlating margins of the South Atlantic." Gondwana Research **28**(3): 1152-1167.

Sanson, M. d. S. R. (2006). "Sistemas deposicionais e tectônica rúptil cenozóica na região de Volta Redonda (RJ): Rift continental do sudeste do Brasil." Anuário do Instituto de Geociências **29**(2): 276-278.

Siga Jr, O., L. F. Cury, I. McReath, L. M. de Almeida Leite Ribeiro, K. Sato, M. Â. Stipp Basei and C. R. Passarelli (2011). "Geology and geochronology of the Betara region in south-southeastern Brazil: Evidence for possible Statherian (1.80–1.75 Ga) and Calymmian (1.50–1.45 Ga) extension events." Gondwana Research **19**(1): 260-274.

Sippel, J., M. Scheck-Wenderoth, K. Reicherter and S. Mazur (2009). "Paleostress states at the southwestern margin of the Central European Basin System—Application of fault-slip analysis to unravel a polyphase deformation pattern." Tectonophysics **470**(1): 129-146.

Suguio, K., C. Riccomini, A. E. M. Sallun, W. S. Filho and P. A. Neto (2010). "Provável Significado Geológico de Idades LOE (Luminescência Opticamente Estimulada) da Formação Itaquaquetuba, SP." Revista do Instituto de Geociências - USP **10**(3): 49-56.

Sykes, L. R. (1978). "Intraplate Seismicity, Reactivation of Preexisting Zones of Weakness, Alkaline Magmatism, and Other Tectonism Postdating Continental Fragmentation." Reviews Of Geophysics And Space Physics **16**(4): 621-688.

Tello Saenz, C. A., J. C. Hadler Neto, P. J. Iunes, S. Guedes, P. C. Hackspacher, L. F. B. Ribeiro, S. R. Paulo and A. M. Osorio A (2005). "Thermochronology of the South American platform in the state of São Paulo, Brazil, through apatite fission tracks." Radiation Measurements **39**(6): 635-640.

Torres-Ribeiro, M. (2004). Fácies microclásticas de um sistema lacustre oligocênico do sudeste do Brasil (Formação Tremembé, bacia de Taubaté). Universidade Federal do Rio de Janeiro, Instituto de Geociências, Rio de Janeiro, Dissertação de Mestrado.

Vauchez, A., A. Tommasi and G. Barruol (1998). "Rheological Heterogeneity, Mechanical Anisotropy And Deformation Of The Continental Lithosphere." Tectonophysics **296**: 61–86.

Zalán, P. V. and J. Oliveira (2005). "Origem e evolução estrutural do Sistema de Riftes Cenozóicos do Sudeste do Brasil." Boletim de Geociências da PETROBRAS **13**(2): 269-300.

Zanão, R., J. C. Castro and A. R. Saad (2006). "Caracterização geométrica de um sistema fluvial, formação Ttaquaquetuba, Terciário da Bacia de São Paulo." Geociências **25**(3): 307-315.

Zitellini, N., M. Rovere, P. Terrinha, F. Chierici and L. Matias (2004). "Neogene Through Quaternary Tectonic Reactivation of SW Iberian Passive Margin." Pure and Applied Geophysics **161**(3): 565-587.